Anx-B

PLI Removal from ECG Signal using Adaptive Algorithms

Author

Javeria Habib

NUST201464399MCEME35014F

Supervisor

Dr. Shahzad Amin Sheikh

DEPARTMENT OF ELECTRICAL ENGINEERING

COLLEGE OF ELECTRICAL & MECHANICAL ENGINEERING

NATIONAL UNIVERSITY OF SCIENCES AND TECHNOLOGY

ISLAMABAD

SEPTEMBER, 2016

Anx-B

PLI Removal from ECG Signal using Adaptive Algorithms

Author

Javeria Habib

NUST201464399MCEME35014F

A thesis submitted in partial fulfillment of the requirements for the degree of

MS Electrical Engineering

Thesis Supervisor:

Dr. Shahzad Amin Sheikh

Thesis Supervisor's Signature:_____

DEPARTMENT OF ELECTRICAL ENGINEERING

COLLEGE OF ELECTRICAL & MECHANICAL ENGINEERING

NATIONAL UNIVERSITY OF SCIENCES AND TECHNOLOGY,

ISLAMABAD

SEPTEMBER, 2016

Declaration

I certify that this research work titled "*PLI Removal from ECG Signal using Adaptive Algorithms"* is my own work. The work has not been presented elsewhere for assessment. The material that has been used from other sources it has been properly acknowledged / referred.

Signature of Student

Javeria Habib

NUST201464399MCEME35014F

Language Correctness Certificate

This thesis has been read by an English expert and is free of typing, syntax, semantic, grammatical and spelling mistakes. Thesis is also according to the format given by the university.

Signature of Student

Javeria Habib

NUST201464399MCEME35014F

Signature of Supervisor

Copyright Statement

Acknowledgements

All praise to my Creator Allah Subana-Watala who showering his countless blessing and courage to complete my MS Degree. He gave me strength and ability to perform my tasks with patience. He showed me the way through difficult time. He send his help through various ways which I may have not known. And His guidance is what I need for every step in my future life.

[36:83] "Verily His command, when He intends a thing, is *only* that He says to it, 'Be!, and it is."

I am profusely thankful to my beloved parents for having hope in me that no matter what the circumstances are, I can do anything possible or impossible. Also for their prayers for my success at every field of my life. I am also grateful to my siblings who have supported me through this journey.

I would also like to express special thanks to my supervisor Dr. Shahazad Amin Sheikh for his help throughout my thesis and also for Dr. Salman Masaud and Adaptive Filters courses which he has taught me. I can safely say that I haven't learned any other engineering subject in such depth than the ones which he has taught.

I would also like to pay special thanks to Dr. Salman Msaud for his tremendous support and cooperation. Each time I got stuck in something, he came up with the solution. Without his help I wouldn't have been able to complete my thesis. I appreciate his patience and guidance throughout the whole thesis.

I would also like to thank Dr. Hamid Mehmood and Dr. Usman Ali for being on my thesis guidance and evaluation committee and for their valuable time.

I gratefully acknowledge College of Electrical and Mechanical Engineering NUST for providing me highly supportive atmosphere during my course and research work.

I would like to express my gratitude to NS Ayesha Zeb, NS Sumbul Gulzar and NS Sana Saleem for their guidance and support throughout my Masters.

Dedicated to my supportive parents and encouraging siblings whose tremendous support and cooperation led me to this wonderful accomplishment.

Abstract

Electrocardiogram (ECG) is the graphical illustration of heart activity to diagnose various cardiovascular diseases. Presence of Power Line Interference (PLI) in ECG makes it difficult for the examiner to identify proper working of heart. To remove such interference different types of adaptive noise cancellers have been implemented. All the adaptive algorithms previously implemented for such purpose have either better convergence, mean square error (MSE) or better complexity. So a new algorithm named SSLMS is implemented to have a compromise between the previously mentioned parameters. Using SSLMS, first impulsive component of PLI has been removed and comparison of it has been made with NLMS, RLS and SSRLS algorithms. In later work, PLI having known frequency is estimated using sinusoidal model of SSLMS algorithm and comparisons are made with SSRLS algorithm. Later PLI with unknown frequency is being tracked by first converging to its true frequency and then estimating it based to the new value of frequency. In the end PLI with unidirectional and bidirectional frequency is being estimated and removed from ECG signal. Moreover, every simulation using SSLMS has also been compared with those of SSRLS algorithm. As SSRLS has better convergence and MSE but exceptionally high computational complexity than that of SSLMS algorithm, so a new hybrid algorithm is proposed that combines the best features of both SSRLS and SSLMS algorithms. This algorithm has faster convergence than that of SSLMS algorithm and lower computational complexity than SSRLS algorithm. Moreover, its MSE is lower than those of both SSRLS and SSLMS algorithm. Simulation results prove the enhanced performance of the proposed hybrid.

Key Words: Power Line Interference, Electrocardiogram, SSLMS, SSRLS,, frequency tracking, adaptive filters, convergence, MSE, computational complexity, robustness

Table of Contents

List of Figures

List of Tables

CHAPTER 1: INTRODUCTION

In this chapter, a short overview of my work is presented. The motivation behind this work, Problem statement and basics of ECG are discussed along with its importance in diagnosing various heart diseases. Moreover, types of noises that usually affect ECG are also discussed in detail in order to elaborate the need of noise removal from ECG.

1.1 Motivation:

Cardiovascular disease includes a group of disorders related to heart and blood vessels. According to World Health Organization (WHO), cardiovascular diseases are on top of the list of diseases causing global deaths annually [1],[2]. WHO reports in 2012 show that approximately 17.5 million deaths, which is 31% of the world population, have occurred due to cardiovascular diseases [2] among which 7.4 million were cases of coronary heart disease and stroke was a cause of 6.7 million [2]. And with this rate, predictions are that death rate due to cardiovascular diseases can reach up to 23.3 million within fifteen years [3]. In order to avoid this predictive death rate, there must be some efficient system to diagnose heart diseases at an early stage. In order to identify such diseases, a graphical illustration of electrical activity by heart are represented in a form of waveform. Such waveforms are called Electrocardiogram (ECG) and are used by medical examiners to identify the disease.

ECG is a very important tool that has been used to identify various cardiovascular issues present. The shape of this waveform has pre-determined amplitudes and duration. ECG signals are obtained by means of electrodes attached to the precise locations on patient's body. But, even with the finest ECG recording machines available, this ECG signal can never be generated without any impurity or noise present in it. Types of noise corrupting ECG signal are Power Line Interference (PLI), Baseline Drift, Electrode Contact Noise, Motion Artifacts, Electromyography (EMG) and instrumentation noise. Among all these, PLI is the major type of noise present in ECG signal and occurs due to Electromagnetic Interference (EMI) in the cable connect to ECG machine. This EMI is from the power line frequency generated by any power line or plug in the surrounding region.

The frequency, phase and amplitude of PLI are not known to any noise cancellation scheme. So, in order to track these characteristics of PLI or ECG signal, we need an adaptive algorithm which leads us to the main motivation i.e. to find an efficient method to remove PLI for ECG signal.

1.1. Electrocardiograph basics:

ECG is one of the most valuable and simplest cardiac diagnostic tools available that provides rich information about the condition of heart. An ECG signal is basically a graphical representation of the electrical activity of heart. One can identify beat disturbance, transmission irregularities and electrolyte inequities by accurately inferring these waveforms. An ECG helps in identifying and intensive care of such diseases like acute coronary syndromes and pericarditis.

For an accurate interpretation of ECG, identification of its key components is necessary and then these components are analyzed separately. The electrical activity of the heart produces currents that transfer through the surrounding tissue to the skin. Electrodes attached to the skin sense these signals and give a graphical representation of them.

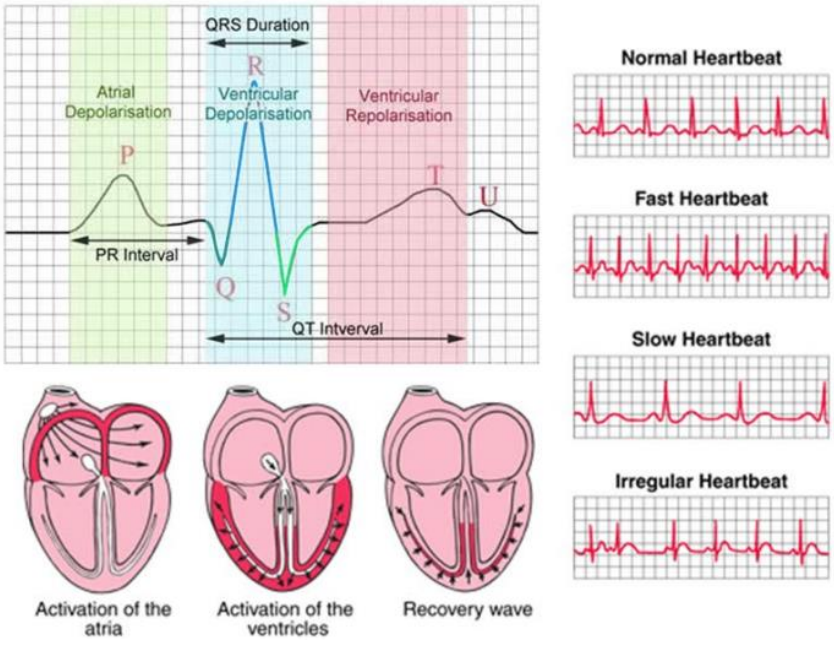

Figure 1.1.1: Heart conditions and ECG

1.2 ECG waveform components:

An ECG complex represents the depolarization-repolarization of the heart occurring in one cardiac cycle. ECG waveform consists of three basic components:

- The P wave
- The QRS complex
- The T wave

The components can be further broken into following intervals and segments:

- PR interval
- ST segment
- QT interval

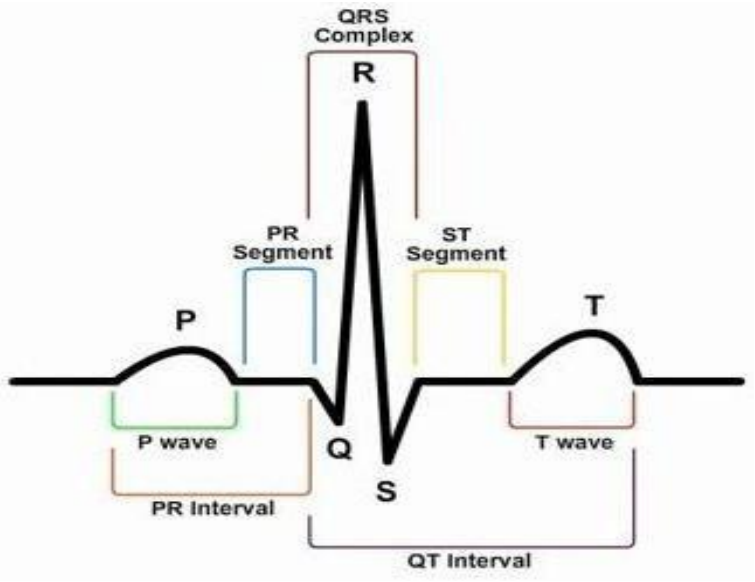

Figure 1.2.1: ECG waveform components

1.3 Sources of noise:

When ECG is acquired from human body, it gets corrupted by various types of noises. Most common types are:

- Power line interference (PLI)
- Baseline Drift
- Electrode Contact Noise
- Motion Artifacts
- Electromyography
- Instrumentational noise

1.3.1 Power Line Interference (PLI):

As mentioned by the name, PLI occurs due to EMI in the power cable connected to the ECG machine. PLI noise is sometimes of such amplitude that it totally conceals the original ECG signal. Due to this reason, American Heart Association has recommended ECG recorders to have a 3dB frequency range from 0.67 Hz to 150 Hz [4], [5], [6].

PLI has two major components reported that are explained as follows:

- Impulsive component comprises of various pulses with high amplitude and short duration which causes the adaptive filters to become unstable..
- Sinusoidal component has unknown frequency which can be a variable parameter in some cases along with unknown amplitude and phase. Removal of this type of PLI has been reported many times in literature. The sinusoidal component of PLI is shown in Figure 1.3.1.

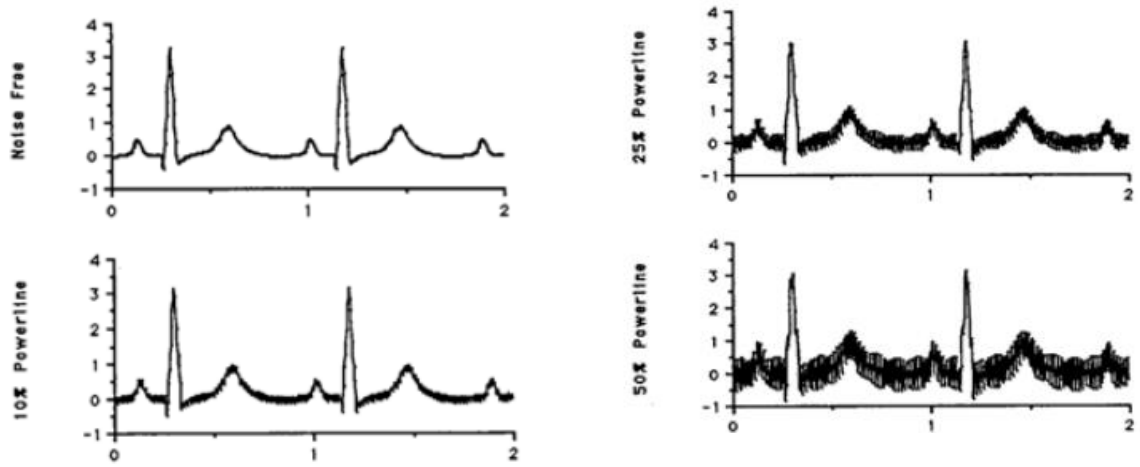

(a) (b)

Figure 1.3.1: ECG signal with (a) 10% PLI, (b) 25% & 50% PLI

This research work focuses on PLI removal techniques from ECG signal.

1.3.2 Baseline Drift:

Baseline drift as shown in Figure 1.3.2 is a sinusoidal signal having low frequency i.e. within 0.5 Hz to 0.5 Hz. Baseline drift occurs due to human respiration, temperature variance, electrode impedance and any bias occurring in the ECG machine. Due to its low frequency, baseline drift causes problem when analyzing low frequency components of ECG and can be removed by passing the corrupted ECG through a high pass filter with cut-off frequency 50 Hz.

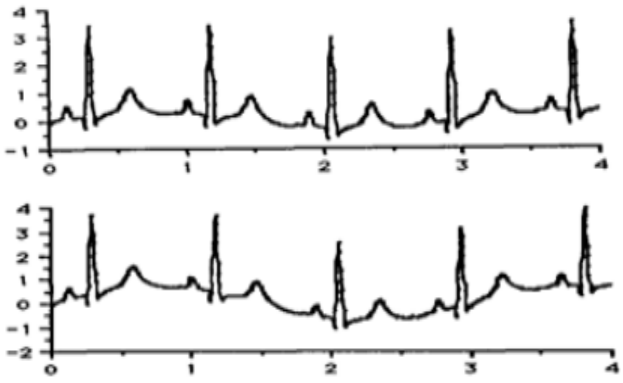

Figure 1.3.2: ECG signal with baseline drift

1.3.3 Electrode Contact Noise:

It occurs due to the loose contact of electrodes with the skin while recording ECG. Figure 1.3.3 shows ECG signal affected by electrode contact noise.

Figure 1.3.3: ECG corrupted with Electrode Contact Noise

1.3.4 Motion artifacts:

The reason for motion artifact shown in Figure 1.3.4 is a dissimilarity between the positions of electrode and heart or any disturbance in the transmission medium between the electrodes and heart. It causes a change in amplitude of ECG signal along with baseline drift.

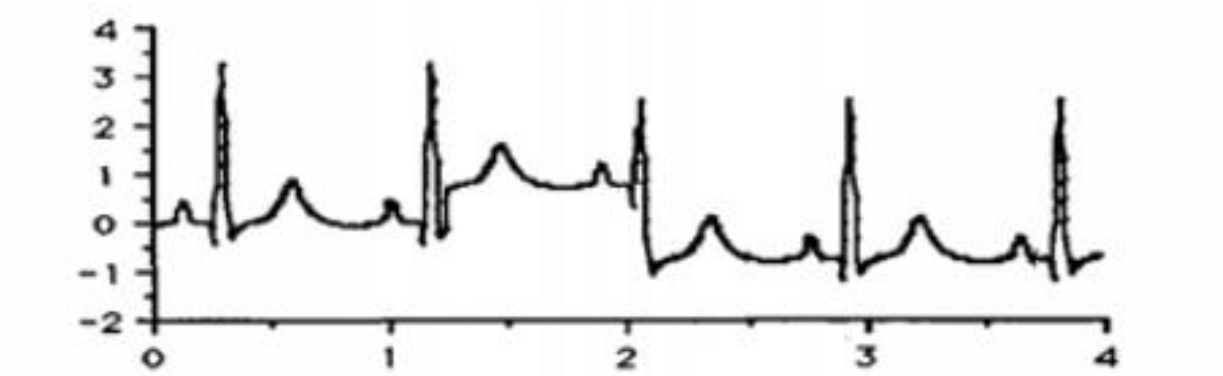

Figure 1.3.4: ECG affected due to Motion artifacts.

1.3.5 Electromyography (EMG) Interference:

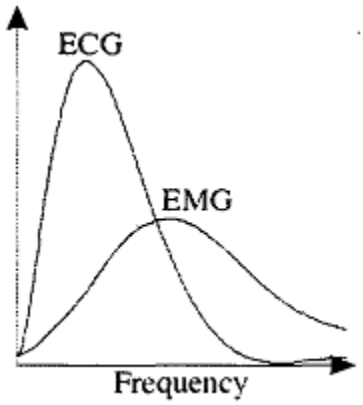

Figure 1.3.5: Frequency spectrum of ECG and EMG.

EMG signal is a random signal with a wide frequency spectrum overlapping with that of ECG signal as shown in Figure 1.3.5. It occurs due to the depolarization and re-polarization waves generated by other muscles besides heart resulting in EMG interference which is represented in Figure 1.3.6. The material of electrodes and muscle contraction decides the extent of EMG noise added.

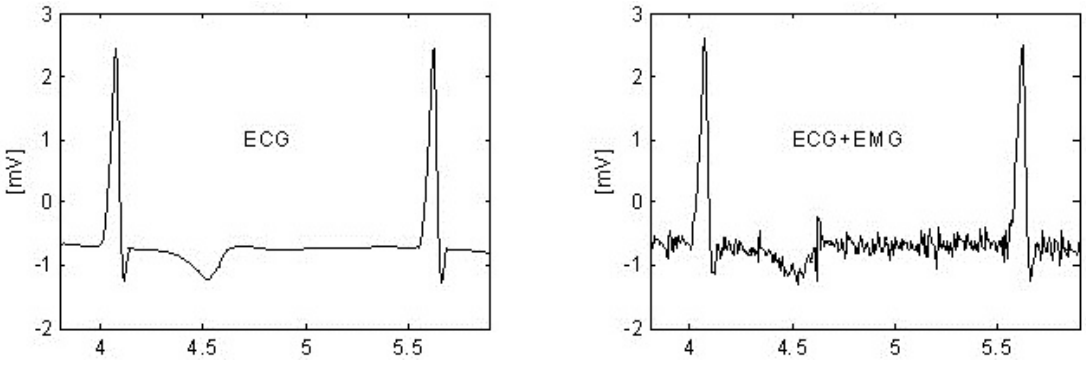

Figure 1.3.6: EMG noise present in ECG.

1.4 Problem Statement:

"Development of efficient solutions for PLI removal from ECG signal with low Computational Complexity and Mean Square Error"

As we will see in Literature Review that Notch Filter Approach is not feasible for removal of PLI with unknown frequency, and in ANC domain the computational complexity of SSRLS is very high. So an algorithm must be proposed with low computational complexity and efficient noise tracking.

CHAPTER 2: OVERVIEW OF EXISTING TECHNIQUES

In this chapter, a brief overview of all the existing techniques for removal of PLI noise from ECG signal has been given. This chapter includes both conference and journal publications for major techniques implemented for problem under consideration.

Electrocardiograph (ECG) is the graphical illustration of electrical signal generated by heart and is an important technique to identify various cardiovascular diseases [7]. ECG signal being corrupted by various types of noise makes it very difficult for the examiner to identify the disease. Types of noise that corrupt ECG signal are Power Line Interference (PLI), Electrode Contact Noise, Motion Artifacts, Electromyography (EMG) and instrumentation noise. PLI is the interference caused in power line cable attached to the ECG machine and is the main source of noise. It occurs through capacitive coupling and inductive coupling, generating high and low frequency noise respectively [8]. A realization of PLI is generated as

$$n_{PLI}[k] = \sigma \sin(\omega kT + \varphi) \tag{2.1}$$

Where σ is the amplitude of PLI, ω is frequency, T is sampling time and φ is phase. Magnitude of PLI must not be more than 0.5% of the peak-to-peak value of ECG signal for it to be detected with accuracy [9]. But for real time ECG signals, it has been observed that PLI noise does not confine to the 0.5% criteria. In literature, two major types of techniques implemented to remove PLI from ECG are named as Notch Filter and Adaptive Noise Canceller (ANC). Notch filter can remove PLI only if its frequency is known as a difference in PLI and notch frequency causes spectrum distortion [10]. Whereas, ANC can also eliminate PLI with unknown or variable frequency [11], [12].

2.1 Notch Filter Approach

IIR notch filters have small filter order as compared to their equivalent FIR notch filters. Due to this reason, IIR notch filters have been used in most of the cases. In order to have less effect

on the spectrum of ECG signal, the suppression band of notch filter must be kept narrow which leads to small ringing effect for impulse response [13]. Moreover, if the frequency of PLI and notch filter is not same, spectrum distortion occurs in ECG recovered ECG signal. Panda et al. [14] have used FIR notch filter to remove various types of noise from ECG signal. They applied various windows for this purpose and compared the techniques on basis of Peak SNR. Rectangular window is proved to be better than other applied windows due to its sharp transition from pass band to stop band and pulsation in stop band. Different types of notch filters are explained as follows:

2.1.1 Q-varying Notch Filter

For a notch filter, its bandwidth and attenuation level are proportional to each other. Whereas, in order to remove a particular frequency, notch filter must have narrow bandwidth at that frequency and high attenuation level. For this purpose, tunable notch filters can tune their notch frequency in a specific range [15]. Adaptive Notch Filters (ANF) have been designed using LMS [16],[17] and RLS[18] to have an adaptable notch frequency.

J. Piskorowski proposed Q-varying notch filter, as a type of ANF, which adjust its Q-factor to have a narrow bandwidth and higher attenuation level than basic notch filter [19] due to which it also reduces the transient response of filter.

2.1.2 Pole Radius Varying Notch Filter

For a noise of short duration, a larger initial distortion leads to lesser accuracy in PLI removal. So for such cases, transient response must be small. Whereas, narrow bandwidth notch filters have larger transient response. Based on pole/zero constrained filter, Li Tan et al [20] suggested a new IIR notch filter to remove PLI from noisy ECG signal. The transient response is reduced by adjusting the pole-placement radius of the filter.

2.2 Adaptive Noise Canceller

The concept of Adaptive Noise Canceller was first proposed by Widrow et al. [11] in 1975. For unknown but constant frequency, once the ANC converges to its true value, it starts working

like Notch Filter [11]-[12]. Due to these reasons, ANC is being used here for noise cancellation from ECG signal.

Adaptive Noise Cancellers are further divided into two categories as reported in literature named as ANC with reference input and without reference input.

2.3 ANC with Reference Input

Under the category of ANC with reference input, S. Z. Islam et. al [22] implemented Least Mean Square (LMS) and Recursive Least Square (RLS) algorithms to remove both AC and DC noises from ECG signal. Further Normalized Least Mean Square (NLMS) algorithm has been proved to remove PLI more efficiently than LMS by comparing the SNR for both [23]. Whereas, RLS has improved convergence and Mean Square Error (MSE) than NMLS but higher computational complexity [24].

2.3.1 Normalized Least Mean Square (NLMS) Algorithm

NLMS is an improved and normalized version of Least Mean Square (LMS) algorithm and exhibits faster convergence and better stability as compared to LMS. For larger input data, LMS encounters 'gradient noise amplification' problem. To resolve this issue, NLMS algorithm [25] is summarized as follows:

$$\widehat{w}_{NLMS}(0) = 0_{Mx1} \tag{2.2}$$

$$For\ k = \ 0,1,2,\ldots.$$

$$X_{NLMS}(k) = [x(k), x(k-1), \ldots, x(k-M+1)]^T \tag{2.3}$$

$$e_{NLMS}(k) = d_{NLMS}(k) - \ \widehat{w}_{NLMS}(k)^H X_{NLMS}(k) \tag{2.4}$$

$$\widehat{w}_{NLMS}(k+1) = \ \widehat{w}_{NLMS}(k) + \frac{\mu_{NLMS} e_{NLMS}(k) X_{NLMS}(k)}{\delta_{NLMS} + ||X_{NLMS}(k)^2||} \tag{2.5}$$

Table 2.3-1 shows the parameters used in NLMS algorithm.

Table 2.3-1: Parameter Description For NLMS Algorithm

Parameter	Description
$\widehat{w}_{NLMS}(k)$	Filter-tap weight vector in the kth iteration

M	Filter order
$e_{NLMS}(k)$	Estimated error for kth iteration
d_{NLMS}	Desired signal
μ_{NLMS}	Step size
δ_{NLMS}	Small number added for stability of NLMS

a. Recursive Least Square (RLS) Algorithm

RLS updates its gain vector $\vec{k}_{RLS}$ recursively and uses auto-correlation of input data. Hence, RLS has faster convergence rate than NLMS algorithm. The recursive parameters of RLS algorithm are updated as follows [25]:

$$\phi_{RLS}(0) = \delta_{RLS}^{-1} I, \qquad \widehat{w}_{RLS}(0) = 0_{Mx1} \tag{2.6}$$

$$For\ k = 0,1,2, \ldots.$$

$$X_{RLS}(k) = [x(k), x(k-1), \ldots, x(k-M+1)]^T \tag{2.7}$$

$$\phi_{RLS}(k) = \lambda_{RLS}^{-1}\phi_{RLS}(k-1) - \lambda_{RLS}^{-1} k_{RLS}(k) X_{RLS}^T(k)\phi_{RLS}(k-1) \tag{2.8}$$

$$\vec{k}_{RLS}(k) = \frac{\phi_{RLS}(k)X_{RLS}(k)}{\lambda_{RLS} + X_{RLS}^T(k)\phi_{RLS}(k)X_{RLS}(k)} \tag{2.9}$$

$$e_{RLS}(k) = d_{RLS}(k) - \widehat{w}_{RLS}(k)^H X_{RLS}(k) \tag{2.10}$$

Table 2.3-2 describes the parameters used in RLS algorithm.

Table 2.3-2: Parameter Description For RLS Algorithm

Parameter	Description
$\widehat{w}_{RLS}(k)$	Filter-tap weight vector in the kth iteration
M	Filter order
$\vec{k}_{RLS}(k)$	Gain vector for kth iteration
$e_{RLS}(k)$	Estimated error for kth iteration
d_{RLS}	Desired signal
λ_{RLS}	Forgetting factor (< 1)

δ_{RLS}	Regularization factor
ϕ_{RLS}	Inverse of Cross Correlation matrix

2.4 ANC without Reference Input

Various adaptive algorithms have been proposed which do not use reference input to estimate the required signal [26], [27], [28], [29] and [30]. Butt et al. [30] proposed State Space RLS (SSRLS) based ANC to remove 50 Hz PLI from ECG signal and compared its performance with conventional notch filter. **Table 2.4-2** compares the investigated algorithms, it is clear from this comparison that SSRLS is better than other algorithms in terms of convergence speed, mean square error and robustness at the cost of high computational complexity.

b. State Space Recursive Least Square Algorithm:

SSRLS [31] is a state space extension of RLS and exhibits faster convergence, better tracking capability but high computational complexity as compared to RLS algorithms. It recursively updates its cross-correlation matrix and observer gain as follows:

$$\bar{x}_{SSRLS}[k] = A_{SSRLS}[k-1]\hat{x}_{SSRLS}[k-1] \tag{2.11}$$

$$\bar{y}_{SSRLS}[k] = C_{SSRLS}[k]\bar{x}_{SSRLS}[k] \tag{2.12}$$

$$\varepsilon_{SSRLS}[k] = y_{SSRLS}[k] - \bar{y}_{SSRLS}[k] \tag{2.13}$$

$$\phi_{SSRLS}[k] = \lambda_{SSRLS}(A_{SSRLS}^{-T}\phi_{SSRLS}[k-1]A_{SSRLS}^{-1} + C_{SSRLS}^{T}C_{SSRLS}) \tag{2.14}$$

$$K_{SSRLS}[k] = \phi_{SSRLS}^{-1}[k]C_{SSRLS}^{T}[k] \tag{2.15}$$

$$\hat{x}_{SSRLS}[k] = \bar{x}_{SSRLS}[k] + K_{SSRLS}[k]\varepsilon_{SSRLS}[k] \tag{2.16}$$

$$\hat{y}_{SSRLS}[k] = C_{SSRLS}[k]\hat{x}_{SSRLS}[k] \tag{2.17}$$

$$e_{SSRLS}[k] = y_{SSRLS}[k] - \hat{y}_{SSRLS}[k] \tag{2.18}$$

Table 2.4-1 describes the parameters used in SSRLS algorithm.

Table 2.4-1: Parameter Description for SSRLS Algorithm

Parameter	Description

$\bar{x}_{SSRLS}[k]$	Predicted state
$\hat{x}_{SSRLS}[k]$	Estimated state
$\bar{y}_{SSRLS}[k]$	Predicted output
$\hat{y}_{SSRLS}[k]$	Estimated output
$\varepsilon_{SSRLS}[k]$	Prediction error
$e_{SSRLS}[k]$	Estimation error
$A_{SSRLS}[k]$	System matrix
$C_{SSRLS}[k]$	Output matrix
$\phi_{SSRLS}[k]$	Cross Correlation Matrix
$K_{SSRLS}[k]$	Observer gain

Other algorithms that have been reported in literature under the category of ANCs are

- Window Adaptive Canceller [33]
- Adaptive Sinusoidal Interference Canceller [34][35]
- Smoothing and Filtering [36]
- Lock-In Amplifier Algorithm [37]
- Median Filter [38]
- Empirical Mode Decomposition [39][40][41][42][43]
- Fusion of Algorithms [44]
- Parabolic Filters [45]

Furthermore, another adaptive algorithm is reported in literature named as State-Space Least Mean Square (SSLMS) algorithm [46] with convergence speed and MSE approaching to that of SSRLS but computational complexity much less than that of SSRLS algorithm. Motivated

by the performance of SSLMS algorithm in [46], in this paper we propose SSLMS algorithm based adaptive noise canceller. In order to further improve the performance of proposed ANC, a hybrid algorithm is proposed that combines the fast convergence speed and low MSE of SSRLS algorithm with the less computational complexity of SSLMS algorithm.

Table 2.4-2 compares the investigated algorithms, it is clear from this comparison that SSRLS is better than other algorithms in terms of convergence speed, mean square error and robustness at the cost of high computational complexity.

Table 2.4-2: Comparison of ANC Algorithms

Algorithm	**Convergence**	**Mean Square Error**	**Robustness**	**Computational Complexity**
NLMS	✓	✓	✓	$5n + 2 + 1$ [25]
RLS	✓✓	✓✓	✓✓	$4n^2 + O(n) + 1$ [25]
SSRLS	✓✓✓✓✓	✓✓✓✓✓	✓✓✓✓✓	$4n^3 + 4n^2 + 5n + 1$ [31]

CHAPTER 3: STATE SPACE LEAST MEAN SQUARE (SSLMS)

In this chapter, State Space Least Mean Square (SSLMS) algorithm, which is the main technique used for estimation and removal of PLI from ECG signal in this this, has been explained and derived step by step with the help of equations. Moreover, its different models have also been explained.

3.1 SSLMS Algorithm Overview

State-space least mean square (SSLMS) is a state-space version of LMS algorithm and makes use of linear state-space model based on the unknown environment. Hence, the system is not limited to the linear regression model, which was the case for LMS and RLS algorithms [25], and handles vector outputs due to its multiple input multiple output (MIMO) nature [46]. State estimator of SSLMS is derived based on the observations noise corrupting the measurements [47].

3.1.1 State Space Model

The output vector $y \in R^m$, m being the maximum number of outputs, is generated by an unforced linear time varying (LTI) discrete time system [47]

$$x_{SSLMS}[k+1] = A_{SSLMS}[k]x_{SSLMS}[k] \tag{3.1}$$
$$y_{SSLMS}[k+1] = C_{SSLMS}[k]x_{SSLMS}[k]$$

Where $x_{SSLMS} \in R^n$ is the state vector, n is the number of states, A_{SSLMS} being the system matrix and C_{SSLMS} is output matrix. Moreover, k is the number of sample under consideration. It is assumed that $m \leq n$ [47] and a system with $m > n$ can be simplified to assumed conditions without losing states information [48]. For every k^{th} sample, $C_{SSLMS}[k]$ is assumed to be full-rank and $(A_{SSLMS}[k], C_{SSLMS}[k])$ pair must be l-step observable [48]. Moreover, $A_{SSLMS}[k]$ is assumed to be invertible resulting in following properties

$$A_{SSLMS}^{-1}[k,j] = A_{SSLMS}[j,k], \qquad \forall\, j,k \tag{3.2}$$
$$A_{SSLMS}[k,i] = A_{SSLMS}[k,j]A_{SSLMS}[j,i], \qquad i \le j \le k$$
$$A_{SSLMS}[k+1,k] = A_{SSLMS}[k]$$

Where the state-transition matrix $A_{SSLMS}[k,j]$ for system is [48]

$$A_{SSLMS}[k,j] = \begin{cases} A_{SSLMS}[k-1]A_{SSLMS}[k-2] \dots A_{SSLMS}[j], & k > j \\ I, & k = j \end{cases} \tag{3.3}$$

3.1.2 State Space Estimator

Suppose that $y_{SSLMS}[k]$ starts appearing sample by sample with first at $k = 1$. The initial state at this stage is assumes to be $x_{SSLMS}[1] = x_o$ which is unknown at this instance. Making use of this initial assumption, SSLMS generates the estimated state $\hat{x}_{SSLMS}[k]$ making use of all the previous values from $y_{SSLMS}[1] \dots y_{SSLMS}[k]$.

Using (3.1) , predicted state and output at k can be computed using the state matrix, output matrix and estimated state at $k-1$.

$$\bar{x}_{SSLMS}[k] = A_{SSLMS}[k-1]\hat{x}_{SSLMS}[k-1] \tag{3.4}$$
$$\bar{y}_{SSLMS}[k] = C_{SSLMS}[k]\bar{x}_{SSLMS}[k] \tag{3.5}$$

The prediction error is now the difference in predicted output and observation y_{SSLMS}.

$$\varepsilon_{SSLMS}[k] = y_{SSLMS}[k] - \bar{y}_{SSLMS}[k] \tag{3.6}$$

Similarly, estimation error is calculated as

$$e_{SSLMS}[k] = y_{SSLMS}[k] - \hat{y}_{SSLMS}[k] \tag{3.7}$$

Where, $\hat{y}_{SSLMS}[k]$ is the estimated output at k

$$\hat{y}_{SSLMS}[k] = C_{SSLMS}[k]\hat{x}_{SSLMS}[k] \tag{3.8}$$

And $\hat{x}_{SSLMS}[k]$ is the estimated state at k. Relating equation (3.6) and (3.7),

$$e_{SSLMS}[k] = \varepsilon_{SSLMS}[k] - C_{SSLMS}[k]\delta[k] \tag{3.9}$$

$$\delta_{SSLMS}[k] = \hat{x}_{SSLMS}[k] - \bar{x}_{SSLMS}[k] \tag{3.10}$$

Assuming $C_{SSLMS}[k]$ to be full rank, we can chose $\hat{x}_{SSLMS}[k]$ such that $e_{SSLMS}[k] = 0$. Hence, rewriting (3.9) as

$$\varepsilon_{SSLMS}[k] = C_{SSLMS}[k]\delta_{SSLMS}[k] \tag{3.11}$$

In order to compute $\hat{x}_{SSLMS}[k]$, $\delta_{SSLMS}[k]$ can be written as [23]

$$\delta_{SSLMS}[k] = C^T_{SSLMS}[k]\varepsilon_{SSLMS}[k] \tag{3.12}$$

$$\hat{x}_{SSLMS}[k] = \bar{x}_{SSLMS}[k] + C^T_{SSLMS}[k]\varepsilon_{SSLMS}[k] \tag{3.13}$$

Based on this analysis, we write estimated states as

$$\hat{x}_{SSLMS}[k] = \bar{x}_{SSLMS}[k] + K_{SSLMS}[k]\varepsilon_{SSLMS}[k] \tag{3.14}$$

Where $K_{SSLMS}[k]$ is the observer gain at k^{th} sample and is defined as

$$K_{SSLMS}[k] = \mu_{SSLMS}G_{SSLMS}C^T_{SSLMS}[k] \tag{3.15}$$

Where μ_{SSLMS} controls the rate of convergence of SSLMS algorithm and is termed as step-size parameter. G_{SSLMS} is selected to make the pair $(A_{SSLMS}[k-1] - K_{SSLMS}[k]C_{SSLMS}[k]A_{SSLMS}[k-1], K_{SSLMS}[k])$ controllable to ensure valid estimation [46].

3.2 Steady State SSLMS

Using equation (3.4) and (3.6) in (3.14),

$$\hat{x}_{SSLMS}[k] = A_{SSLMS}[k-1]\hat{x}_{SSLMS}[k-1] + K_{SSLMS}[k](y_{SSLMS}[k] - C_{SSLMS}[k]A_{SSLMS}[k-1]\hat{x}_{SSLMS}[k-1]) \quad (3.16)$$

If $\lim_{k\to\infty} C_{SSLMS}[k] = C_{SSLMS}$ exists, then by (3.15), $\lim_{k\to\infty} K_{SSLMS}[k] = \mu_{SSLMS}G_{SSLMS}C_{SSLMS}^{T}$.

Moreover, if $\lim_{k\to\infty} A_{SSLMS}[k] = A_{SSLMS}$ also exists, then (3.16) can be written as

$$\hat{x}_{SSLMS}[k] = A_{SSLMS}\hat{x}_{SSLMS}[k-1] + K_{SSLMS}(y_{SSLMS}[k] - C_{SSLMS}A_{SSLMS}\hat{x}_{SSLMS}[k-1]) \quad (3.17)$$

As $\hat{x}_{SSLMS}[k]$ in (3.17) is an LTI system, its transfer function mapping from $y_{SSLMS}[k]$ to $\hat{x}_{SSLMS}[k]$ can be written as follows [47]

$$H(z) = z(zI - A_{SSLMS} + K_{SSLMS}C_{SSLMS}A_{SSLMS})^{-1}K_{SSLMS} \quad (3.18)$$

Steady state SSLMS is numerically efficient as compared to standard SSLMS algorithm.

3.3 State space models

For different types of unknown environments, SSLMS uses various models in order to track a signal. In [46], different state-space models for SSRLS have been proposed which can also be implemented for tracking using SSLMS algorithm. Most commonly used models are as follows:

3.3.1 Constant Model

Constant model for SSLMS is represented as

$$A_{SSLMS} = \mathrm{I} \quad (3.19)$$

$$C_{SSLMS} = \mathrm{I}$$

Using these parameter in (3.18), we get

$$H(z) = z(zI - I + K_{SSLMS}I)^{-1}K_{SSLMS} \tag{3.20}$$
$$H(z) = z(I - K_{SSLMS}) + K_{SSLMS}$$

3.3.2 Velocity Model

Velocity model is given as

$$A_{SSLMS} = \begin{bmatrix} 1 & T \\ 0 & 1 \end{bmatrix} \tag{3.21}$$
$$C_{SSLMS} = \begin{bmatrix} 1 & 0 \end{bmatrix}$$

Where T is the sampling time. Using these parameter in (3.18), and $G_{SSLMS} = \begin{bmatrix} 1 & 0 \\ 0 & 1 \end{bmatrix}$ in (3.15) we get

$$K_{SSLMS} = \begin{bmatrix} \mu \\ 0 \end{bmatrix} \tag{3.22}$$
$$H(z) = \frac{\begin{bmatrix} \mu z^2 - \mu z \\ 0 \end{bmatrix}}{z^2 - 2z + z(\mu - 1) + 1}$$
$$H(z) = \begin{bmatrix} \frac{\mu z(z-1)}{z^2 + z(\mu - 3) + 1} \\ 0 \end{bmatrix}$$

3.3.3 Acceleration Model

Acceleration model is demonstrated as follows

$$A_{SSLMS} = \begin{bmatrix} 1 & T & \frac{T^2}{2} \\ 0 & 1 & T \\ 0 & 0 & 1 \end{bmatrix} \quad (3.23)$$

$$C_{SSLMS} = [1 \quad 0 \quad 0]$$

Updating (3.18), and using $G_{SSLMS} = \begin{bmatrix} 1 & 0 \\ 0 & 1 \end{bmatrix}$ in (3.15) we get

$$K_{SSLMS} = \begin{bmatrix} \mu \\ 0 \\ 0 \end{bmatrix} \quad (3.24)$$

$$H(z) = \mathrm{z}\begin{bmatrix} z-1+\mu & T(\mu-1) & \frac{T^2}{2}(\mu-1) \\ 0 & z-1 & -T \\ 0 & 0 & z-1 \end{bmatrix}^{-1} \begin{bmatrix} \mu \\ 0 \\ 0 \end{bmatrix}$$

3.3.4 Sinusoidal Model

As PLI is assumed to sinusoidal in nature, a sinusoidal SSLMS model has been selected. The system and output matrix of model are as follows [46]

$$A_{SSLMS} = \begin{bmatrix} \cos(wT) & sin(wT) \\ -sin(wT) & cos(wT) \end{bmatrix} \quad (3.25)$$

$$C_{SSLMS} = [1 \quad 0]$$

Where w is the frequency in rad/sec and T is the sampling time. Moreover, for sinusoidal case, matrix G_{SSLMS} is not required [46]. Updating (3.18), we get

$$K_{SSLMS} = \begin{bmatrix} \mu \\ 0 \end{bmatrix} \quad (3.26)$$

$$H(z) = \frac{\begin{bmatrix} \mu(z - \cos(wT)) \\ -\mu sin(wT) \end{bmatrix}}{z^2 - z(\mu - z)\cos(wT) + (\mu - 1)\cos^2(wT) + \sin^2(wT) - \mu \sin(wT)}$$

CHAPTER 4: TRACKING AND REMOVAL OF IMPULSIVE PLI FROM ECG SIGNAL

In this chapter, the performance of the proposed SSLMS based noise canceller is compared with the reported algorithms for ECG signal corrupted with impulsive noise using MATLAB version R2012a.

4.1 Impulsive Noise Generation

The impulsive noise is generated using the method reported in [52]. Table 4.1-1 shows the parameters which are used to generate impulsive noise.

Table 4.1-1: Parameter set for impulsive noise generation

Parameter	Symbol	Description
Total Time	T	100
Sampling Frequency	f	10
Average Time between samples	B	1
Mean of Additive Gaussian Noise	μ_n	0.1
Standard Deviation of Gaussian Noise	σ_n	0.5
Mean of Log Amplitude	A	10 dB
Standard Deviation of Log Amplitude	B	5 dB

The impulsive noise generated using the above mentioned parameters, is shown in **Figure 4.1.1**(a). **Figure 4.1.1**(b) shows pure as well as noisy ECG signal taken from MIT-BIH database [49] with peak to peak amplitude normalized at 1 and sampling frequency 360 Hz.

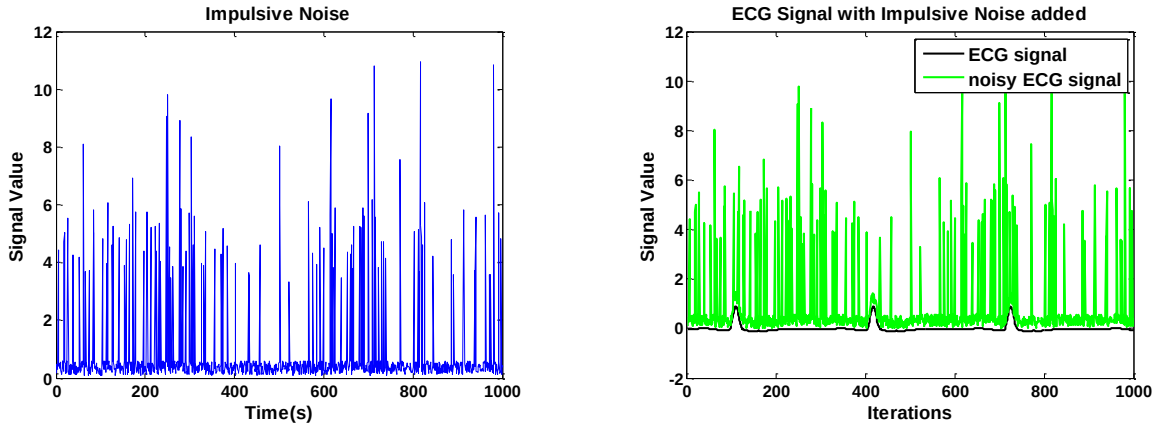

(a) (b)

Figure 4.1.1: (a) Impulsive Noise (b) Pure and Noisy ECG signal.

4.2 Impulsive Noise Reduction using previous techniques

In this section, impulsive noise is estimated and removed using NLMS [25], RLS [25] and SSRLS [32] algorithms

Table 4.2-1: Parameter value for NLMS, RLS and SSLMS

Parameter	Value
M	3
μ_{NLMS}	0.001
λ_{RLS}	0.9
λ_{SSRLS}	0.01

The parameters for all the underlying algorithms are mentioned in **Table 4.2-1**. It is proved from simulation results that higher order models can better track sharp transitions in the reference

signal but at the expense of increased computational complexity. For tracking impulsive noise we have used third order model i.e. an acceleration model. For SSLMS matrix G is selected as in [46]

$$G = \begin{bmatrix} 1 & 0 & 0 \\ 0.3 & 0 & 0 \\ 0.3 & 0 & 0 \end{bmatrix}$$

Figure 4.2.1 shows the comparison of output of the investigated adaptive filters with the original ECG signal. The result shows that best noise reduction from noisy ECG signal is achieved by the SSLMS algorithm.

Figure 4.2.1 (a) shows that RLS filter has better performance than that of NLMS filter. In Figure 4.2.1 (b) and (c) it is observed that SSRLS algorithm is reducing impulsive noise from the noisy ECG signal more efficiently than NLMS and RLS algorithms. Moreover, it is clearly indicated that SSLMS algorithm has reduced all the high peaks of noisy ECG signal.

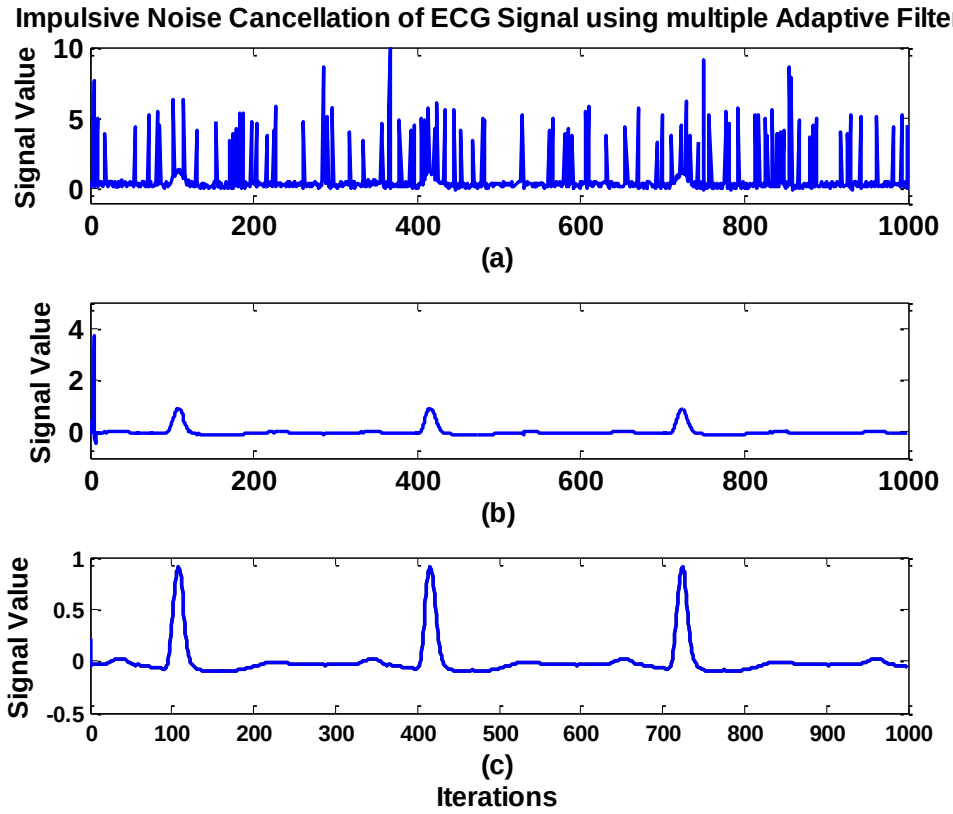

Figure 4.2.1: Comparison of ECG signal recovered using (a) NLMS (b) RLS (c) SSLMS

Figure 4.2.2 represents the MSE in dB, which also explains the results shown in Figure 4.2.1.

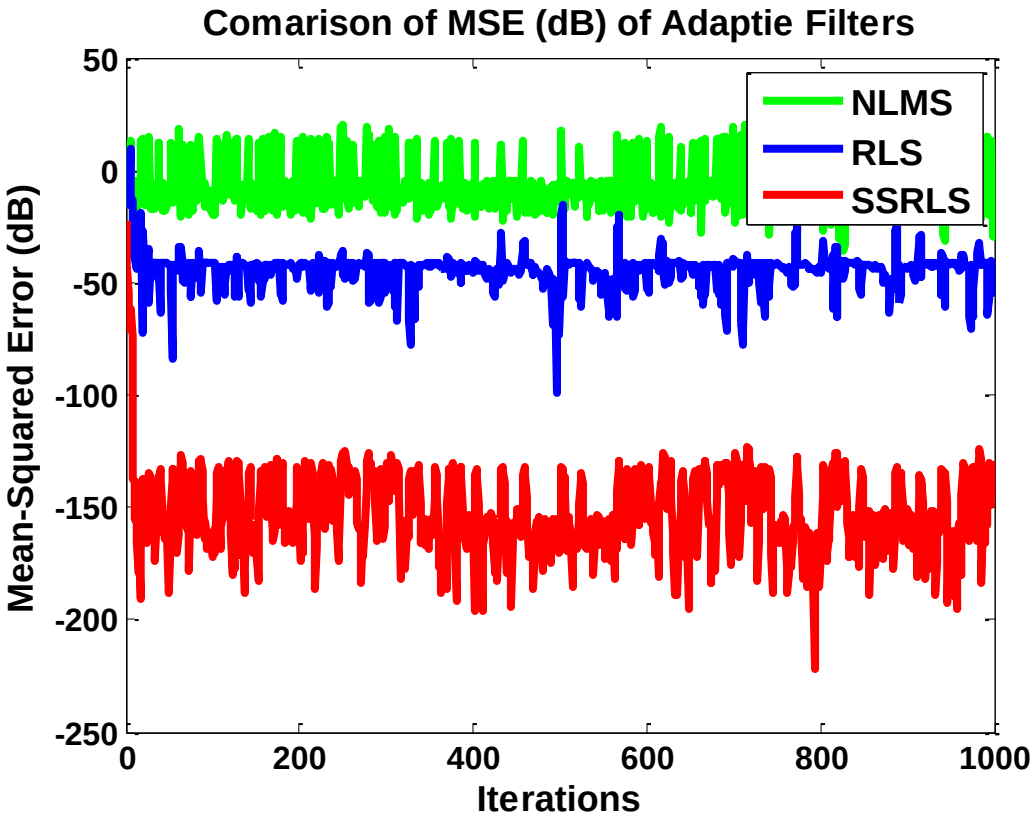

Figure 4.2.2: Comparison of MSE (dB) of NLMS, RLS and SSRLS

4.3 Impulsive Noise reduction using SSLMS algorithm

In this section, SSLMS is implemented to remove impulsive noise, with $\mu_{SSLMS} = 0.999$, from ECG and simultaneously the results are compared with those of SSRLS algorithm.

Figure 4.3.1 shows that from the plots of estimated ECG signal, both SSLMS and SSRLS algorithms are estimating the unknown ECG signal efficiently. Whereas, going further into the details of estimation, we can see that in **Figure 4.3.2** that there is a minor difference between their MSE which shows that the estimation of two algorithms is approximately same.

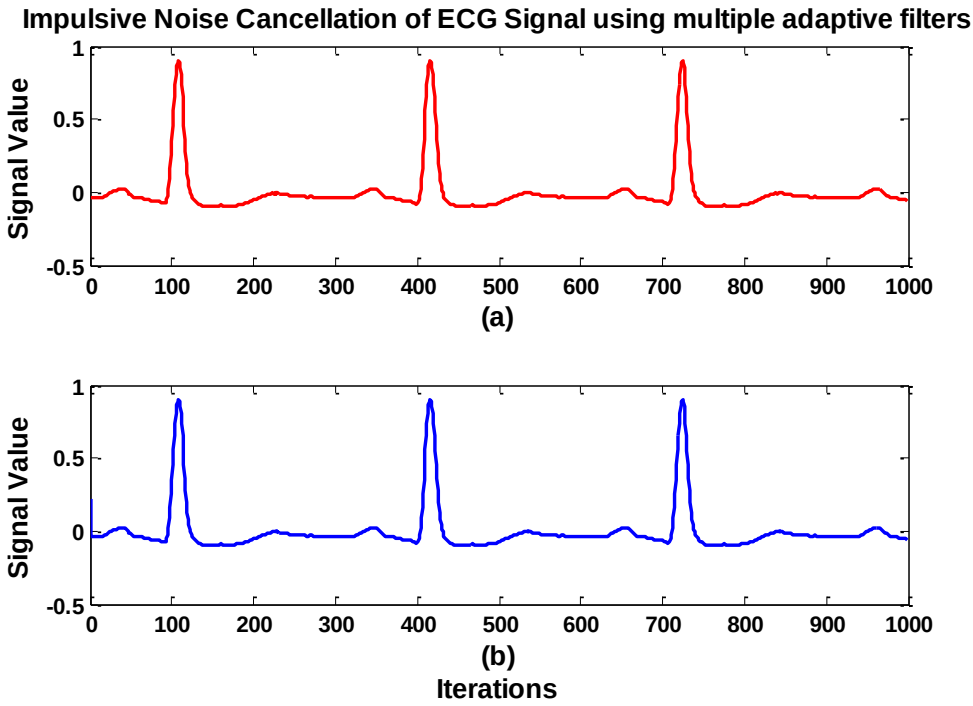

Figure 4.3.1: Comparison of ECG signal recovered using (a) SSLMS (b) SSRLS

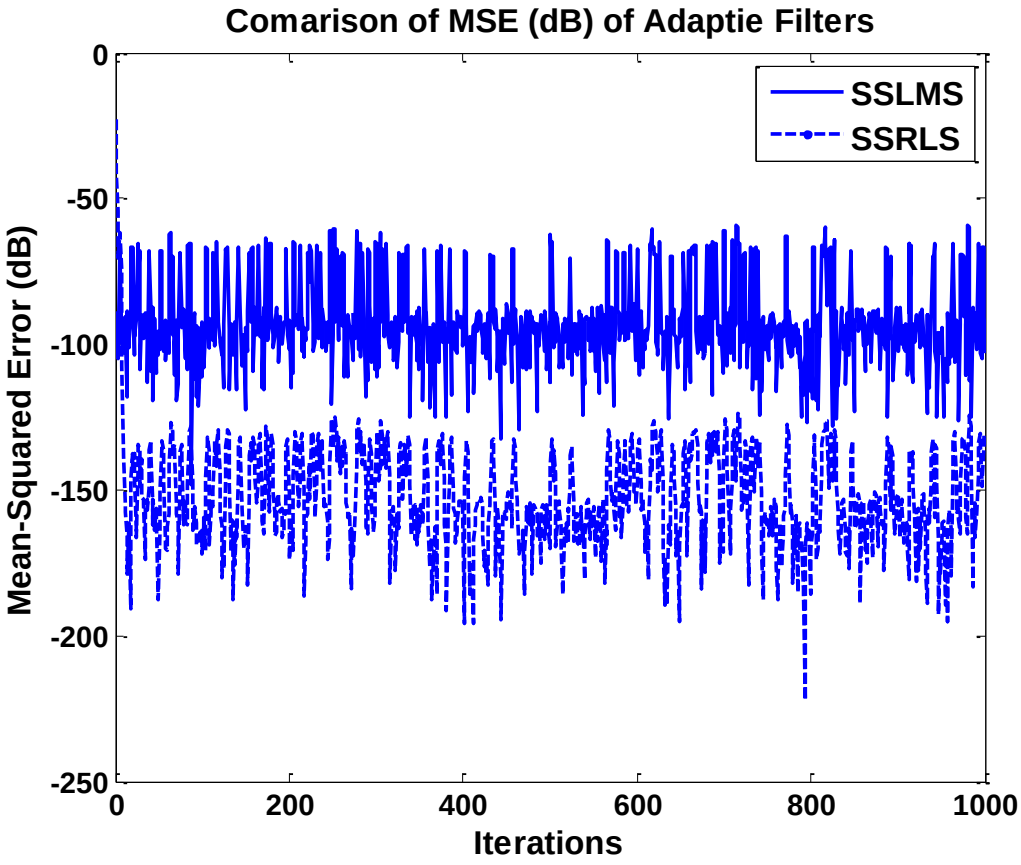

Figure 4.3.2: Comparison of MSE (dB) of NLMS, RLS and SSRLS

4.4 Computational Complexity

The computational complexities of the investigated algorithms are mentioned in Table 5.3-1.

Table 4.4-1: Computational Complexities of Adaptive Algorithms [32]

Algorithm	**Multiplication and Addition**	**Division**
SSLMS	$4n^2 + 2n$	-
SSRLS	$4n^3 + 4n^2 + 5n + 1$	-

Algorithm	Multiplication and Addition	Division
RLS	$4n^2 + O(n)$	1
NLMS	$5n + 2$	1

4.5 Conclusion

The computational complexity of SSLMS algorithm is greater than NLMS and RLS algorithm but it outperforms NLMS and RLS algorithms in terms of low MSE and excellent tracking capability. Whereas, it has high MSE than low computational complexity than that of SSRLS but it can be seen from section 4.4 that it has computational complexity much better than SSRLS which makes it to be overall better than other algorithms.

CHAPTER 5: TRACKING AND REMOVAL OF SINUSOIDAL PLI WITH KNOWN FREQUENCY FROM ECG SIGNAL

This chapter explains the tracking of sinusoidal component of PLI having known frequency from ECG signal using SSLMS Algorithm. The results are generated using MATLAB R2012a. The comparison of SSLMS is done with SSRLS algorithm with respect to convergence, mean square error and computational complexity.

5.1 Standard ECG Signal

Standard ECG Signal is generated using MIT-BIH database [49] with peak-to-peak amplitude normalized at 1 and sampling frequency of 360 Hz as shown in Figure 5.1.1 (a). This database has been frequently used by the community doing medical research. Figure 5.1.1 (b) shows the frequency response of pure ECG signal and it can be seen that there is no component of 50 Hz in pure ECG signal.

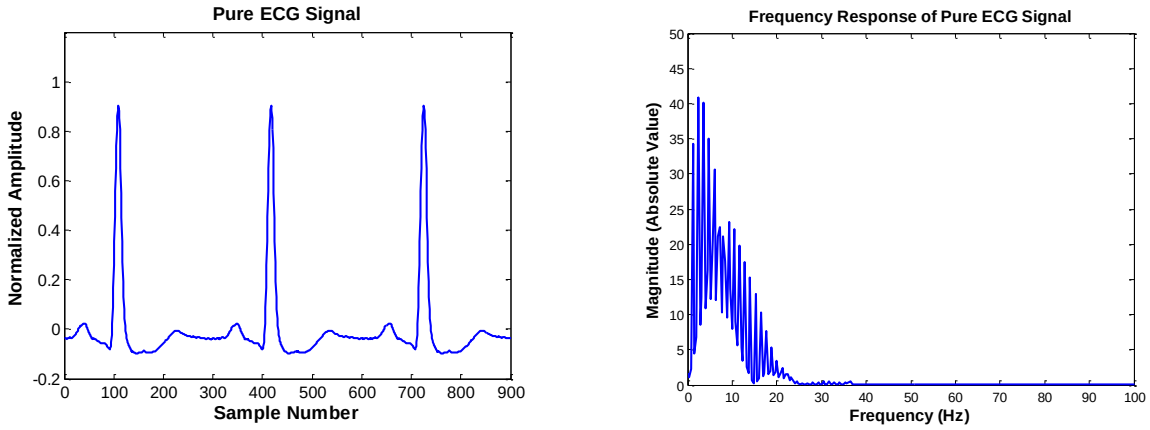

(a) (b)

Figure 5.1.1: Pure ECG Signal using MIT-BIH database (a) Amplitude (b) Frequency response

Table 5.1-1: Parameters to generate Sinusoidal PLI

Parameter	Symbol	Value
Amplitude	σ_s	0.1

Frequency	ω	$2\pi \times 50$
Phase	φ	0
Sampling Time	T_s	$\frac{1}{360} = 0.028$

Figure 5.1.2 shows the pure ECG signal corrupted by PLI generated using parameters in Table 5.1-1 along with its frequency response. As we can see in Figure 5.1.2 (b) that there is a peak at 50 Hz showing the addition of 50 Hz PLI to ECG signal.

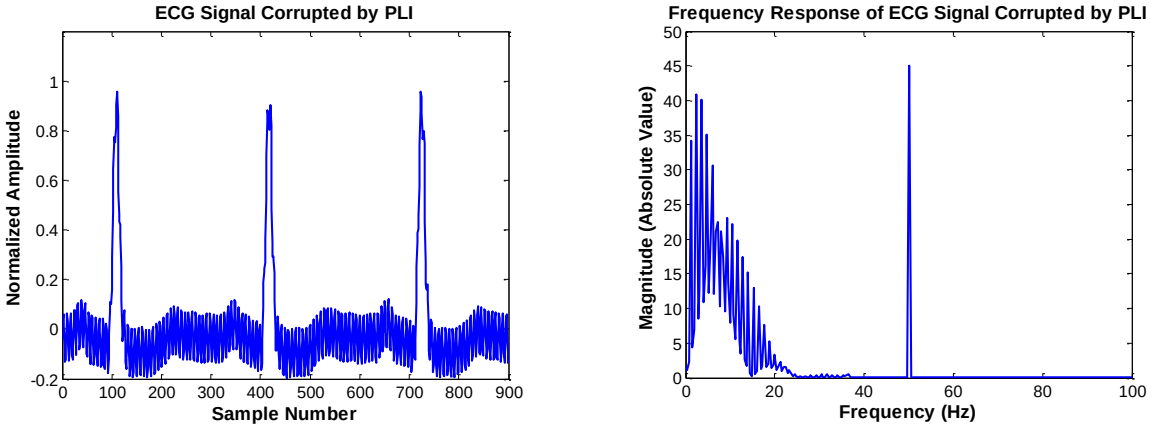

(a) (b)

Figure 5.1.2: PLI Corrupted ECG Signal (a) Amplitude (b) Frequency response

5.2 Implementation of SSLMS Algorithm

Figure 5.2.1 shows the mechanism used to remove PLI with known frequency. SSLMS algorithm estimates the PLI using the following state space model

$$A_{SSLMS} = \begin{bmatrix} \cos(2\pi \times 50 \times 0.028) & \sin(2\pi \times 50 \times 0.028) \\ -\sin(2\pi \times 50 \times 0.028) & \cos(2\pi \times 50 \times 0.028) \end{bmatrix} \quad (5.1)$$

$$C_{SSLMS} = [1 \quad 0]$$

The output of SSLMS Filter is the estimated PLI (i.e. $\hat{y}_{SSLMS}[k] = n'_{SSLMS}[k]$), which is subtracted from noisy ECG signal to produce clean ECG signal at the output of noise canceller.

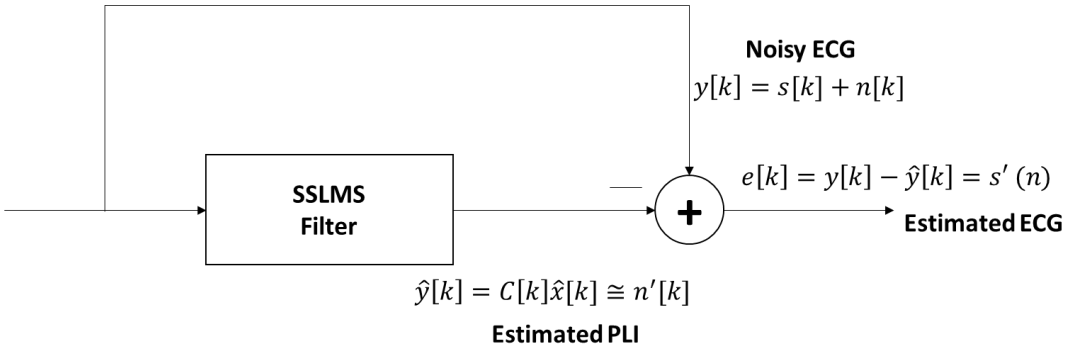

Figure 5.2.1: Block Diagram for Cancelation of PLI with known frequency

SSLMS is initialized with $x_o = \begin{bmatrix} 0 \\ 0 \end{bmatrix}$ and $\mu_{SSLMS} = 0.05$. Figure 5.2.2 shows the output of SSLMS algorithm. It can be seen from Figure 5.2.2 (b) that along with other frequencies having minimal presence, the signal with 50 Hz has also been tracked by SSLMS algorithm. Subtracting the estimated PLI signal from corrupted ECG gives the desired ECG signal.

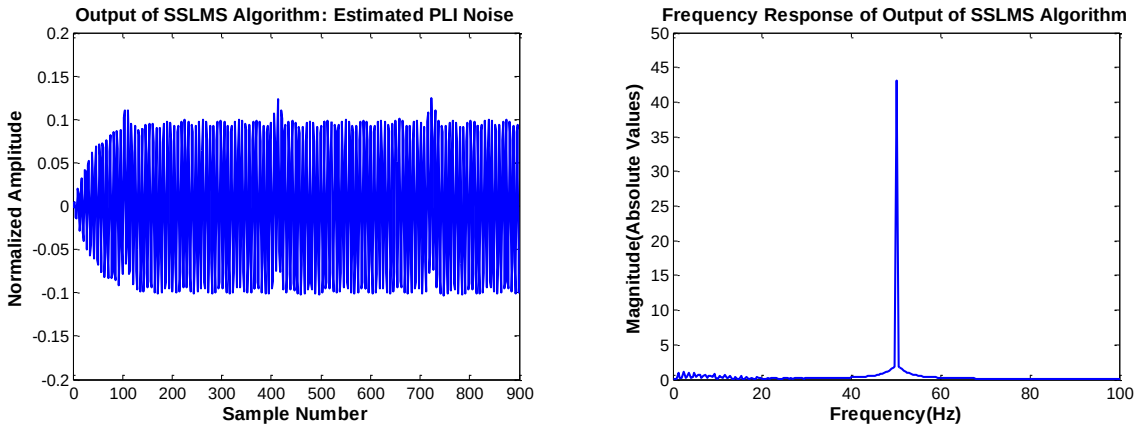

(a) (b)

Figure 5.2.2: Output of SSLMS Algorithm with $\mu_{SSLMS} = 0.05$ (a) Amplitude (b) Frequency response

As we can see in Figure 5.2.3 (a) that initially it takes some time for the canceller to track ECG and with further iterations, the tracking is improved. Similarly the frequency response in Figure 5.2.3 (b) is similar to that in Figure 5.1.1 (b) showing that SSLMS based ANC removes the noise effectively.

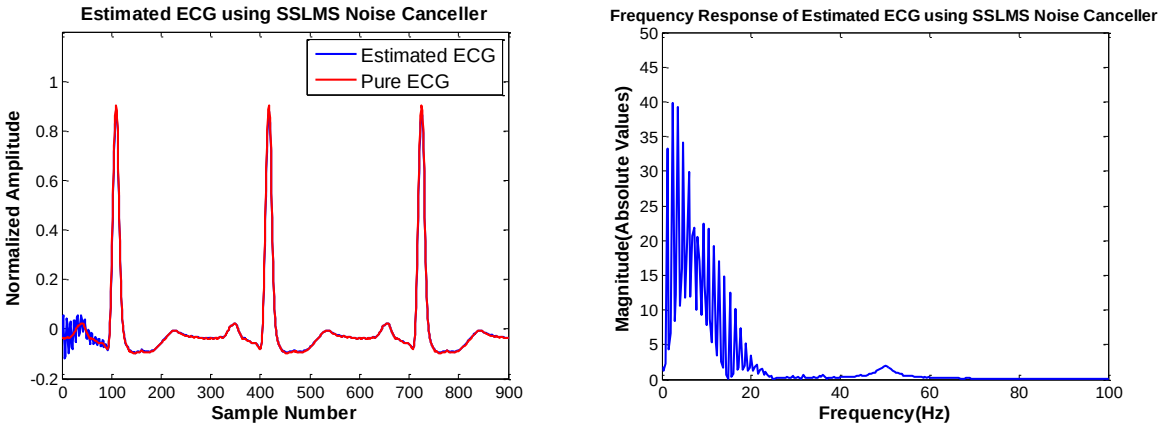

(a) (b)

Figure 5.2.3: Estimated ECG signal using SSLMS based ANC with $\mu_{SSLMS} = 0.05$ (a) Amplitude (b) Frequency response

Moreover, it can be observed in **Figure 5.2.4** that after SSLMS converges, there is very small error at the stages where QRS complex peaks have occurred in ECG signal. These results demonstrate that SSLMS based ANC removes PLI efficiently from ECG signal. Further results will demonstrate its comparison with SSRLS algorithm with respect to noise removal efficiency and computational complexity.

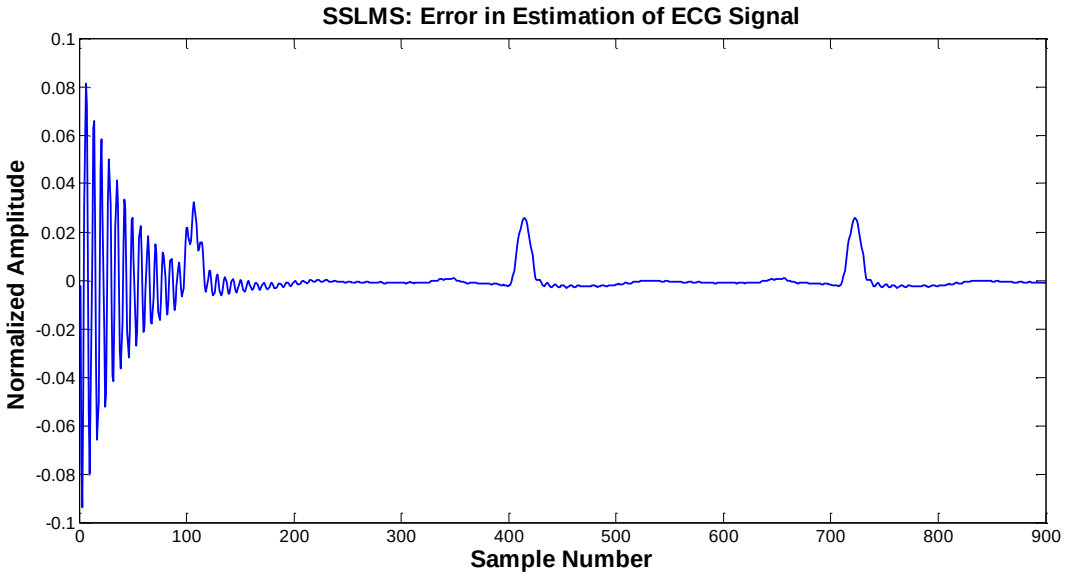

Figure 5.2.4: Estimation Error of SSLMS based ANC using $\mu_{SSLMS} = 0.05$

5.3 Comparison with SSRLS Algorithm

Comparison between SSLMS based ANC using step-size $\mu_{SSLMS} = 0.05$ and SSRLS based ANC using forgetting factor $\lambda_{SSRLS} = 0.99$ based upon error and MATLAB elapsed time has been made in this section.

Error signal plot of SSRLS in **Figure 5.3.1** shows convergence and error at later samples. The error peaks occur due to QRS complex peaks, which give a little disturbance in the estimation of PLI from noisy ECG. Comparing it with estimation error using SSLMS as shown in **Figure 5.2.4**, it can be seen that SSLMS has slower convergence than SSRLS.

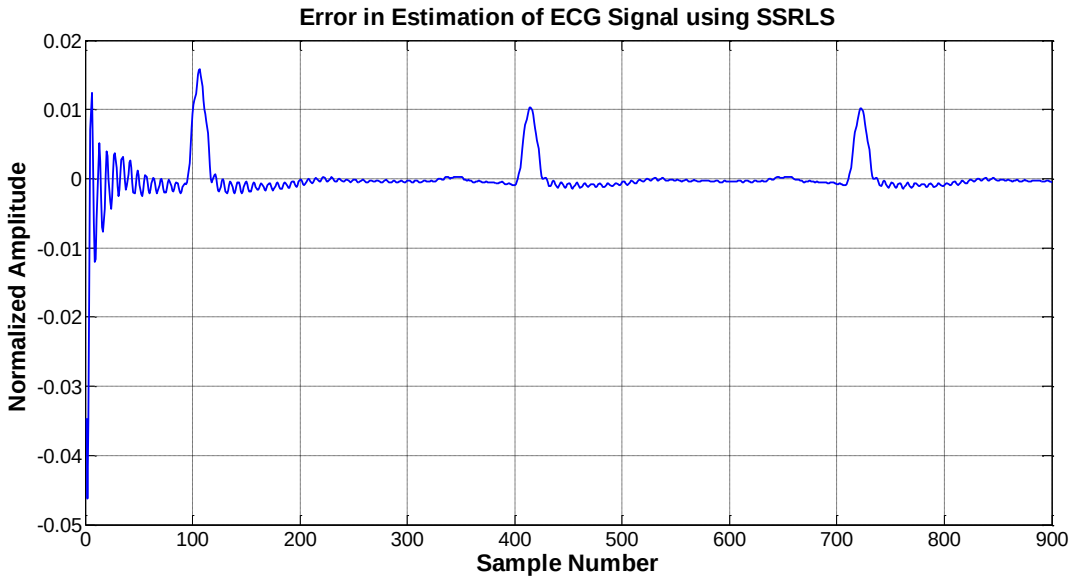

Figure 5.3.1: ECG Estimation error using SSRLS ($\lambda_{SSRLS} = 0.99$)

Moreover, comparing the mean square error (MSE) plots of both algorithms in **Figure 5.3.2**, it can be seen that after convergence, there is a difference of approximately 10dB in the error estimation of both algorithms.

Hence, the performance of SSLMS degrades than that of SSRLS with a small ratio. However, comparing the elapsed time for MATLAB simulations in Table 5.3-1, it is clear that SSLMS is sixty times faster than that of SSRLS algorithm proving SSLMS to be overall better than SSRLS algorithm.

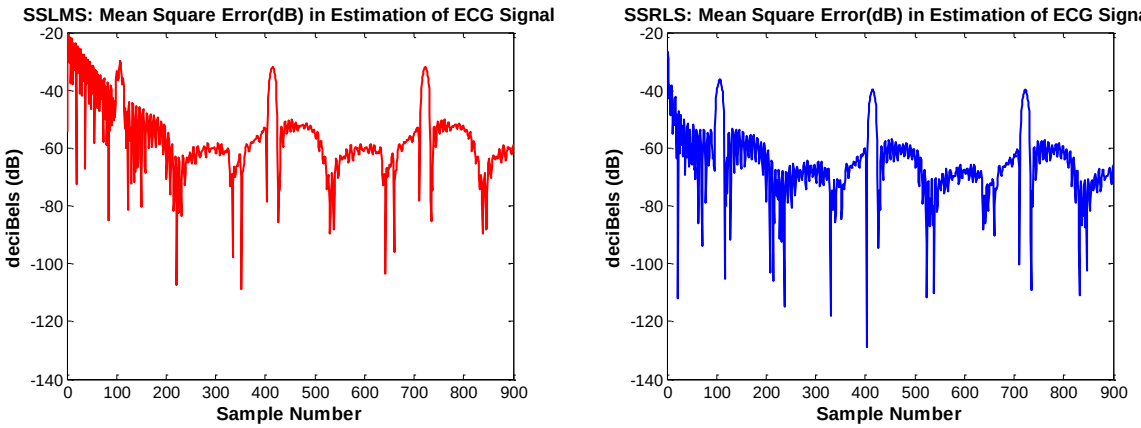

(a) (b)

Figure 5.3.2: MSE using (a) SSLMS ($\mu_{SSLMS} = 0.05$) (b) SSRLS ($\lambda_{SSRLS} = 0.99$) algorithm

Table 5.3-1: Computational complexity and elapsed time for MATLAB simulations of SSLMS and SSRLS algorithms

Parameter	**SSLMS**	**SSRLS**
Computational Complexity	$4n^2 + 2n$ [32]	$4n^3 + 4n^2 + 5n + 1$ [32]
Elapsed Time	0.013704 seconds	0.849161 seconds

5.4 Conclusion

Concluding this part of thesis, it is clear from the results shown in above figures that although SSRLS algorithm has better estimation performance than that of SSLMS algorithm, but it can be seen from the comparison between Figure 5.3.2 and Table 5.3-1 that such small reduction in MSE is subsided by exceptionally high computational complexity. Hence, SSLMS is better than SSRLS algorithm on overall basis.

CHAPTER 6: TRACKING AND REMOVAL OF SINUSOIDAL PLI WITH UNKNOWN FREQUENCY FROM ECG SIGNAL

This chapter explains the tracking of sinusoidal component of PLI having unknown frequency from ECG signal using SSLMS Algorithm. The results are generated using MATLAB R2012a. The parameter for tracking are analyzed for their performance. The comparison of SSLMS is done with SSRLS algorithm with respect to convergence, mean square error and computational complexity.

6.1 SSLMS based Adaptive Tracking scheme

It is very rare to have PLI with known frequency. So in order to track a sinusoidal with unknown frequency, an adaptive tracking scheme has been proposed using SSRLS algorithm [50].

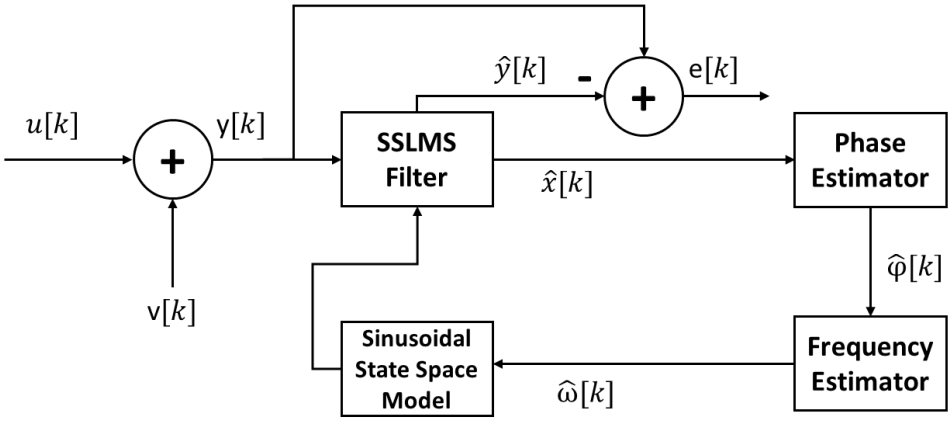

Figure 6.1.1 Adaptive tracking of Sinusoidal Signal using SSLMS Algorithm

A modified block diagram of adaptive tracking system integrated with SSLMS based noise canceller has been shown in Figure 6.1.1. ECG signal generated using MIT-BIH database [49] as shown in **Figure 5.1.1** is represented by $u[k]$. $v_{PLI}[k]$ is the PLI signal having unknown frequency as is mathematically formulated as

$$v_{PLI}[k] = \sigma_s \sin(\omega k T + \varphi) \tag{6.1}$$

Where $\sigma_s =$ amplitude, $\omega =$ frequency, $\varphi =$ phase and $T =$ sampling time of the unknown PLI signal. State space model for this LTI model is

$$A_{SSLMS}[k] = \begin{bmatrix} \cos(\omega[k]T) & \sin(\omega[k]T) \\ -\sin(\omega[k]T) & \cos(\omega[k]T) \end{bmatrix} \tag{6.2}$$

$$C_{SSLMS} = [1 \quad 0]$$

As the purpose of this scheme is to track the unknown parameter, the state transition matrix is a time-varying parameter. The states $x_{SSLMS}[k]$ and coefficients are related as

$$x_{SSLMS}[k] = A_{SSLMS}^{k} \begin{bmatrix} a \\ b \end{bmatrix} \tag{6.3}$$

Where $a = \sigma_s \cos(\varphi)$and $\mathrm{b} = \sigma_s \sin(\varphi)$ are the initial conditions. Rearranging above equation

$$\begin{bmatrix} \hat{a} \\ \hat{b} \end{bmatrix} = A_{SSLMS}^{-k} \hat{x}_{SSLMS}[k] \tag{6.4}$$

The inverse of A_{SSLMS} can be calculated using (3.2) and (3.3) whereas $\hat{x}[k]$ can be updated recursively using (3.14). Using $\hat{a}$ and $\hat{b}$, we can track the phase using the following relation

$$\hat{\varphi}_{SSLMS}[k] = \tan^{-1}\left(\frac{\hat{b}}{\hat{a}}\right) \tag{6.5}$$

As the phase is being updated recursively, any discontinuities in its tracking can be handled by unwrapping its value [51]. Further, the frequency of unknown sinusoid can be updated using a stochastic gradient like equation as follows

$$\hat{\omega}_{SSLMS}[k] = \hat{\omega}_{SSLMS}[k-1] + \eta(\hat{\varphi}_{SSLMS}[k] - \hat{\varphi}_{SSLMS}[k-1]) \tag{6.6}$$

Where η is the step-size parameter for adaptive tracking system. The difference between the estimated values of phase can also be computed using a discrete filter with transfer function.

$$H(z) = z^{-2}(z-1) \tag{6.7}$$

Using the updated frequency, the state space model can be updated as follows

$$\mathrm{A_{SSLMS}}[k] = \begin{bmatrix} \cos(\hat{\omega}(k)T) & \sin(\hat{\omega}(k)T) \\ -\sin(\hat{\omega}(k)T) & \cos(\hat{\omega}(k)T) \end{bmatrix} \tag{6.8}$$

$$\mathrm{C_{SSLMS}}[k] = [1 \quad 0]$$

The summarized block diagram is shown in **Figure 6.1.2** along with the computations at each step of tracking.

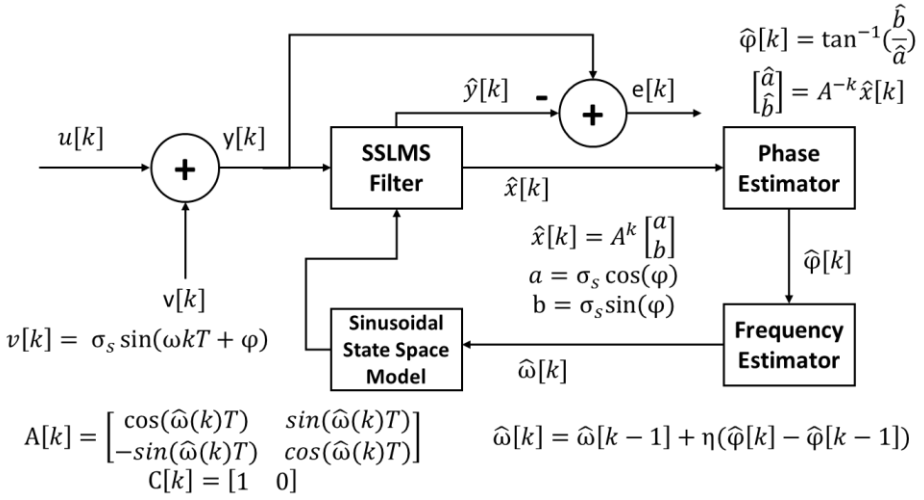

Figure 6.1.2: Adaptive tracking of Sinusoidal Signal using SSLMS Algorithm with equations

The unknown sinusoidal signal $v_{PLI}[k]$ has been generated using the following parameters

Table 6.1-1: Parameters to generate Sinusoidal Noise of frequency 49.5

Parameter	**Symbol**	**Value**
Amplitude	σ_s	0.1

Frequency	ω	$2\pi \times 49.5$
Phase	φ	$\frac{\pi}{4}$
Sampling Time	T_s	$\frac{1}{360} = 0.028$

Figure 6.1.3 shows pure ECG signal $u[k]$ from MIT-BIH database [49]. Adding $v_{PLI}[k]$ generated using parameters shown in Table 6.1-1, we get PLI corrupted signal as mentioned in Figure 6.1.4.

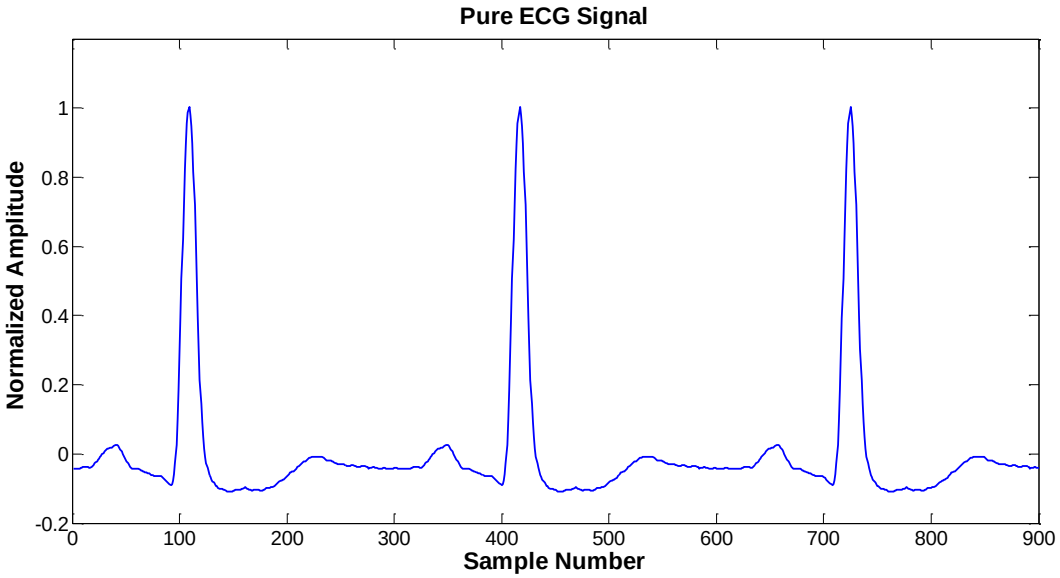

Figure 6.1.3: Pure ECG Signal using MIT-BIH database

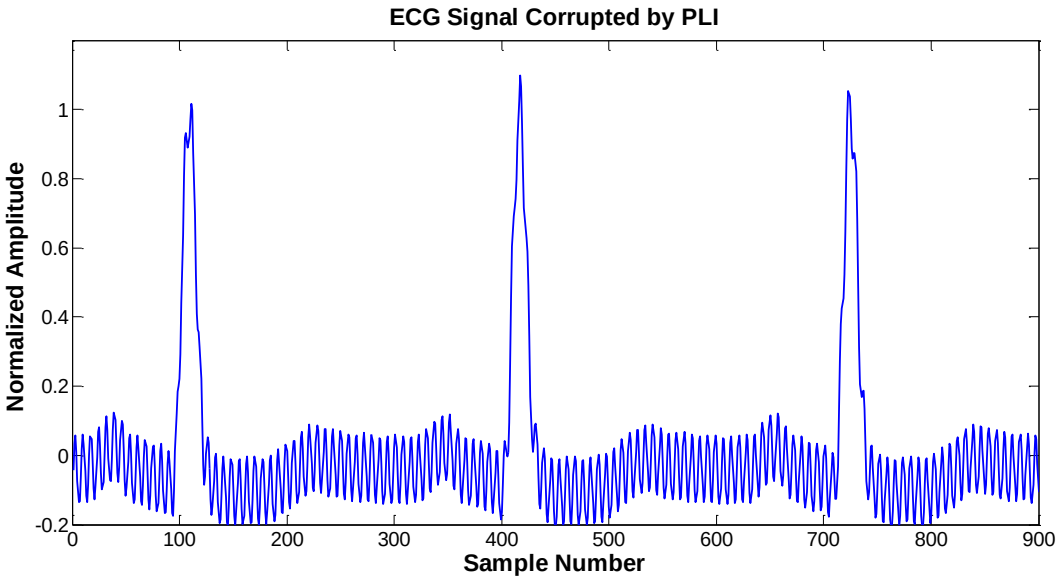

Figure 6.1.4: 49.5 Hz Sinusoidal PLI corrupted ECG Signal

6.2 Simulation Results

The adaptive frequency system has been initialized as $\omega_o = 2\pi \times 50$ and $\varphi_o = 0$. In order to analyze the tracking ability of SSLMS based ANC, the value of frequency and phase are different from those of PLI. SSLMS algorithm is initialized as $\mu_{SSLMS} = 0.005$ and the value of η is 0.02. Further discussion shows the simulation results for tracking the frequency and estimation PLI noise and recovery of noise-free ECG signal. It can be shown in Figure 6.2.1 that initially the frequency is 50 Hz and slowly it tracks down to 49.5 Hz. Once the frequency reaches its true value, it stays constant.

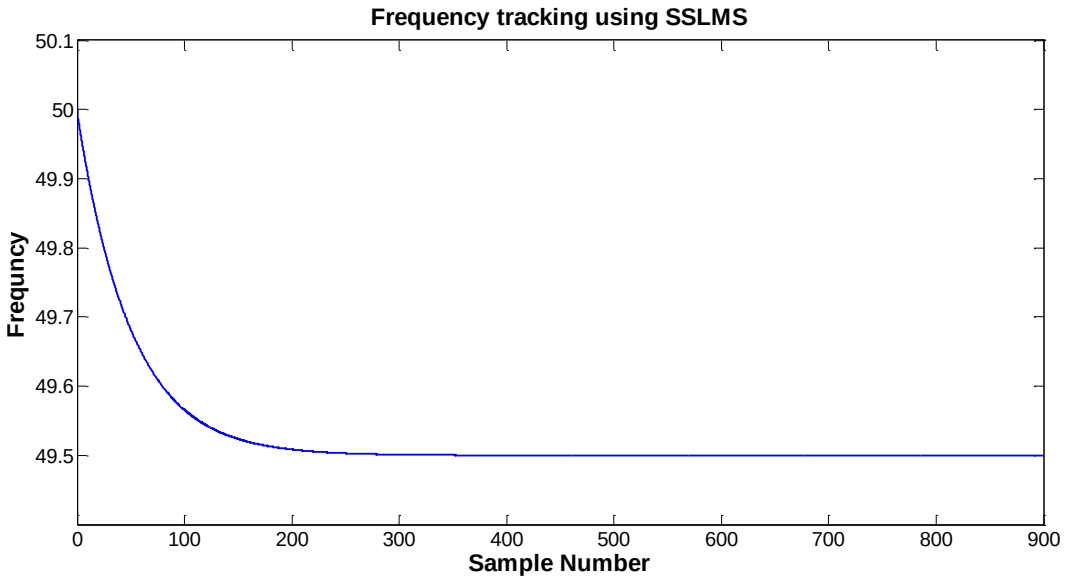

Figure 6.2.1: Frequency tracking of PLI using $\mu_{SSLMS} = 0.005$ and η = 0.02

Figure 6.2.2 shows that as the frequency converges, estimated PLI signal reaches its correct amplitude i.e. 0.1.

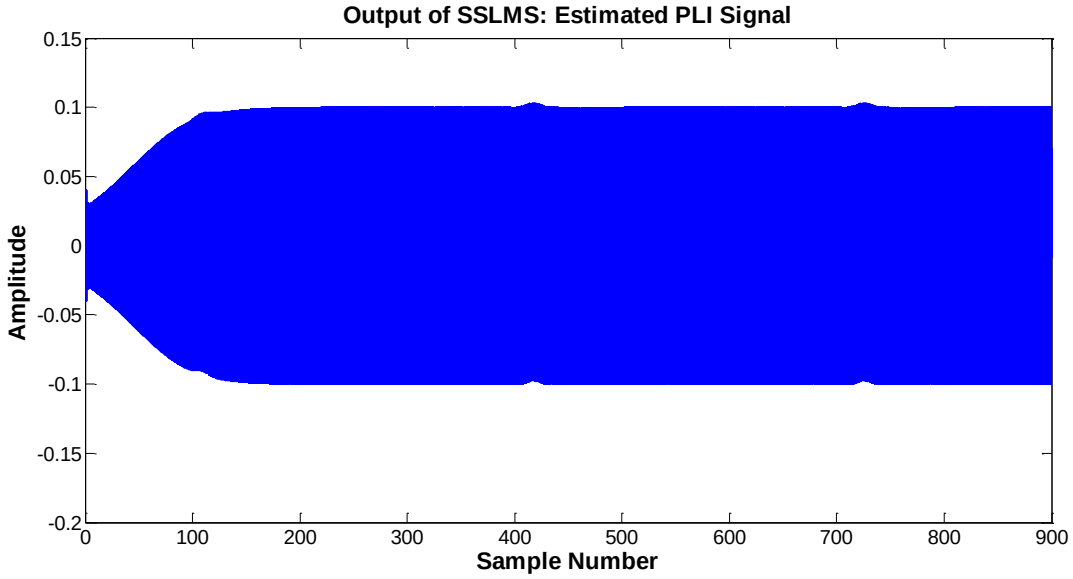

Figure 6.2.2: Estimated PLI of 49.5 Hz using $\mu_{SSLMS} = 0.005$ and η = 0.02

Moreover, as shown in Figure 6.2.3 and Figure 6.2.4, the estimated ECG is being tracked efficiently and the error signal reduces to zero as the system converges to correct frequency value. It must be seen that initially the amplitude of error is close to that of PLI signal. But as the estimated PLI converges, the error reduces to zero.

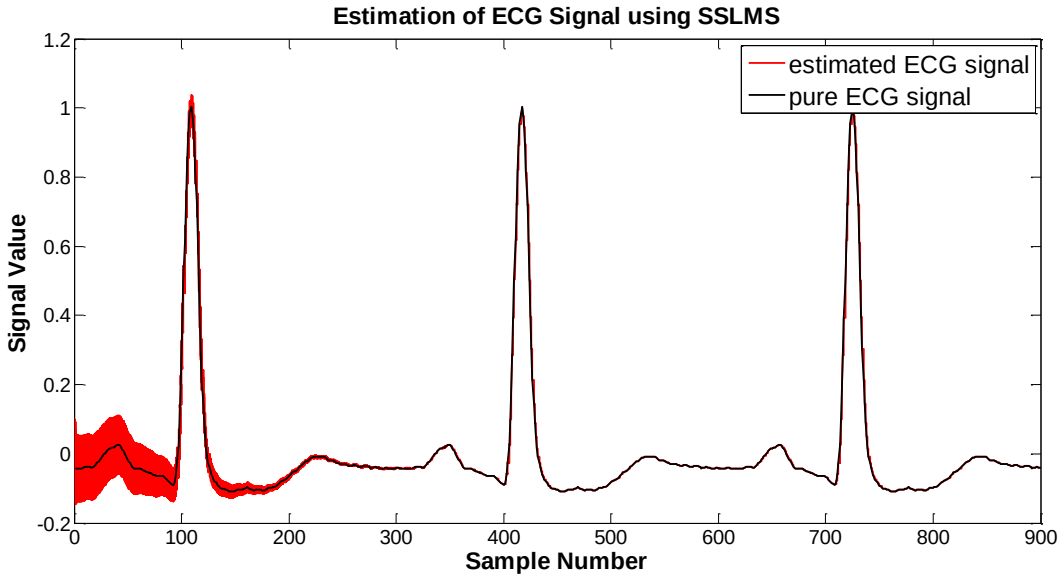

Figure 6.2.3: Estimated ECG Signal using $\mu_{SSLMS} = 0.005$ and η = 0.02

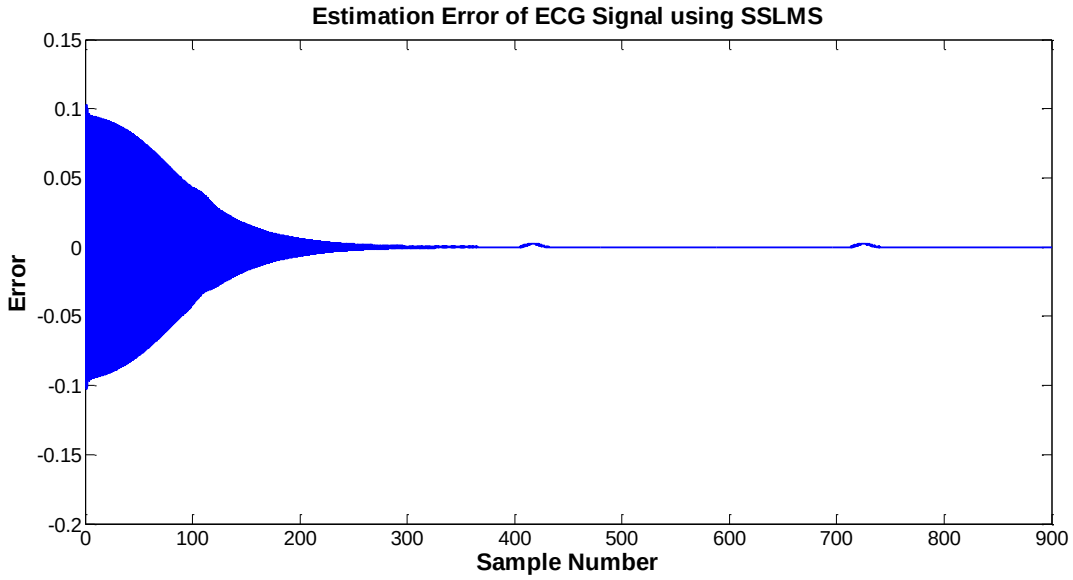

Figure 6.2.4: Error in estimation of ECG Signal using $\mu_{SSLMS} = 0.005$ and η = 0.02

6.3 Effect of η on frequency tracking

Step-size parameter η in (6.6) controls the convergence of frequency in the adaptive tracking mechanism as it controls the effect of phase-difference at each step. Before, we have concluded from the analysis in 6.2 that as soon as correct frequency is tracked, the SSLMS algorithm also converges. So, indirectly, parameter η is controlling the convergence of SSLMS. To elaborate the effect of step-size on frequency tracking, different values of η have been chosen in Table 6.3-1 along with their point of convergence.

Table 6.3-1: Effect of step-size η on frequency convergence

Parameter η	Convergence after samples
0.01	550
0.02	300
0.05	130
0.1	60
0.2	30
0.5	15
1	10

It can be seen in Table 6.3-1 that as η increases, the convergence speed of adaptive tracking has increased. There is a difference of only three sample for $\eta = 0.5$ and $\eta = 1$, so it is clear that beyond $\eta = 0.5$, the converegence speed does not improve distinctively. Hence, 0.5 has been chosed as the maximum value of η and the comparison between two different values has been shown in Figure 6.3.1 to further explain frequency convergence phenomenon.

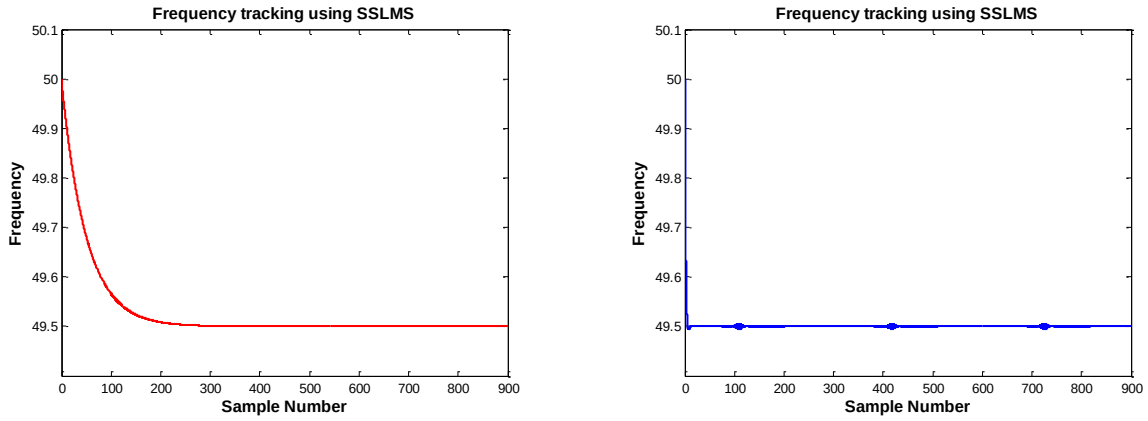

(a) (b)

Figure 6.3.1: Frequency tracking of PLI using μ_{SSLMS}=0.005 with (a) η = 0.02 (b) η = 0.5

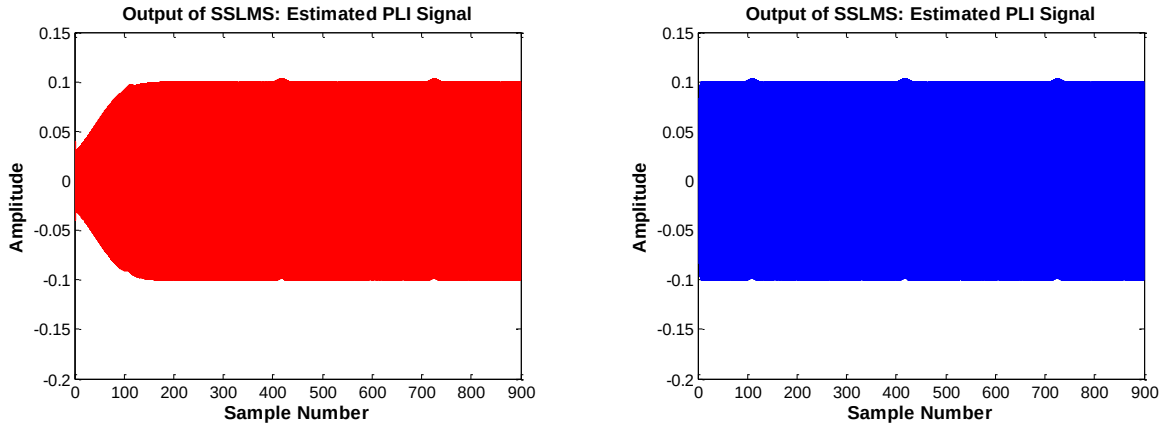

(a) (b)

Figure 6.3.2: Estimated PLI of 49.5 Hz using μ_{SSLMS}=0.005 with (a) η = 0.02 (b) η = 0.5

It's elaborated in the plots of Figure 6.3.1 that for larger η, frequency convergence takes much lesser time and similarly estimated PLI reaches its true amplitude much faster as shown in Figure 6.3.2. According to this, the effect of η on estimated ECG signal and error in estimation is shown in Figure 6.3.3 and Figure 6.3.4.

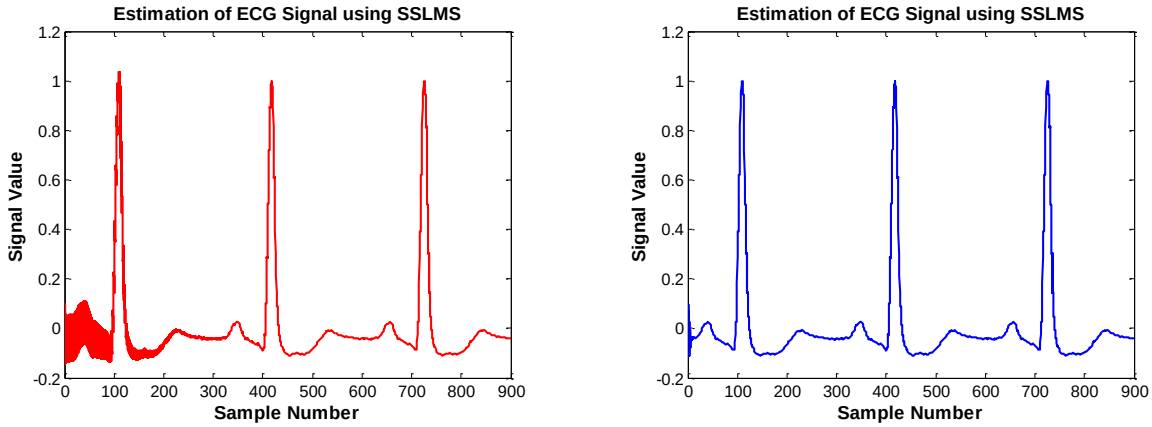

(a) (b)

Figure 6.3.3: Estimated ECG Signal using μ_{SSLMS}=0.005 with (a) η = 0.02 (b) η = 0.5

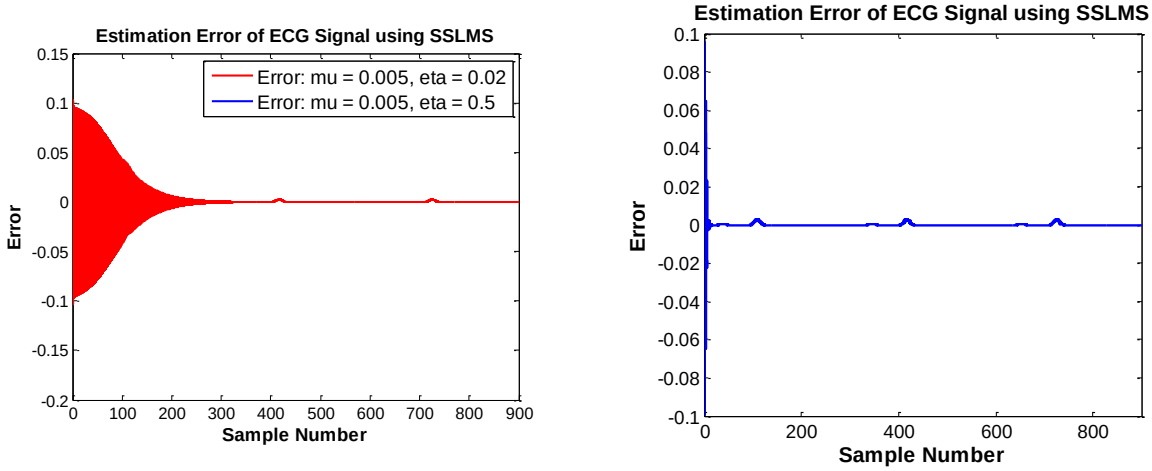

(a) (b)

Figure 6.3.4: Error in estimation of ECG Signal using μ_{SSLMS}=0.005 with (a) η = 0.02 (b) η = 0.5

6.4 Effect of μ_{SSLMS} on convergence and error

The value of μ_{SSLMS} does not affect the frequency tracking but it is directly related to the convergence of SSLMS algorithm and its estimation error. This section shows the simulation results for comparison between SSLMS performance using $\mu_{SSLMS} = 0.005$ and $\mu_{SSLMS} = 0.05$. In order to analyze this process in detail, the value of η has been kept smaller. As we can see in

Figure 6.4.1 that frequency tracking is not affected by changes in μ_{SSLMS}. However, we can see the in **Figure 6.4.4** that for smaller value of μ_{SSLMS} , SSLMS takes longer to converge but has small estimation error at the QRS complex peaks of ECG signal and vice versa.

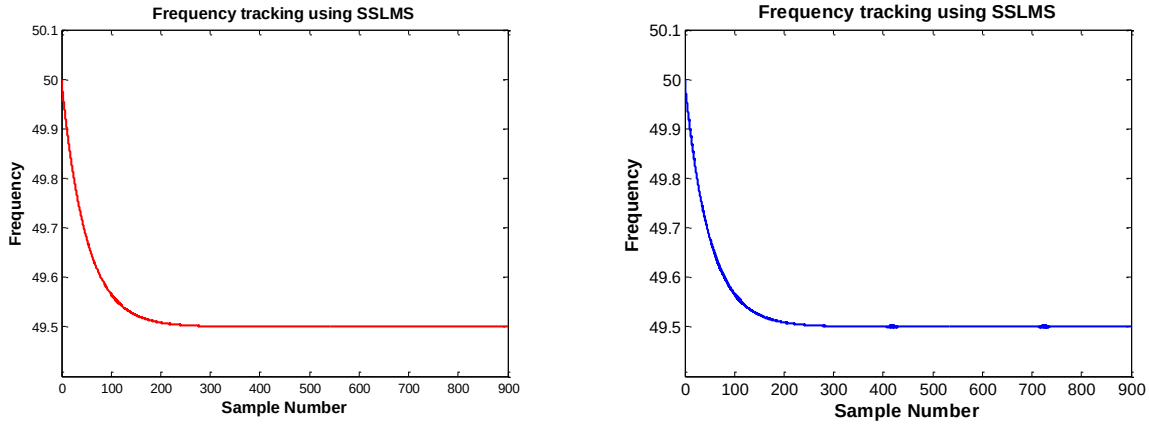

(a) (b)

Figure 6.4.1: Frequency tracking of PLI using η = 0.02 with (a) μ_{SSLMS}=0.005 (b) μ_{SSLMS} =0.05

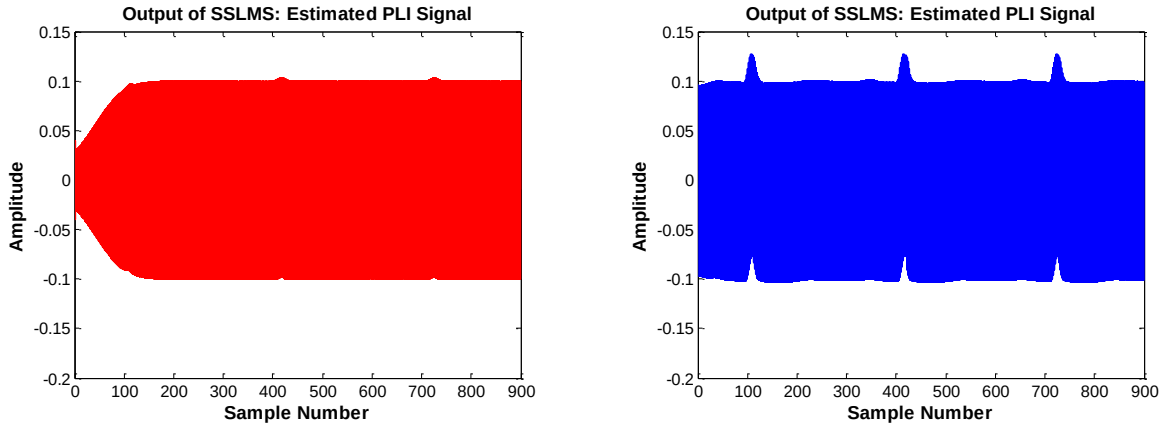

(a) (b)

Figure 6.4.2: Estimated PLI of 49.5 Hz using η = 0.02 with (a) μ_{SSLMS}=0.005 (b) μ_{SSLMS} =0.05

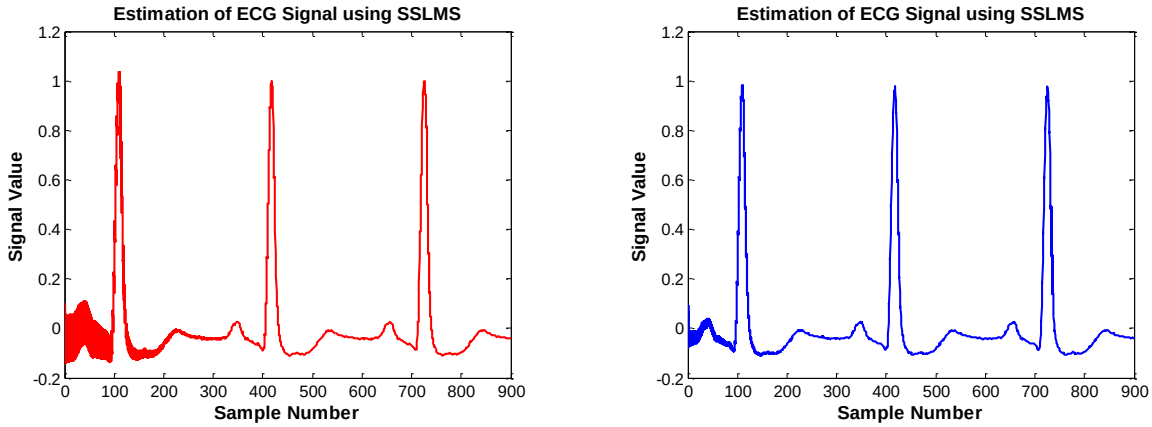

(a) (b)

Figure 6.4.3: Estimated ECG Signal using η = 0.02 with (a) μ_{SSLMS}=0.005 (b) μ_{SSLMS} =0.05

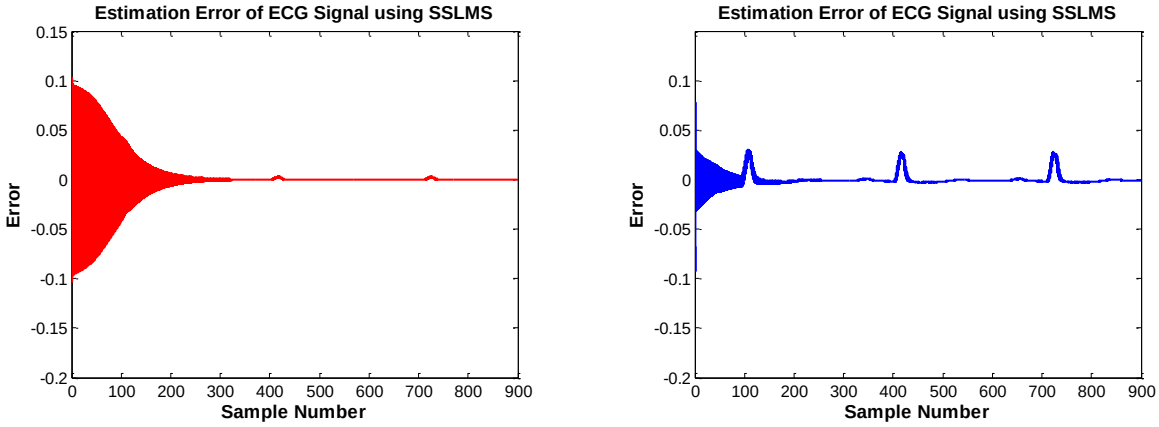

(a) (b)

Figure 6.4.4: Error in estimation of ECG Signal using η = 0.02 with (a) μ_{SSLMS}=0.005 (b) μ_{SSLMS} =0.05

For specific signal to noise ratio (SNR), PLI parameter and sampling frequency, a suitable $[\mu_{SSLMS}, \eta]$ pair must be decided which in this case is [0.005,0.5].

6.5 Comparison with SSRLS algorithm

Simulation results for estimating unknown PLI signal using SSRLS algorithm [50] and SSLMS algorithm shown in Figure 6.1.1 have been compared in this section. The step-size

parameter for SSLMS is $\mu_{SSLMS} = 0.005$ and forgetting factor used for SSRLS is $\lambda_{SSRLS} = 0.999$. Moreover, in order to observe convergence in details, η has been set at 0.02. Figure 6.5.1 shows that as far as η is same for both adaptive tracking schemes, change of noise canceller does not affect the convergence of frequency. It can be seen in Figure 6.5.2 that the convergence speed of SSLMS is faster than that of SSRLS algorithm due to model uncertainty factor. This performance analysis is also exhibited in Figure 6.5.3 and Figure 6.5.4.

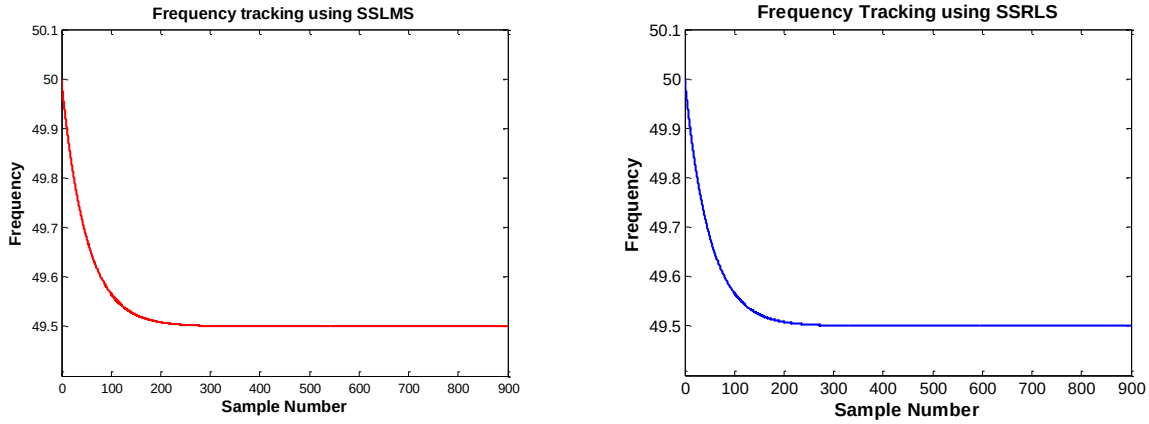

(a) (b)

Figure 6.5.1: Frequency tracking of PLI using η = 0.02 with (a) SSLMS (μ_{SSLMS}=0.005) (b) SSRLS (λ_{SSRLS} = 0.999)

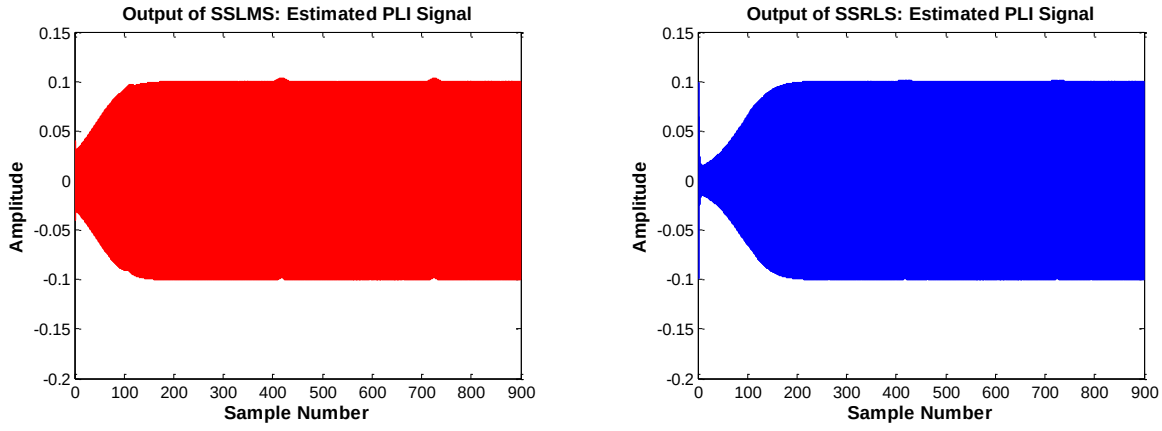

(a) (b)

Figure 6.5.2: Estimated PLI of 49.5 Hz using η = 0.02 with (a) SSLMS (μ_{SSLMS}=0.005) (b) SSRLS (λ_{SSRLS} = 0.999)

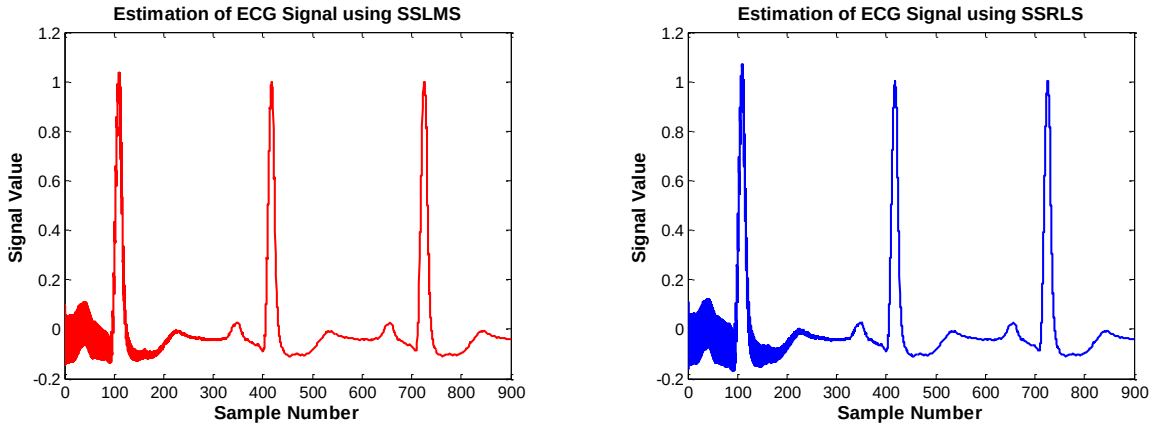

(a) (b)

Figure 6.5.3: Estimated ECG Signal using η = 0.02 with (a) SSLMS (μ_{SSLMS}=0.005) (b) SSRLS (λ_{SSRLS} = 0.999)

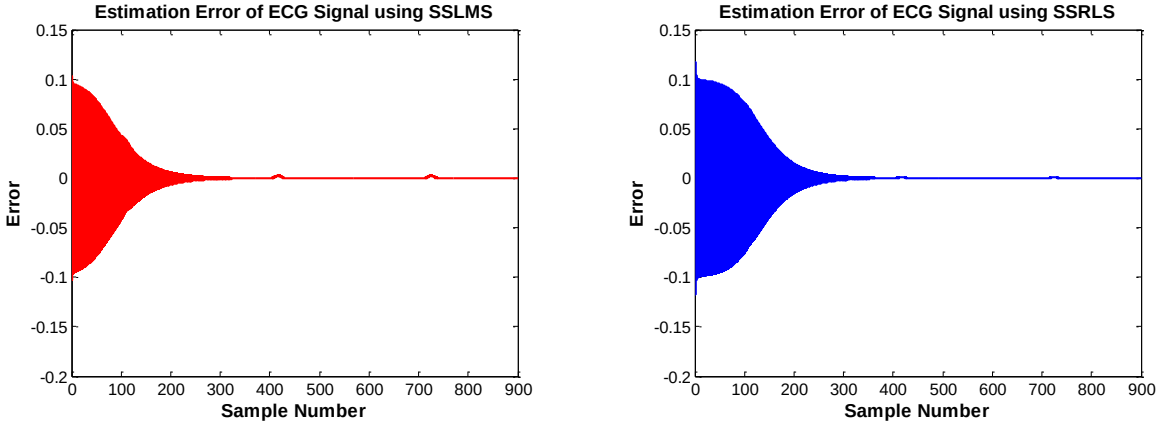

(a) (b)

Figure 6.5.4: Error in estimation of ECG Signal using η = 0.02 with (a) SSLMS (μ_{SSLMS}=0.005) (b) SSRLS (λ_{SSRLS} = 0.999)

Table 6.5-1 compares the MATLAB simulations elapsed time and it is clear that SSLMS is approximately twenty six times faster than that of SSRLS algorithm hence proving SSLMS to be better than that of SSRLS algorithm.

Table 6.5-1: Elapsed time of MATLAB simulations for SSLMS and SSRLS algorithms

SSLMS	**SSRLS**
0.033861 seconds	0.868233 seconds

6.6 Conclusion

From this chapter, PLI with frequency unknown to the system has been removed from noisy ECG signal by first tracking its frequency and then estimating it. From the simulation results, we have concluded that, in case of unknown frequency, SSLMS gives better results for a larger value of η and smaller value of μ_{SSLMS} where former determines frequency tracking and later leads to convergence. Moreover, SSLMS has better convergence speed and computational complexity than SSRLS algorithm for a fixed value of η.

CHAPTER 7: TRACKING AND REMOVAL OF SINUSOIDAL PLI WITH VARYING FREQUENCY FROM ECG SIGNAL

This chapter explains the tracking of sinusoidal component of PLI having frequency which is varying unidirectional or bidirectional from ECG signal using SSLMS Algorithm. The results are generated using MATLAB R2012a. The parameter for tracking are analyzed for their performance. The comparison of SSLMS is done with SSRLS algorithm with respect to convergence, mean square error and computational complexity.

7.1 SSLMS based Adaptive Tracking of Varying Frequency

In real life situations, there is a chance for PLI frequency to vary within a certain range. This drifting PLI is hard to estimate and can be modeled as a chirp signal and it has been shown in literature that SSLMS can track a chirp signal [50]. In this chapter, SSLMS will be implemented to first track the frequency of signal and then estimating it. In order to track the variable frequency, the mechanism mentioned in section 6 has been used. However, the noisy signal $v_{PLI}[k]$ is generated as follows:

$$v_{PLI}[k] = \sigma \sin[\omega kT + \partial (kT)^2 + \varphi] \tag{7.1}$$

Where $\sigma =$ amplitude, $\omega =$ frequency, $\partial =$ frequency drift rate, $\varphi =$ phase and $T =$ sampling time of the unknown and variable PLI signal.

7.2 Tracking PLI with Unidirectional Drifting Frequency

For any signal with unidirectional varying frequency, its frequency increases or decrease till the last sample. Figure 7.2.1 shows ten cycles of pure ECG signal $u[k]$ from MIT-BIH database [49] normalized.

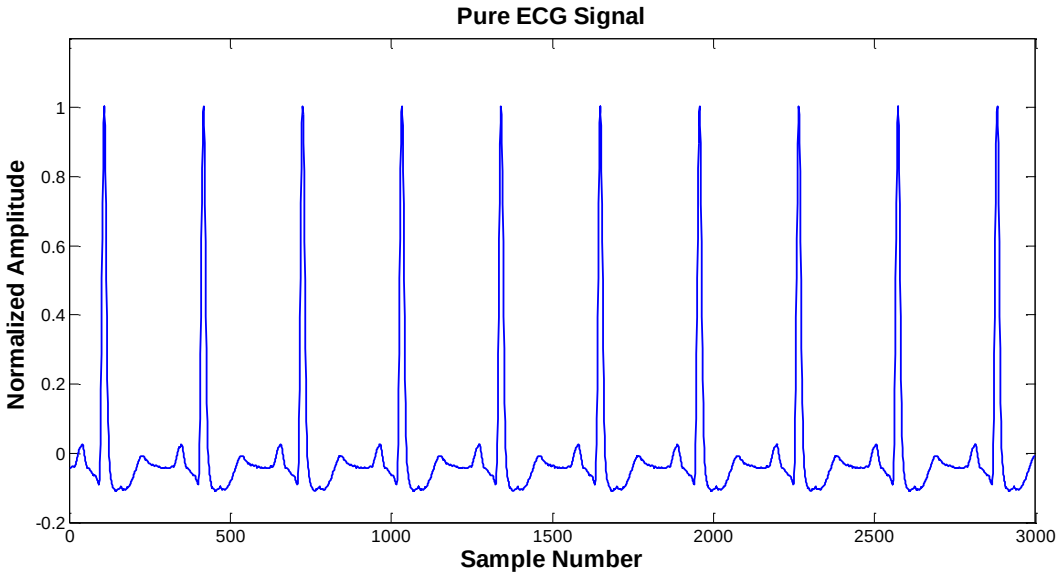

Figure 7.2.1: Pure ECG Signal using MIT-BIH database

The unknown sinusoidal $v_{PLI}[k]$ has been generated using the parameter mentioned in Table 7.2-1. The frequency has been linearly increased from 49.5 Hz to 50.5 Hz.

Table 7.2-1: Parameters to generate Sinusoidal Noise with linearly varying frequency

Parameter	Symbol	Value
Amplitude	σ_s	0.1
Frequency	ω	$2\pi \times 49.5$ to $2\pi \times 50.5$
Phase	φ	$\frac{\pi}{4}$
Sampling Time	T_s	$\frac{1}{360} = 0.028$

Adding $v_{PLI}[k]$ we get PLI corrupted signal as mentioned in Figure 7.2.2.

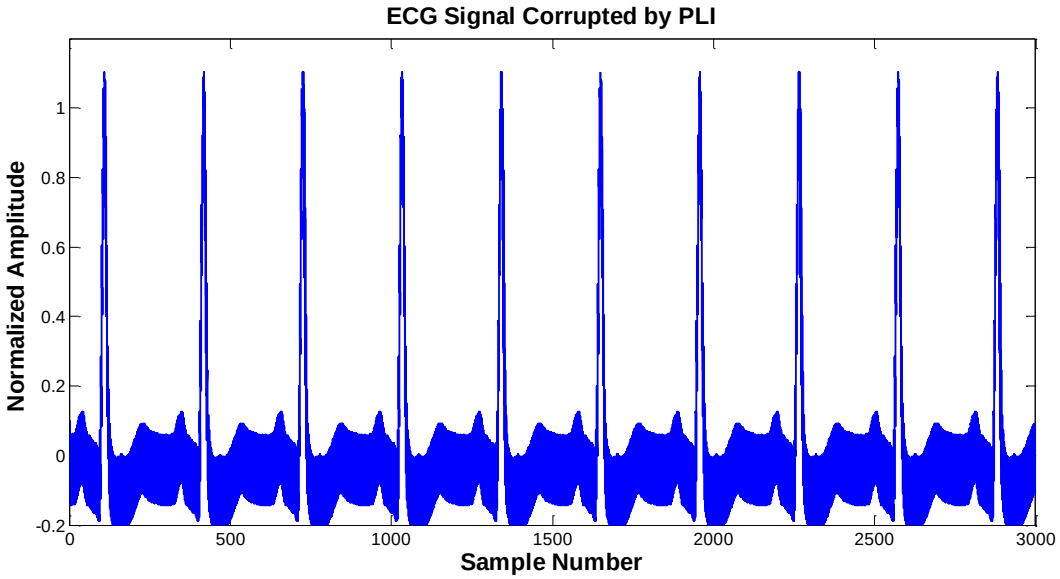

Figure 7.2.2: Unidirectional Frequency Sinusoidal PLI corrupted ECG Signal

7.2.1 Simulation Results

SSLMS based ANC has been initialized with $\omega_o = 2\pi \times 50$, $\varphi_o = 0$, $\mu_{SSLMS} = 0.005$ and $\eta = 0.5$. Value of η is kept higher than 0.02 as the frequency is varying and such small step-size will not be able to track the desired results.

It can be seen in Figure 7.2.3 that the tracked frequency is varying from 49.5 Hz to 50.5 Hz, hence the frequency is being track correctly. Due to larger value of η, Figure 7.2.4 shows that the output of SSLMS algorithm converges in the beginning. Moreover, Figure 7.2.5 exhibit that the ECG is estimated correctly and Figure 7.2.6 shows that due to small estimation error, SSLMS is an efficient algorithm in tracking and removing unidirectional varying PLI.

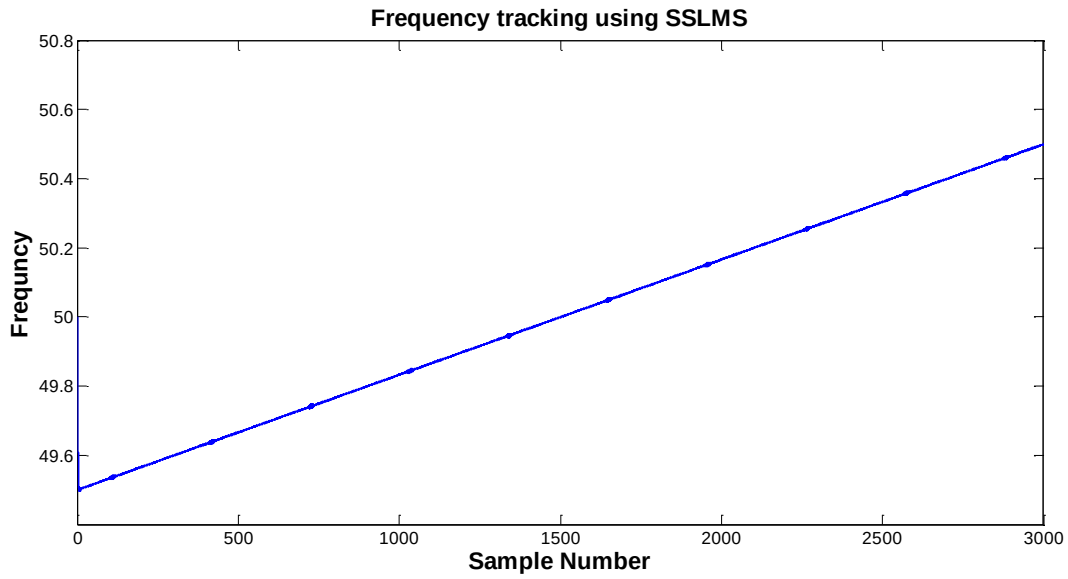

Figure 7.2.3: Frequency tracking unidirectional varying of PLI using $\mu_{SSLMS} = 0.005$ and η = 0.5

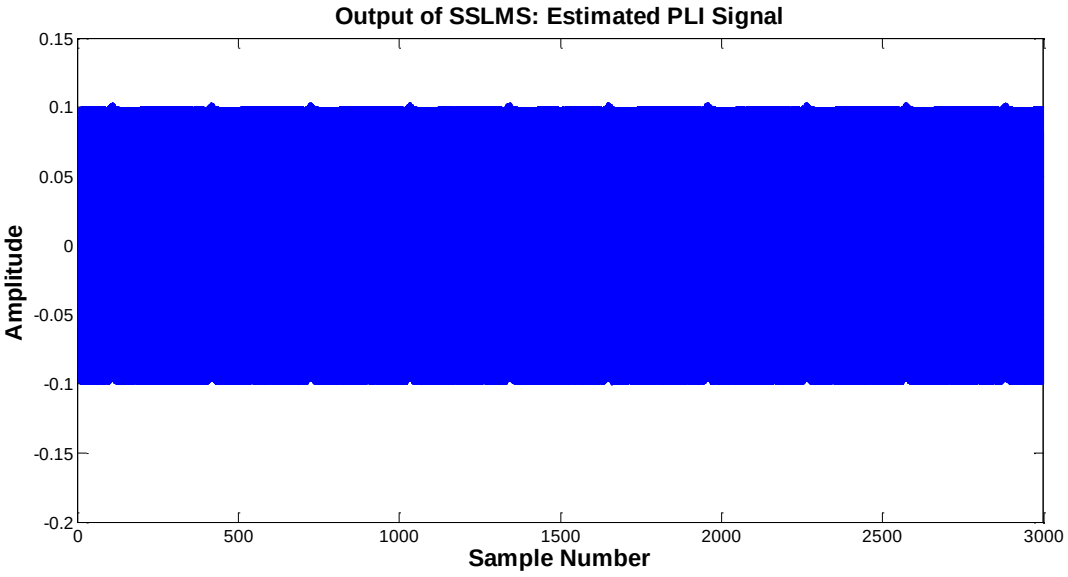

Figure 7.2.4: Estimated unidirectional varying PLI using $\mu_{SSLMS} = 0.005$ and η = 0.5

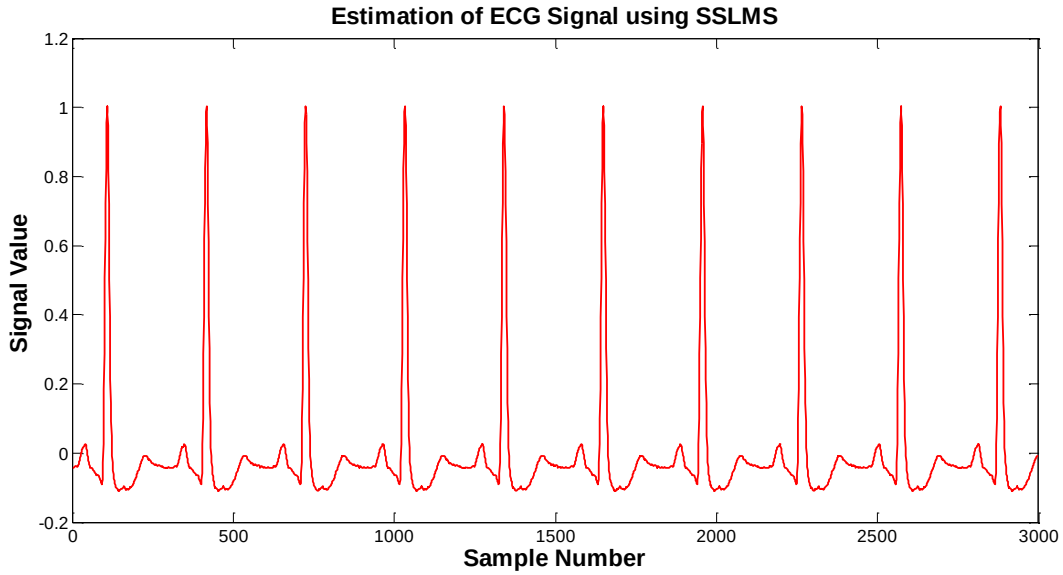

Figure 7.2.5: Estimated ECG Signal using $\mu_{SSLMS} = 0.005$ and η = 0.5

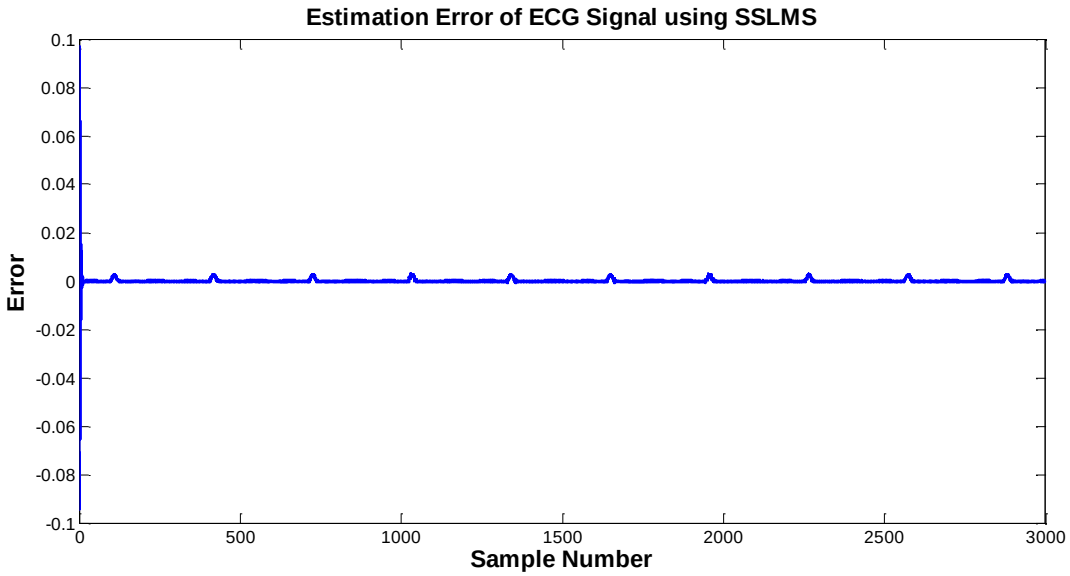

Figure 7.2.6: Error in estimation of ECG Signal using $\mu_{SSLMS} = 0.005$ and η = 0.5

7.2.2 Effect of η on frequency tracking

Values of η chosen for analysis are $\eta = 0.02$ and $\eta = 0.5$. Figure 7.2.7 show that for $\eta = 0.02$, frequency converges from 50Hz, which the initial frequency of the system, and takes some iterations to reach near its correct value. Moreover, the estimated PLI signal at the output of SSLMS algorithm with smaller η also takes longer to converge than with larger η as shown in Figure 7.2.8.

In Figure 7.2.9, it can be seen that for SSLMS with smaller η, estimated ECG is not accurate. The reason for this behavior is that due to frequency varying at every step, it is very difficult to track it with a smaller value of η. This inaccuracy in ECG estimation can also be shown in the error plots of Figure 7.2.10.

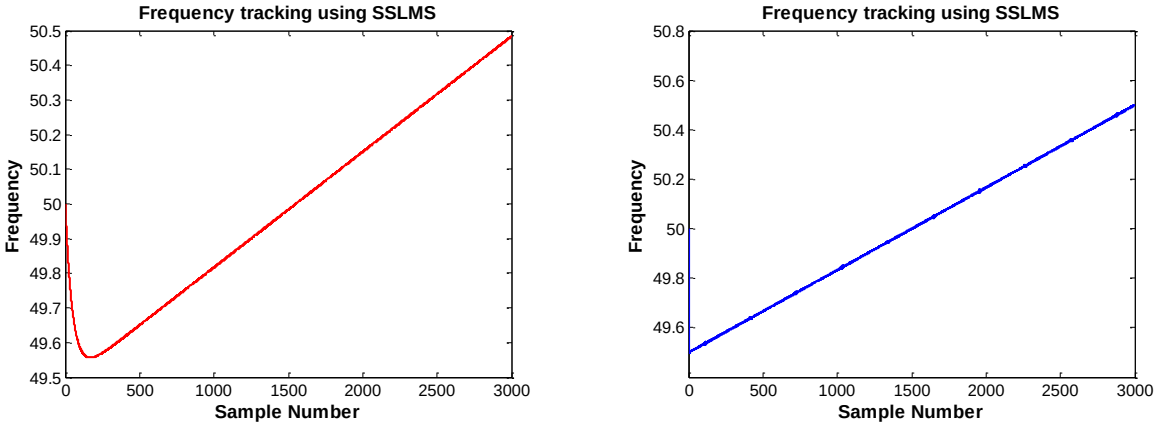

(a) (b)

Figure 7.2.7: Frequency tracking of unidirectional varying PLI using μ_{SSLMS}=0.005 with (a) η = 0.02 (b) η = 0.5

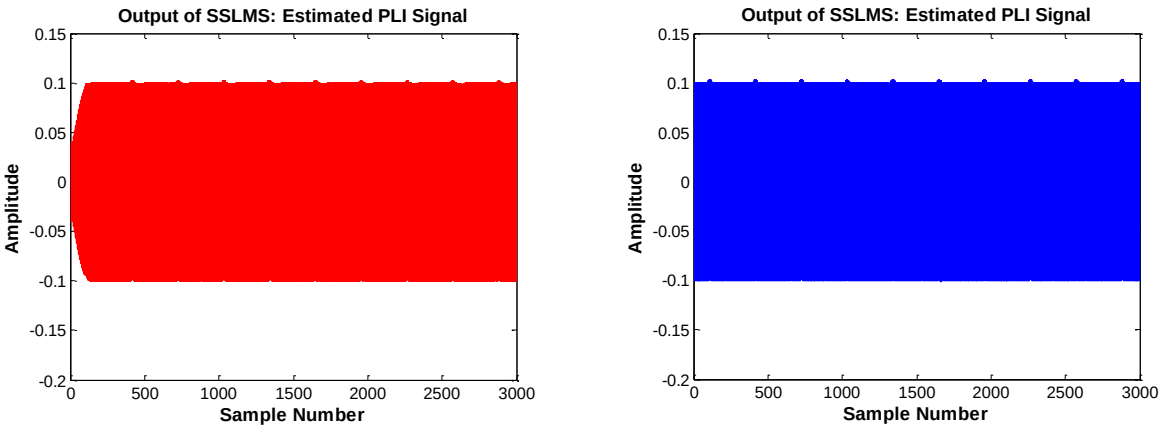

(a) (b)

Figure 7.2.8: Estimated unidirectional varying PLI using μ_{SSLMS}=0.005 with (a) η = 0.02 (b) η = 0.5

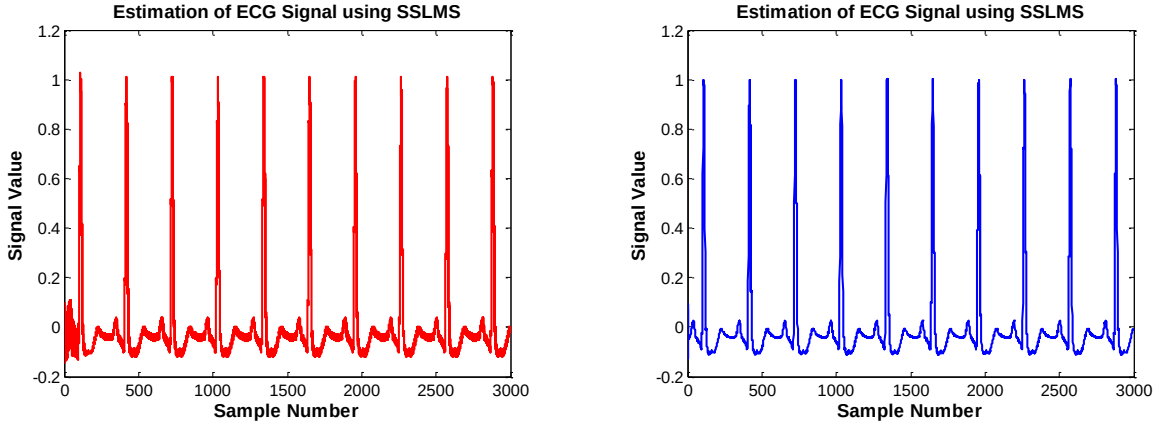

(a) (b)

Figure 7.2.9: Estimated ECG Signal using μ_{SSLMS}=0.005 with (a) η = 0.02 (b) η = 0.5

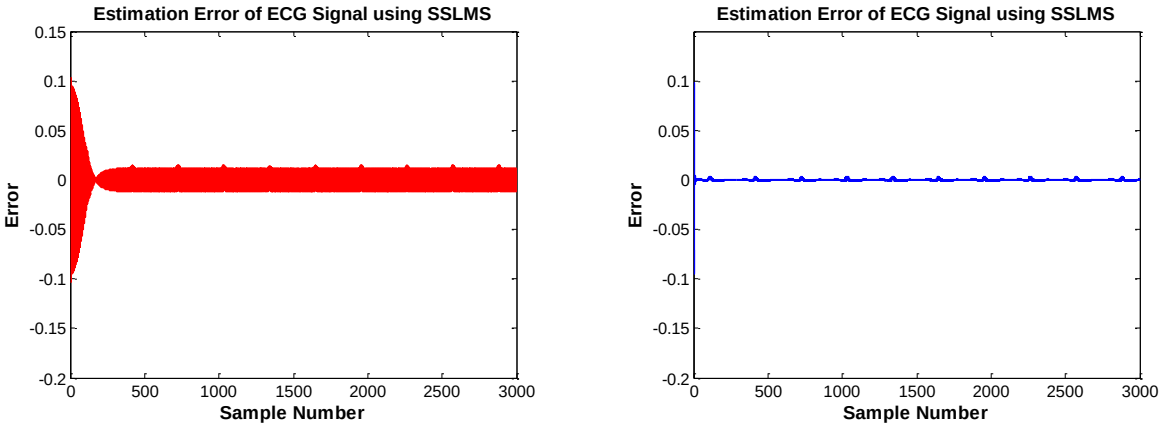

(a) (b)

Figure 7.2.10: Error in estimation of ECG Signal using μ_{SSLMS}=0.005 with (a) η = 0.02 (b) η = 0.5

7.2.3 Effect of μ_{SSLMS} on convergence and error

Figure 7.2.14 shows that for larger value of μ_{SSLMS} i.e. 0.05, SSLMS algorithm exhibits poor estimation at the occurrence of QRS complex peaks in ECG. This estimation performance also affects the tracking of frequency as shown in Figure 7.2.11.

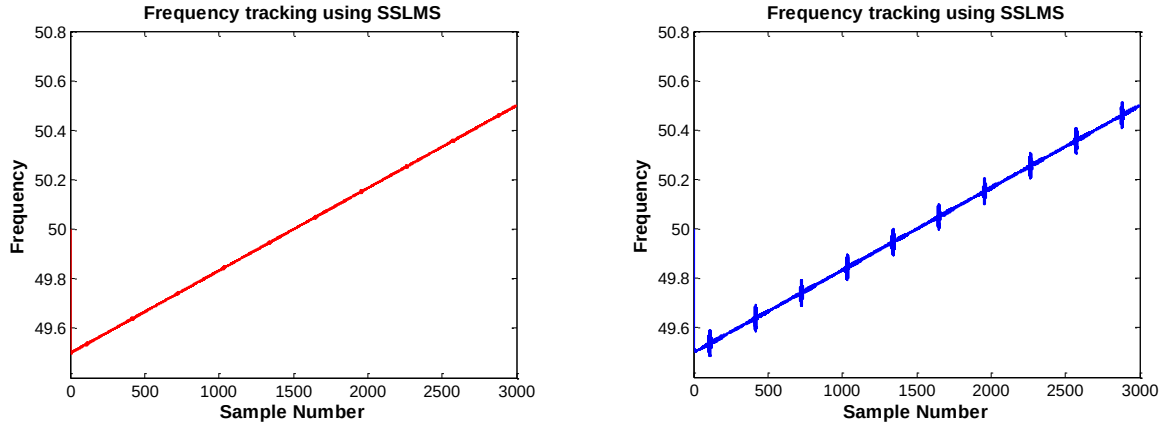

(a) (b)

Figure 7.2.11: Frequency tracking of unidirectional varying PLI using η = 0.5 with (a) μ_{SSLMS}=0.005 (b) μ_{SSLMS} =0.05

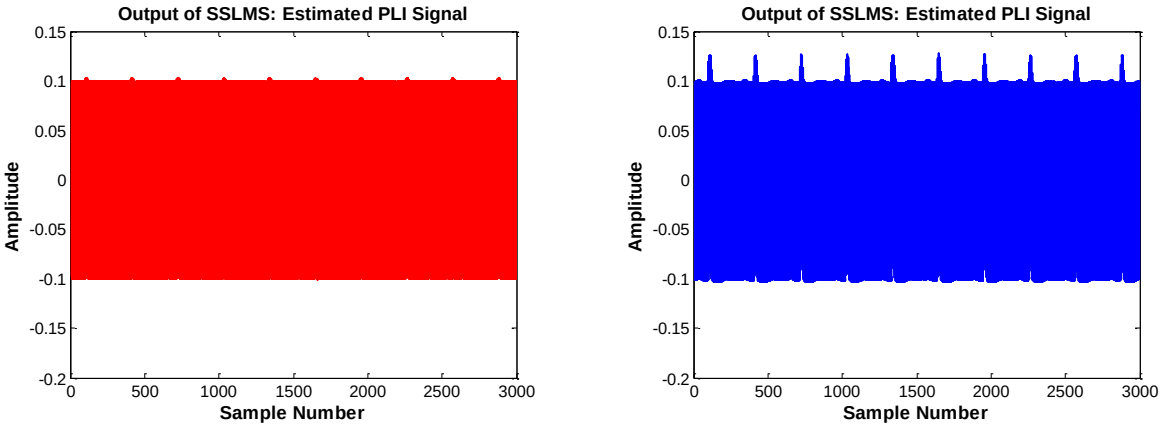

(a) (b)

Figure 7.2.12: Estimated unidirectional varying PLI using η = 0.5 with (a) μ_{SSLMS}=0.005 (b) μ_{SSLMS} =0.05

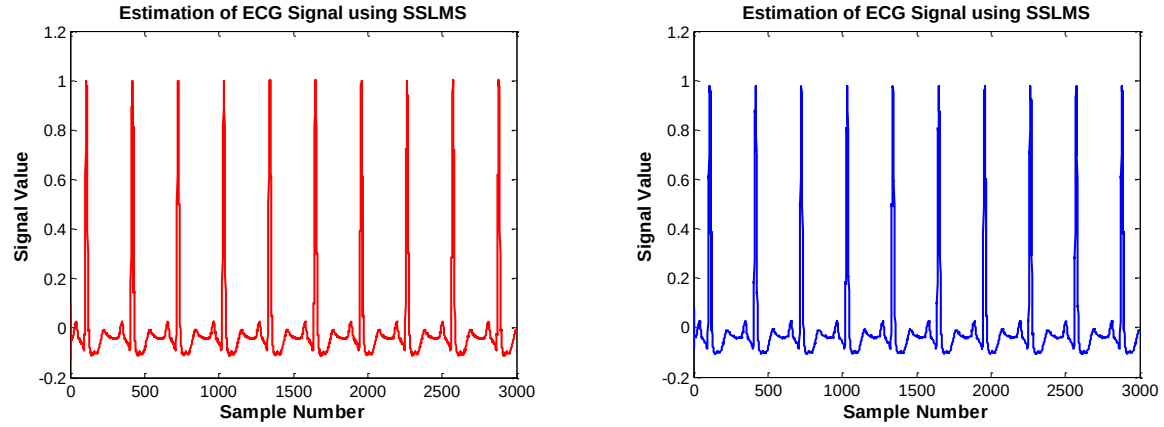

(a) (b)

Figure 7.2.13: Estimated ECG Signal using η = 0.5 with (a) μ_{SSLMS}=0.005 (b) μ_{SSLMS} =0.05

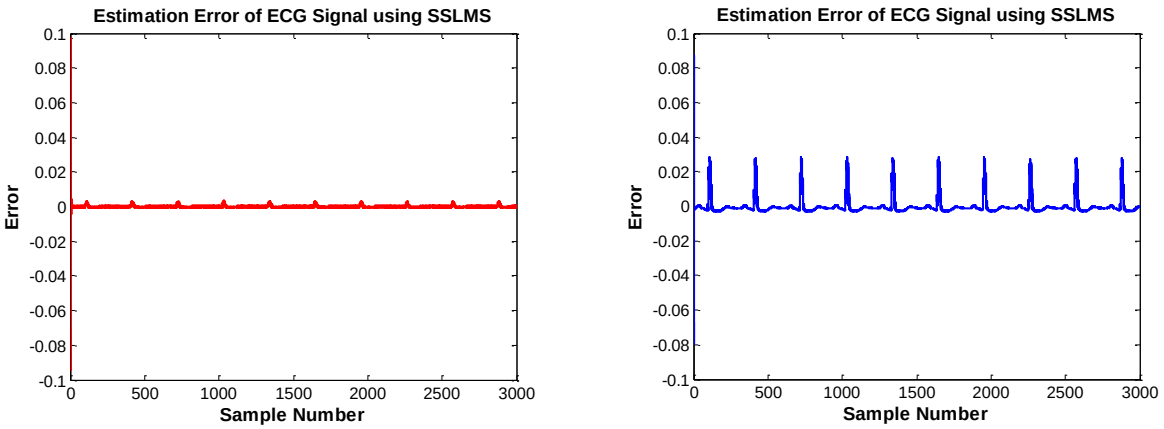

(a) (b)

Figure 7.2.14: Error in estimation of ECG Signal using η = 0.5 with (a) μ_{SSLMS}=0.005 (b) μ_{SSLMS} =0.05

7.2.4 Comparison with SSRLS algorithm

Tracking of variable frequency PLI has been shown in this section using $\mu_{SSLMS} = 0.005$, $\lambda_{SSRLS} = 0.999$ and $\eta = 0.5$ for both adaptive filters. As shown earlier in Figure 6.5.1, it can also be observed from Figure 7.2.15 that the change of algorithm does not affect frequency convergence as far as η is constant. Figure 7.2.18 shows that the estimation error of SSLMS is better that that of SSRLS in this specific case.

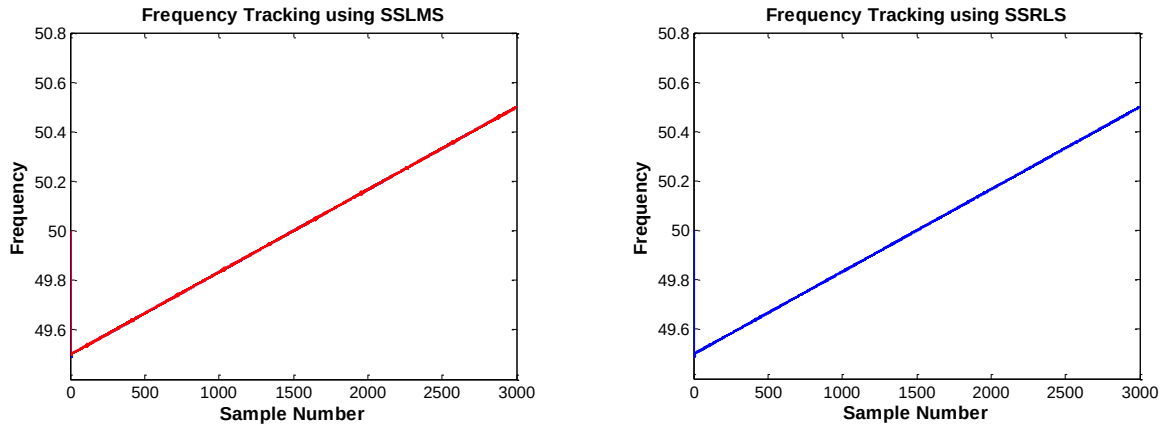

(a) (b)

Figure 7.2.15: Frequency tracking of unidirectional varying PLI using η = 0.5 with (a) SSLMS (μ_{SSLMS}=0.005) (b) SSRLS (λ_{SSRLS} = 0.999)

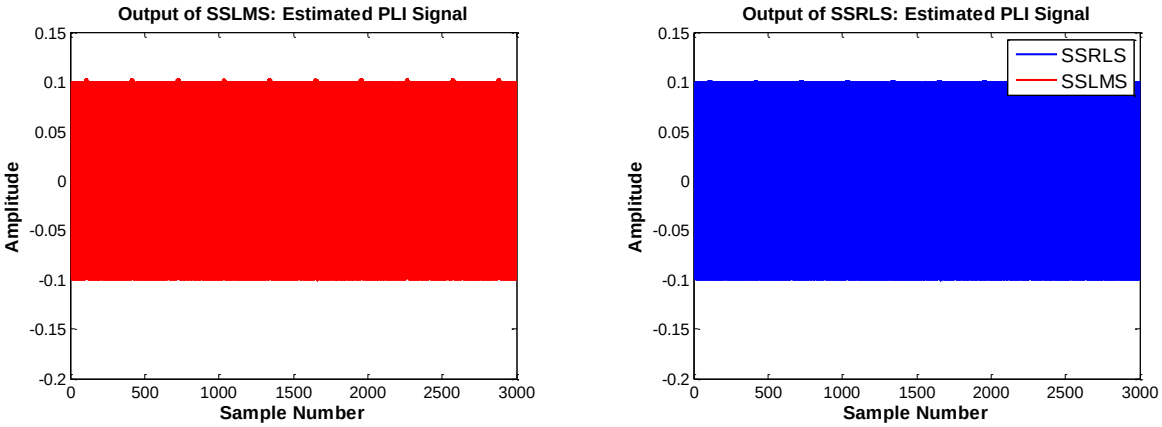

(a) (b)

Figure 7.2.16: Estimated unidirectional varying PLI using η = 0.5 with (a) SSLMS (μ_{SSLMS}=0.005) (b) SSRLS (λ_{SSRLS} = 0.999)

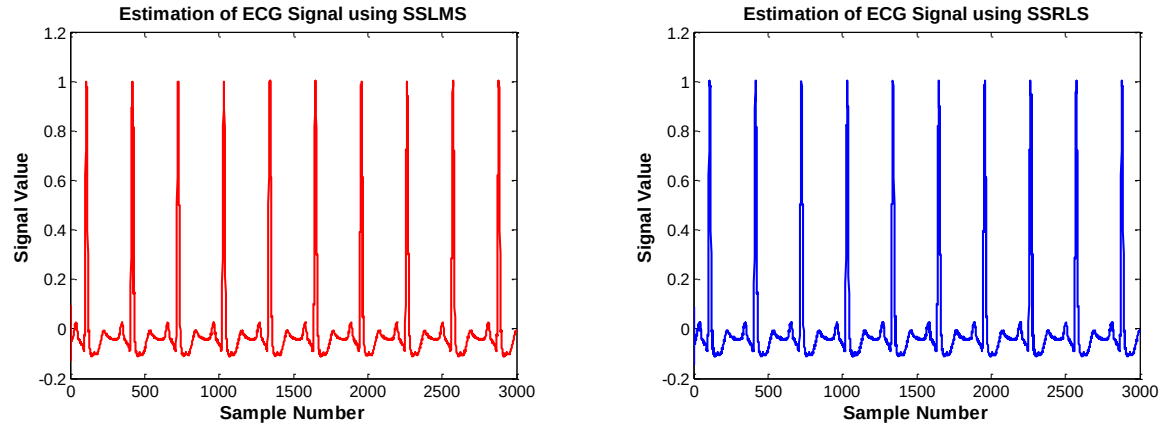

(a) (b)

Figure 7.2.17: Estimated ECG Signal using η = 0.5 with (a) SSLMS (μ_{SSLMS}=0.005) (b) SSRLS (λ_{SSRLS} = 0.999)

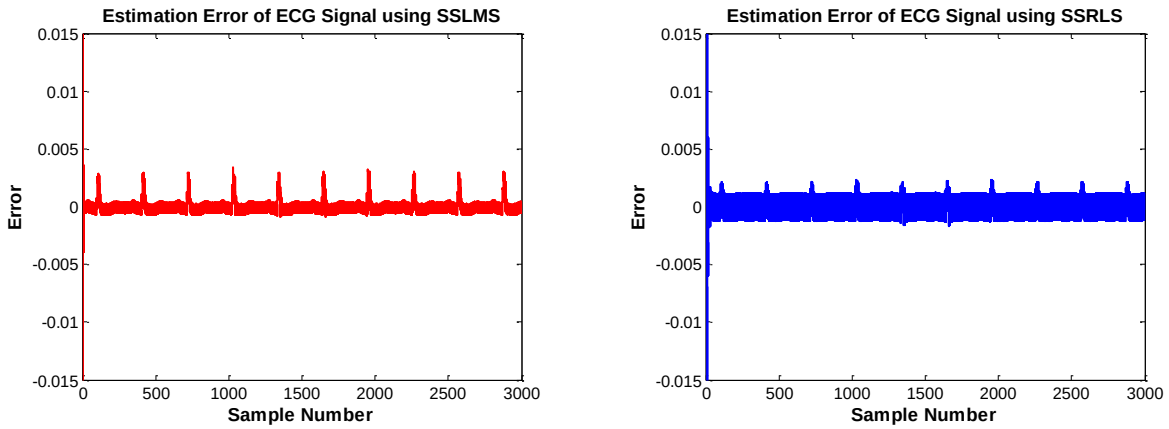

(a) (b)

Figure 7.2.18: Error in estimation of ECG Signal using η = 0.5 with (a) SSLMS (μ_{SSLMS}=0.005) (b) SSRLS (λ_{SSRLS} = 0.999)

In Table 7.2-2, it is shown that SSLMS requires lesser time to execute than SSRLS algorithm.

Table 7.2-2: Elapsed time of MATLAB simulations for SSLMS and SSRLS algorithms

SSLMS	**SSRLS**
0.065857 seconds	0.217688 seconds

Hence the simulation results and elapsed time analysis prove SSLMS based adaptive noise canceller to be better than SSRLS one in case of unidirectional varying frequency.

7.3 PLI with Bidirectional Drifting Frequency

Bidirectional frequency means that it increases or decreases in one direction to a specific sample and then goes vice versa and so on. Figure 7.2.1 shows ten cycles of pure ECG signal $u[k]$ from MIT-BIH database [49] normalized. In order to test the working of SSLMS on bidirectional varying frequency, $v_{PLI}[k]$ has been increased from 49.5 Hz to 50.5 Hz till the center of the signal and then decreased back to 49.5 Hz as shown in

Table **7.3-1**.

Table 7.3-1: Parameters to generate Sinusoidal Noise with bidirectional varying frequency

Parameter	Symbol	Value
Amplitude	σ_s	0.1
Frequency	ω	Sample 1:1500 → $2\pi \times 49.5$ to $2\pi \times 50.5$
		Sample 1501:3000 → $2\pi \times 50.5$ to $2\pi \times 49.5$
Phase	φ	$\frac{\pi}{4}$
Sampling Time	T_s	$\frac{1}{360} = 0.028$

Adding $v_{PLI}[k]$ we get PLI corrupted signal as mentioned in **Figure 7.3.1**.

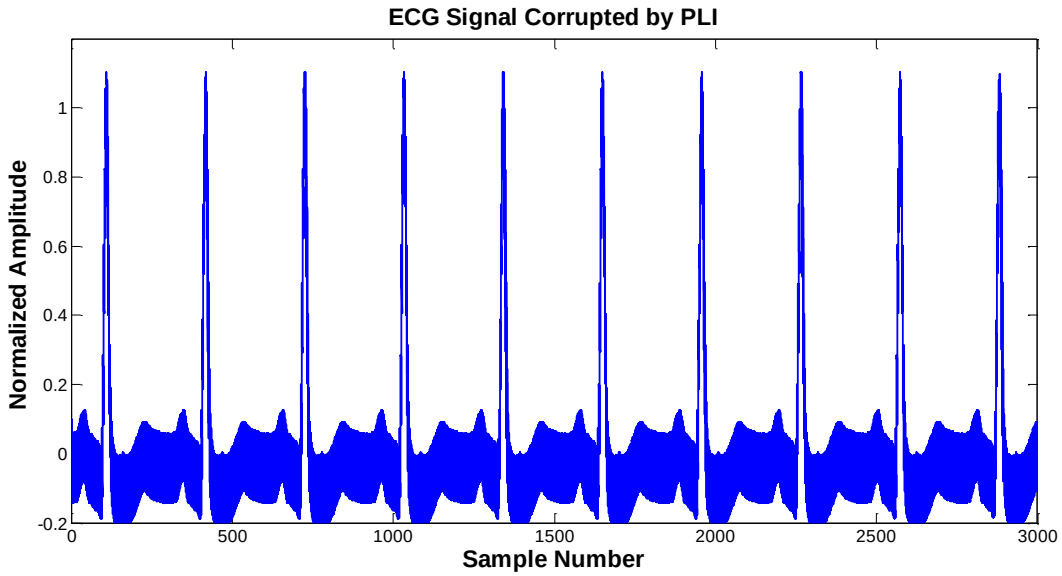

Figure 7.3.1: Bidirectional Frequency Sinusoidal PLI corrupted ECG Signal

7.3.1 Simulation Results

SSLMS has been initialized with $\omega_o = 2\pi \times 50$, $\varphi_o = 0$, $\mu_{SSLMS} = 0.005$ and step-size parameter for adaptive tracking scheme in section 6 is $\eta = 0.5$.

Figure 7.3.2 shows that SSLMS based adaptive tracking algorithm has traced frequency efficiently. Also Figure 7.3.4 and Figure 7.3.5 show excellent interference cancellation ability of SSLMS algorithm.

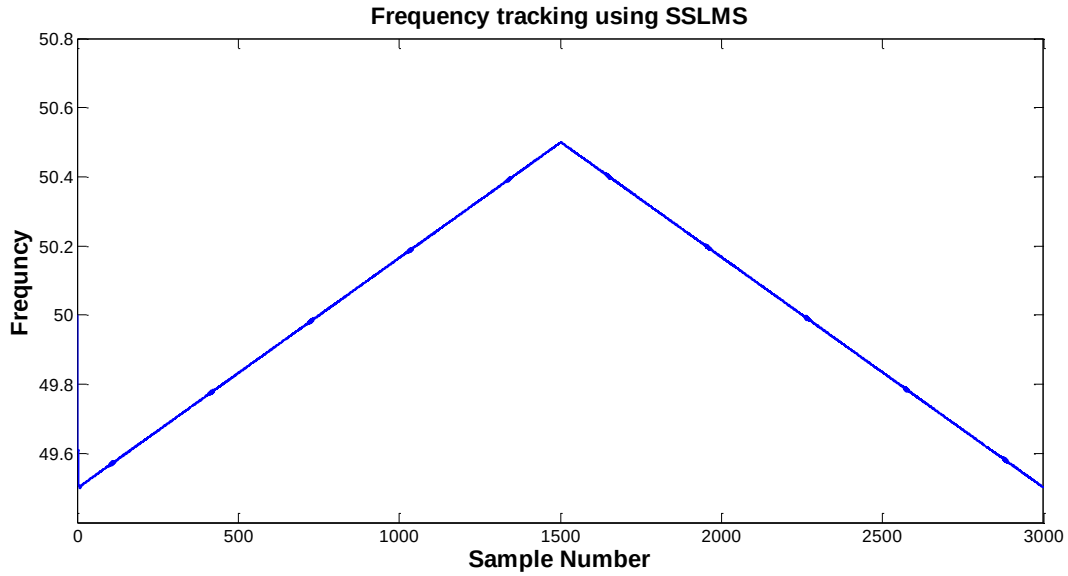

Figure 7.3.2: Frequency tracking bidirectional varying of PLI using $\mu_{SSLMS} = 0.005$ and η = 0.5

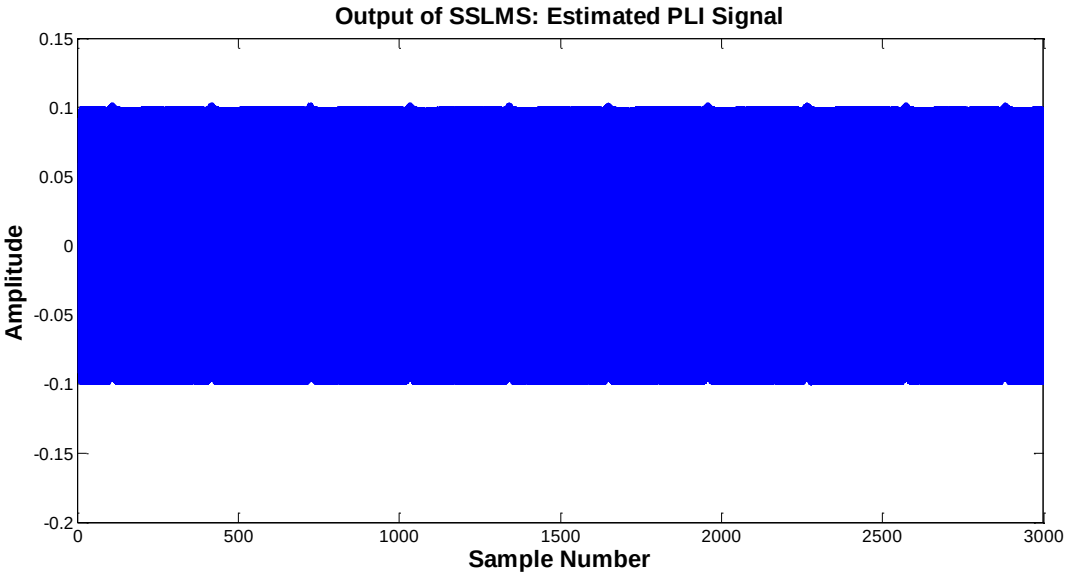

Figure 7.3.3: Estimated bidirectional varying PLI using $\mu_{SSLMS} = 0.005$ and η = 0.5

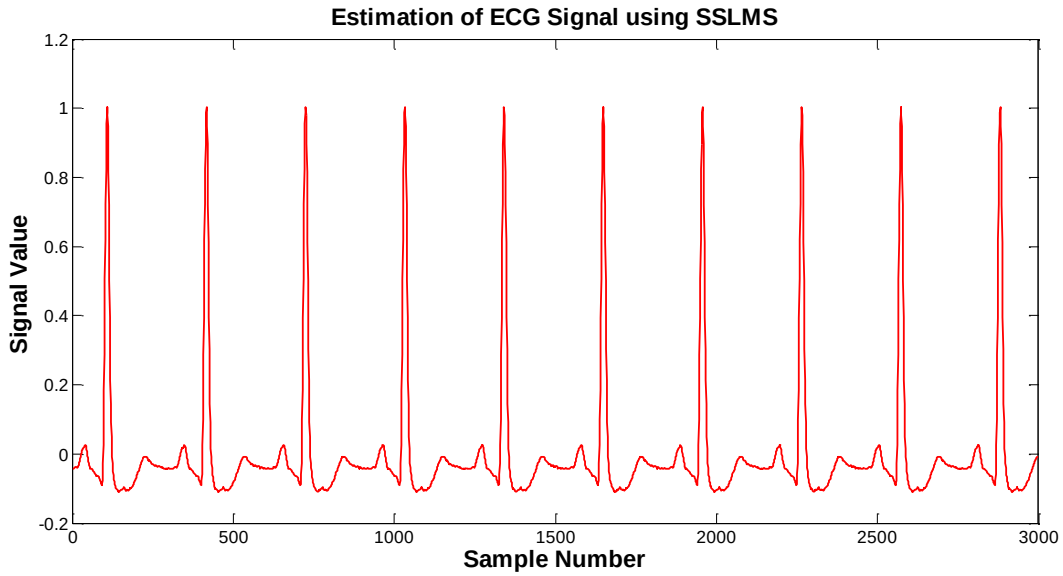

Figure 7.3.4: Estimated ECG Signal using $\mu_{SSLMS} = 0.005$ and η = 0.5

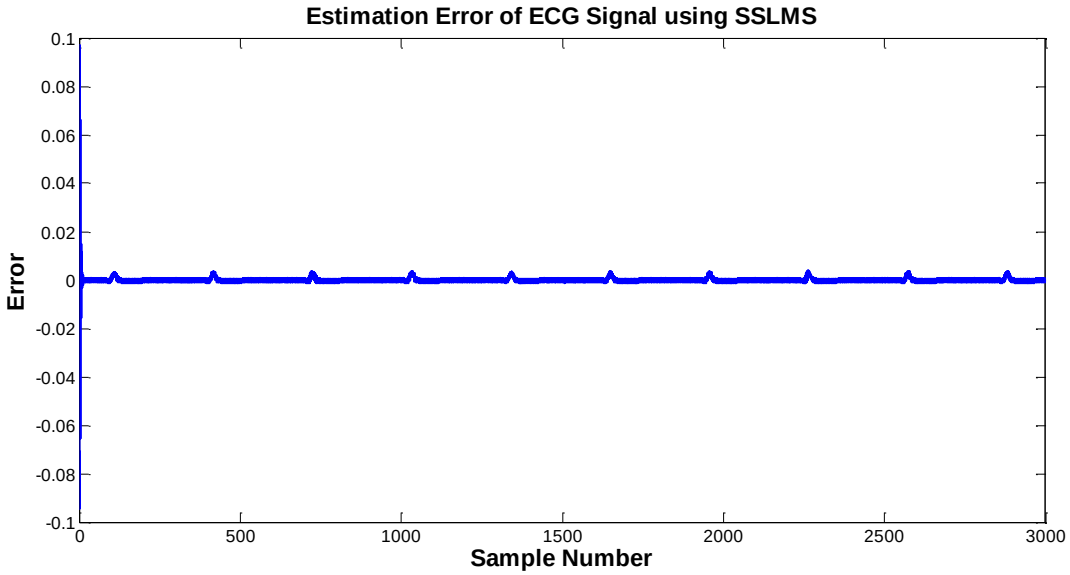

Figure 7.3.5: Error in estimation of ECG Signal using $\mu_{SSLMS} = 0.005$ and η = 0.5

7.3.2 Effect of η on frequency tracking

$\eta = 0.02$ and $\eta = 0.5$ have been chosen for this comparative analysis. Figure 7.3.6 shows that for smaller η, the frequency is not being tracked correctly and even after convergence, it's value is slightly lesser than true value hence giving out more error in estimation as shown in Figure 7.3.8 and Figure 7.3.9.

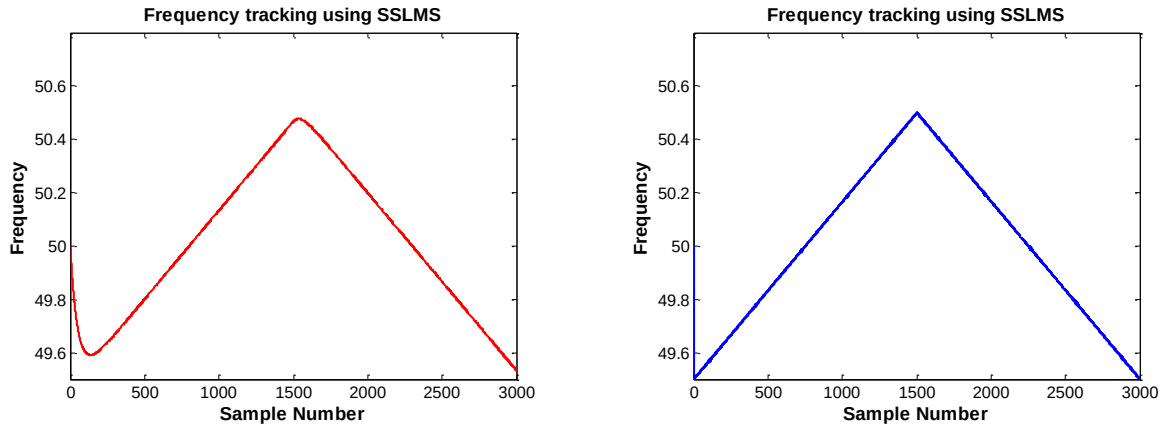

(a) (b)

Figure 7.3.6: Frequency tracking of bidirectional varying PLI using μ_{SSLMS}=0.005 with (a) η = 0.02 (b) η = 0.5

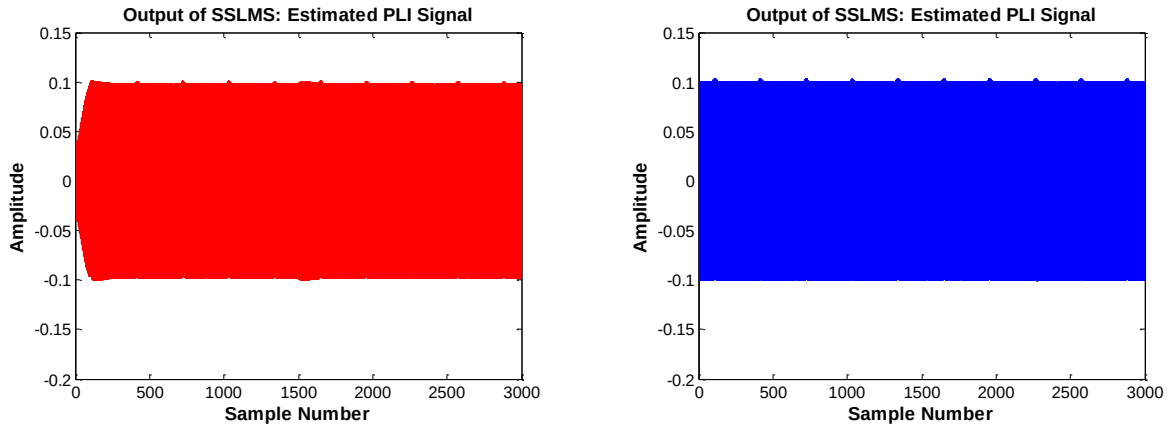

(a) (b)

Figure 7.3.7: Estimated bidirectional varying PLI using μ_{SSLMS}=0.005 with (a) η = 0.02 (b) η = 0.5

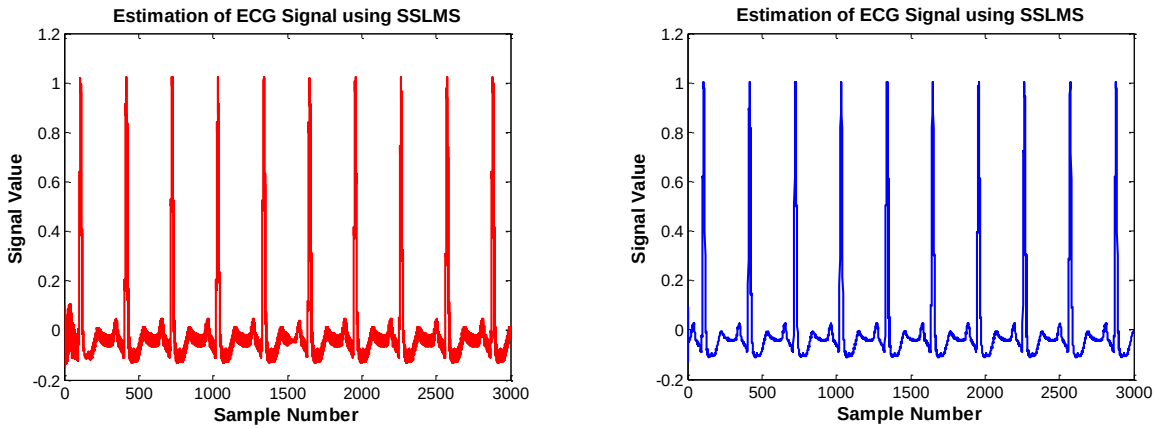

(a) (b)

Figure 7.3.8: Estimated ECG Signal using μ_{SSLMS}=0.005 with (a) η = 0.02 (b) η = 0.5

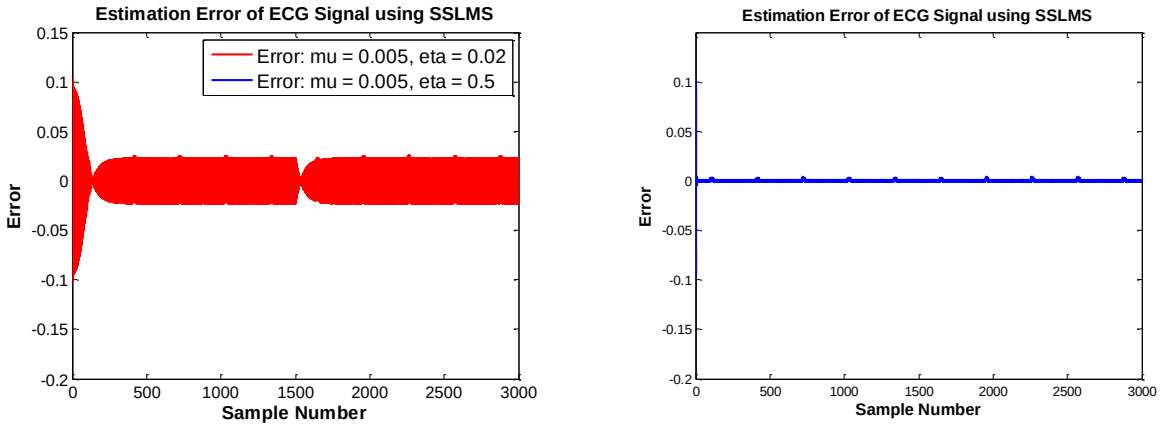

(a) (b)

Figure 7.3.9: Error in estimation of ECG Signal using μ_{SSLMS}=0.005 with (a) η = 0.02 (b) η = 0.5

7.3.3 Effect of μ on convergence and error

Results in this section exhibit that smaller the value of μ_{SSLMS}, smaller the estimation error at QRS complex peaks of ECG signal. It can be seen in Figure 7.3.10 that for smaller μ_{SSLMS}, frequency tracking is also affected at the point of occurrence of ECG signal peaks which also leads to error in estimation as shown in Figure 7.3.13.

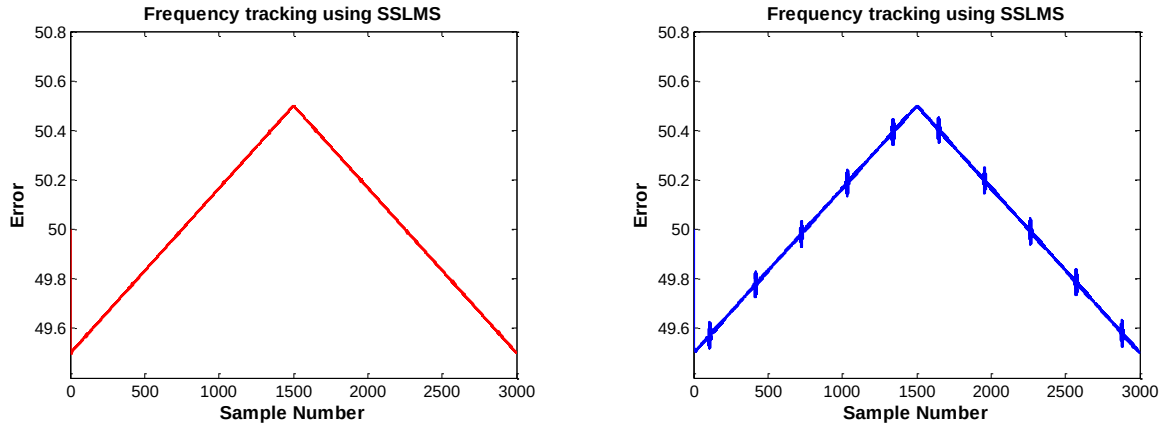

(a) (b)

Figure 7.3.10: Frequency tracking of bidirectional varying PLI using η = 0.5 with (a) μ_{SSLMS}=0.005 (b) μ_{SSLMS} =0.05

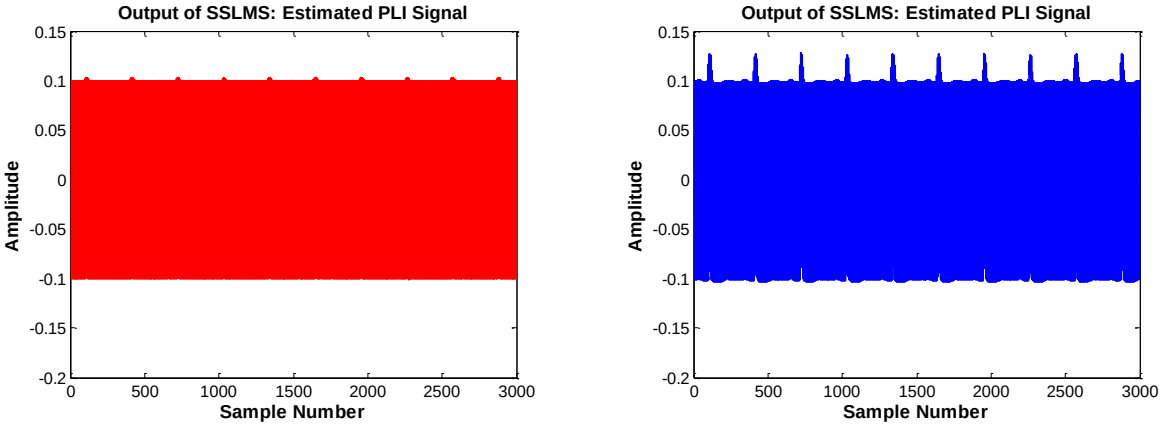

(a) (b)

Figure 7.3.11: Estimated bidirectional varying PLI using η = 0.5 with (a) μ_{SSLMS}=0.005 (b) μ_{SSLMS} =0.05

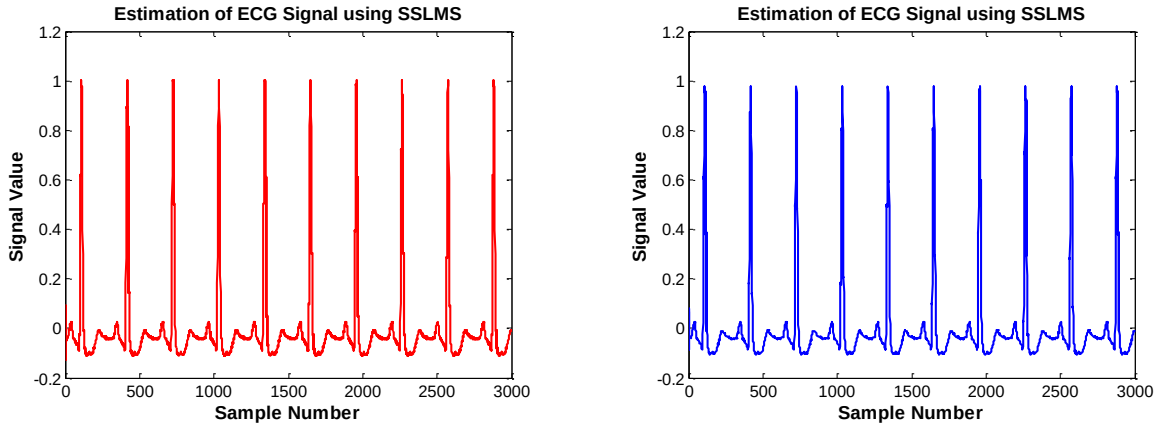

(a) (b)

Figure 7.3.12: Estimated ECG Signal using η = 0.5 with (a) μ_{SSLMS}=0.005 (b) μ_{SSLMS} =0.05

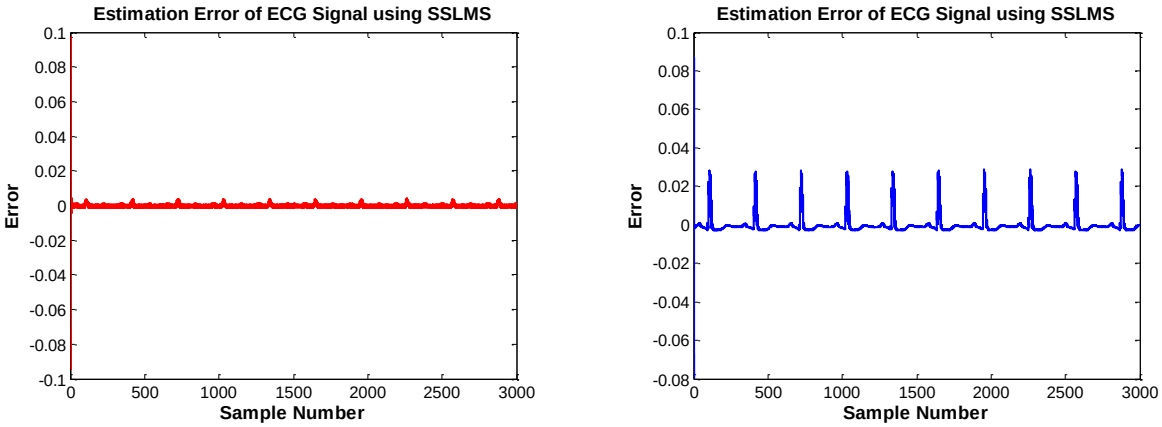

(a) (b)

Figure 7.3.13: Error in estimation of ECG Signal using η = 0.5 with (a) μ_{SSLMS}=0.005 (b) μ_{SSLMS} =0.05

7.3.4 Comparison with SSRLS algorithm

Figure 7.3.14 shows the frequency tracking of PLI with bidirectional variable using $\mu_{SSLMS} = 0.005$, $\lambda_{SSRLS} = 0.999$ and $\eta = 0.5$. Figure 7.3.17 shows that the estimation error of SSLMS is better that that of SSRLS for such type of frequency variation.

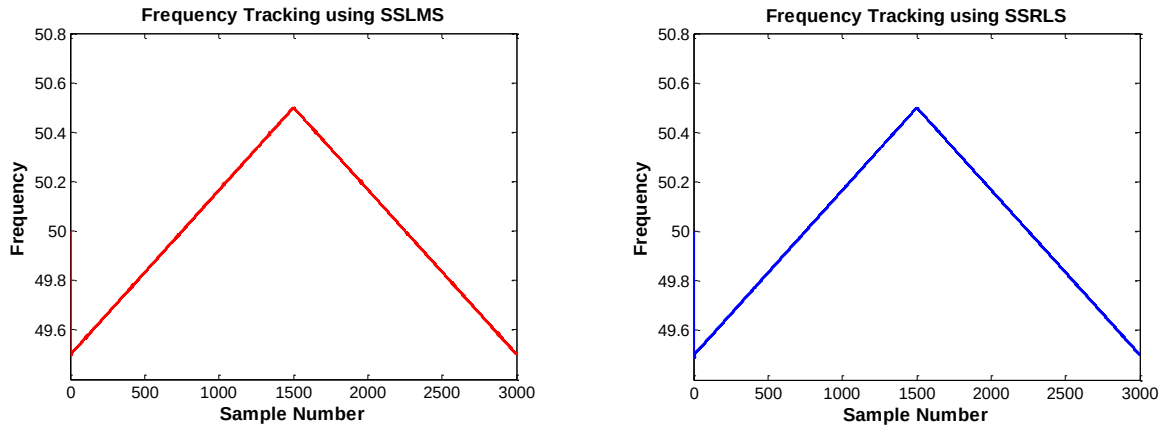

(a) (b)

Figure 7.3.14: Frequency tracking of bidirectional varying PLI using η = 0.5 with (a) SSLMS (μ_{SSLMS}=0.005) (b) SSRLS (λ_{SSRLS} = 0.999)

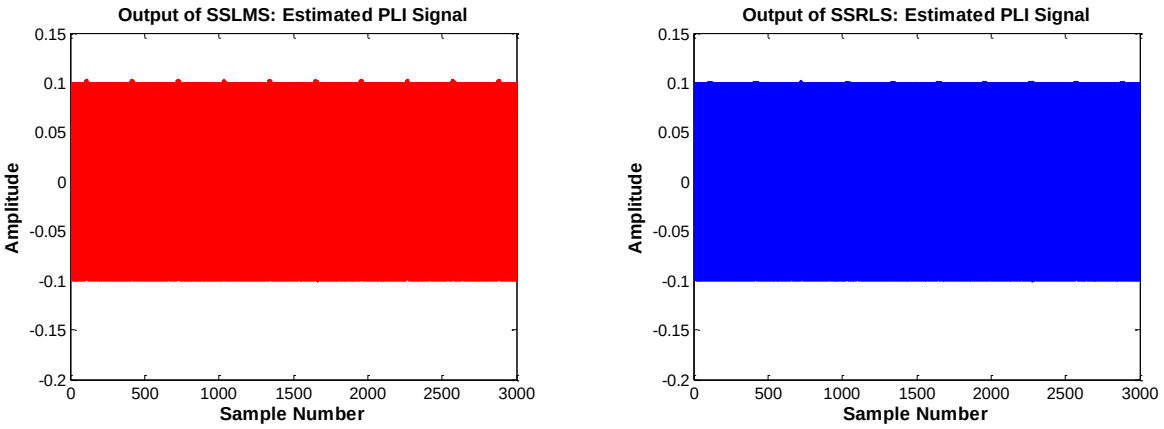

(a) (b)

Figure 7.3.15: Estimated bidirectional varying PLI using η = 0.5 with (a) SSLMS (μ_{SSLMS}=0.005) (b) SSRLS (λ_{SSRLS} = 0.999)

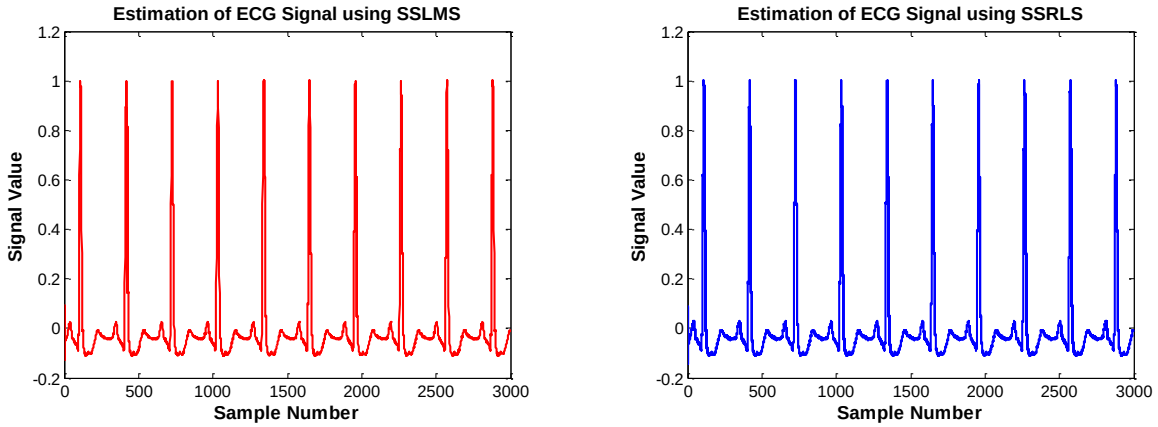

(a) (b)

Figure 7.3.16: Estimated ECG Signal using η = 0.5 with (a) SSLMS (μ_{SSLMS}=0.005) (b) SSRLS (λ_{SSRLS} = 0.999)

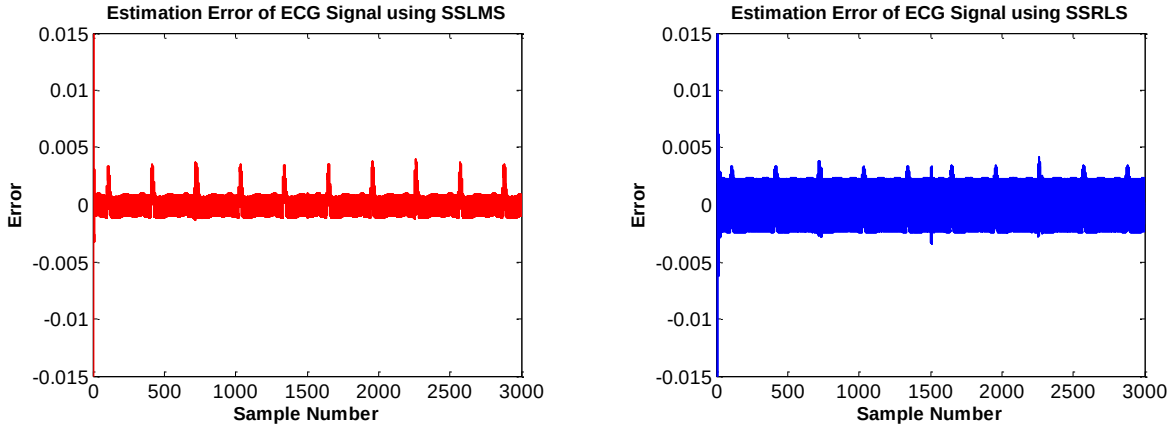

(a) (b)

Figure 7.3.17: Error in estimation of ECG Signal using η = 0.5 with (a) SSLMS (μ_{SSLMS}=0.005) (b) SSRLS (λ_{SSRLS} = 0.999)

In **Table 7.3-2**, it is shown that for SSLMS, MATLAB requires lesser time to execute than that for SSRLS algorithm.

Table 7.3-2: Elapsed time of MATLAB simulations for SSLMS and SSRLS algorithms

SSLMS	**SSRLS**
0.120216 seconds	1.437904 seconds

Hence the simulation results and elapsed time analysis proves SSLMS based adaptive noise canceller to be better than SSRLS one in case of unidirectional varying frequency.

7.4 Conclusion

From this chapter, PLI with frequency unidirectional and bidirectional varying has been removed from noisy ECG signal by first tracking its frequency and then estimating it. From the simulation results, we have concluded that, in case of drifting frequency, SSLMS gives better results for a larger value of η and smaller value of μ_{SSLMS} where former determines frequency tracking and later leads to convergence. Moreover, SSLMS has better convergence speed and computational complexity than SSRLS algorithm for a fixed value of η.

CHAPTER 8: SSRLS-SSLMS HYBRID ALGORITHM BASED ADAPTIVE NOISE CANCELLER

In this chapter a hybrid of SSRLS and SSLMS algorithm has been proposed to remove sinusoidal PLI with known frequency from ECG signal. The results are generated using MATLAB R2012a. The parameter for hybrid to switch from one algorithm to another has been explained. Moreover, the results have been compared with those of SSLMS and SSRLS algorithm.

8.1 Overview of Hybrid$_{\text{SSRLS-SSLMS}}$ Algorithm

In Table 8.1-1, SSRLS and SSLMS algorithms have been compared in light of previous simulations mentioned in section 5.3. It is clear that SSRLS algorithm has better convergence speed and MSE but has very high computational complexity (Table 2.4-2So in order to benefit from both algorithms, a hybrid of SSRLS and SSLMS has been proposed which combines convergence and MSE of former and computational complexity of later algorithm as shown in Table 8.1-1.

Table 8.1-1: Comparison of SSRLS, SSLMS and Hybrid algorithm with respect to convergence, MSE and computational complexity

	Convergence	**Mean Square Error**	**Computational Complexity**
SSRLS	✓	✓	✗
SSLMS	✗	✗	✓
SSRLS-SSLMS Hybrid	✓	✓	✓

In order to have better convergence for the proposed hybrid, SSRLS algorithm is being executed for first ψ iteration, and after that for the rest of the estimation SSLMS based adaptive noise cancellation has been implemented. Value of ψ is decided according to the convergence property of respective SSRLS algorithm.

$$Iteration \underset{>}{\overset{<}{\gtrless}} \psi \qquad (8.1)$$

SSRLS

SSLMS

The selection of λ_{SSRLS} for faster convergence and μ_{SSLMS} for improved mean square error in later iterations is further explained in Section 8.2.

8.2 Implementation of Hybrid SSRLS-SSLMS Algorithm

SSRLS-SSLMS Hybrid algorithm has been used to remove PLI noise generated parameters using Table 5.1-1. Figure 5.1.1 and Figure 5.1.2 show the pure ECG signal [49] and noisy ECG signal respectively along with their frequency response. For SSRLS algorithm, larger value of forgetting factor λ_{SSRLS} leads to slow convergence. Similarly for SSLMS algorithm, in order to have efficient estimation at QRS complex peaks of the ECG signal, μ_{SSLMS} must be kept smaller. Keeping this in view, hybrid algorithm is initialized with $x_o = \begin{bmatrix} 0 \\ 0 \end{bmatrix}$, $\lambda_{Hybrid} = 0.99$ and $\mu_{Hybrid} = 0.01$. Moreover, SSRLS algorithm has been executed for the first cycle of ECG signal in this case which leads to $\psi = 300$.

Figure 8.2.1 shows the amplitude and frequency response of proposed hybrid algorithm. It can be seen that after convergence, estimated PLI reaches its true amplitude i.e. 0.1. Frequency response in **Figure 8.2.1** (b) shows that it has estimated the 50 Hz PLI very efficiently.

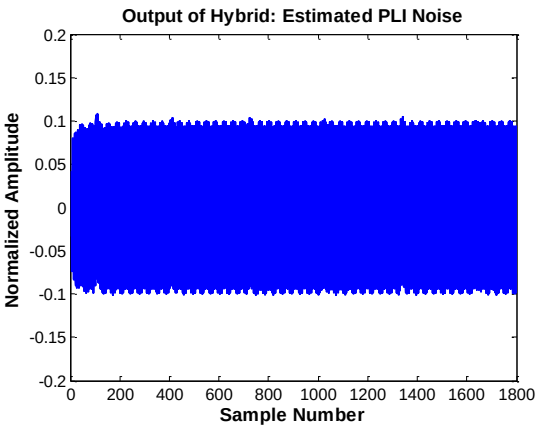

(a)

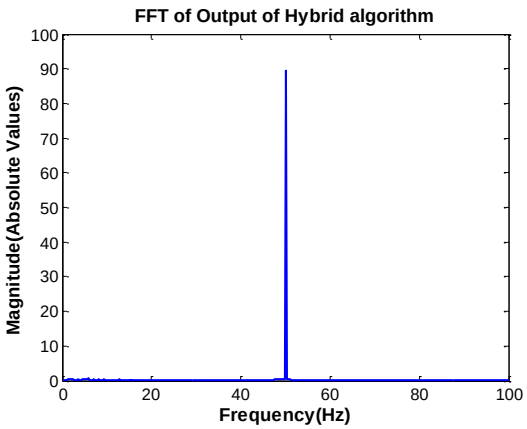

(b)

Figure 8.2.1: Output of SSRLS-SSLMS Hybrid algorithm (a) Amplitude (b) Frequency response

Figure 8.2.2 shows the amplitude and frequency response using the Hybrid algorithm based adaptive noise canceller and it can be seen from frequency response that 50 Hz component has been significantly removed by the improved ANC.

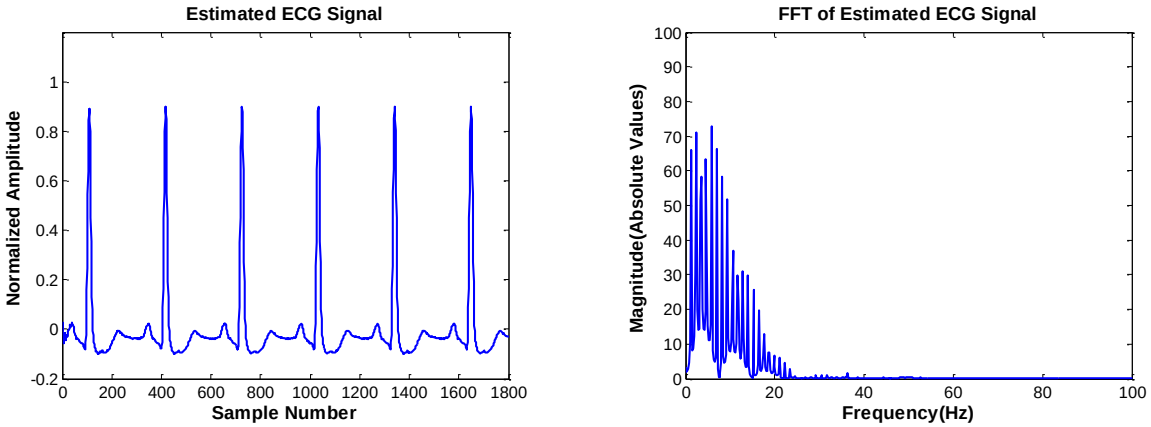

(a) (b)

Figure 8.2.2: Estimated ECG signal using proposed hybrid based ANC (a) Amplitude (b) Frequency response

Figure 8.2.3 shows the error in the estimation of the noise-free ECG signal and it can be seen that this proposed technique reduce the error remarkably.

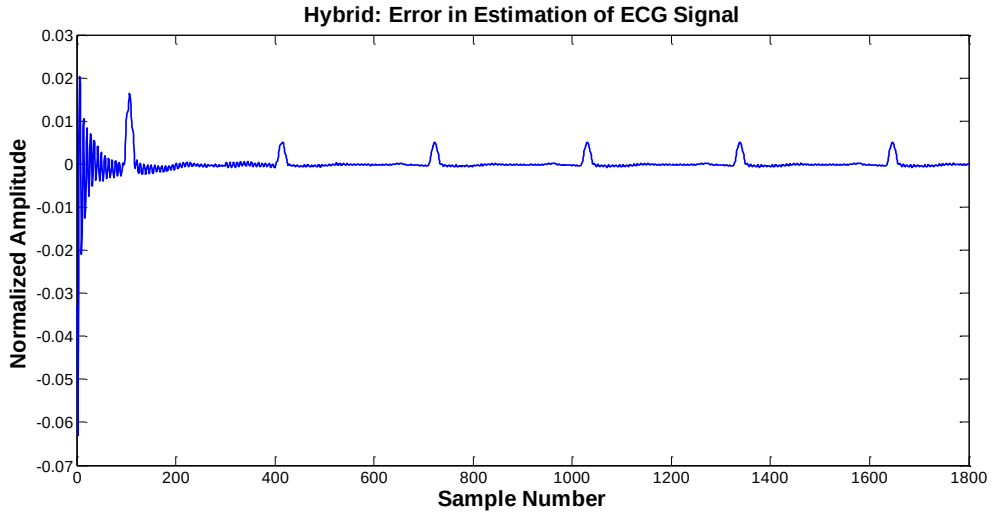

Figure 8.2.3: Estimation error using SSRLS-SSLMS Hybrid based ANC

8.3 Comparison with SSLMS and SSRLS algorithms

This section shows the comparison of proposed hybrid algorithm with SSRLS and SSLMS algorithms. The parameters used are $\mu_{SSLMS} = 0.05$, $\lambda_{SSLMS} = 0.99$, $\mu_{Hybrid} = 0.01$ and $\lambda_{Hybrid} = 0.99$. Analyzing Figure 8.3.1, we can see that MSE of Hybrid algorithm is lowest than both SSRLS and SSLMS algorithms making it better in sense of convergence and MSE than both existing algorithms.

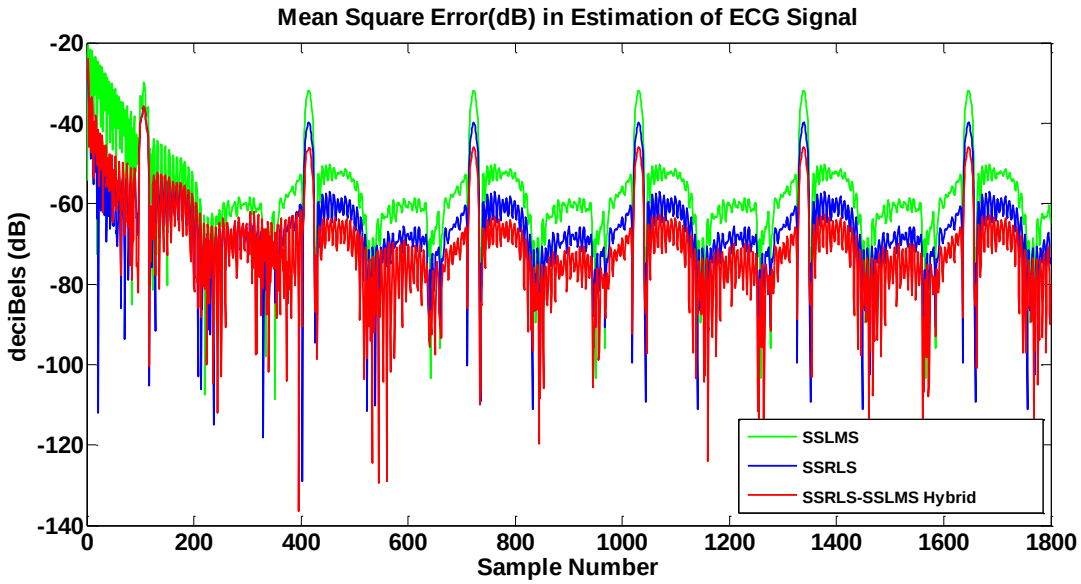

Figure 8.3.1: Comparison of MSE of SSLMS, SSRLS and Hybrid $_{SSRLS\text{-}SSLMS}$ based ANCs for noise cancellation

Moreover, it can be seen in Figure 8.3.2 that estimated PLI using hybrids algorithm shows no peaks at the occurrence points of ECG QRS complex peaks. Figure 8.3.3 shows the estimated ECG signal and it can be shown that Hybrid algorithm has better tracking efficiency than SSLMS and SSRLS based ANCs. Figure 8.3.4 shows that after the hybrid converges, it has lower error that the other two algorithms under consideration.

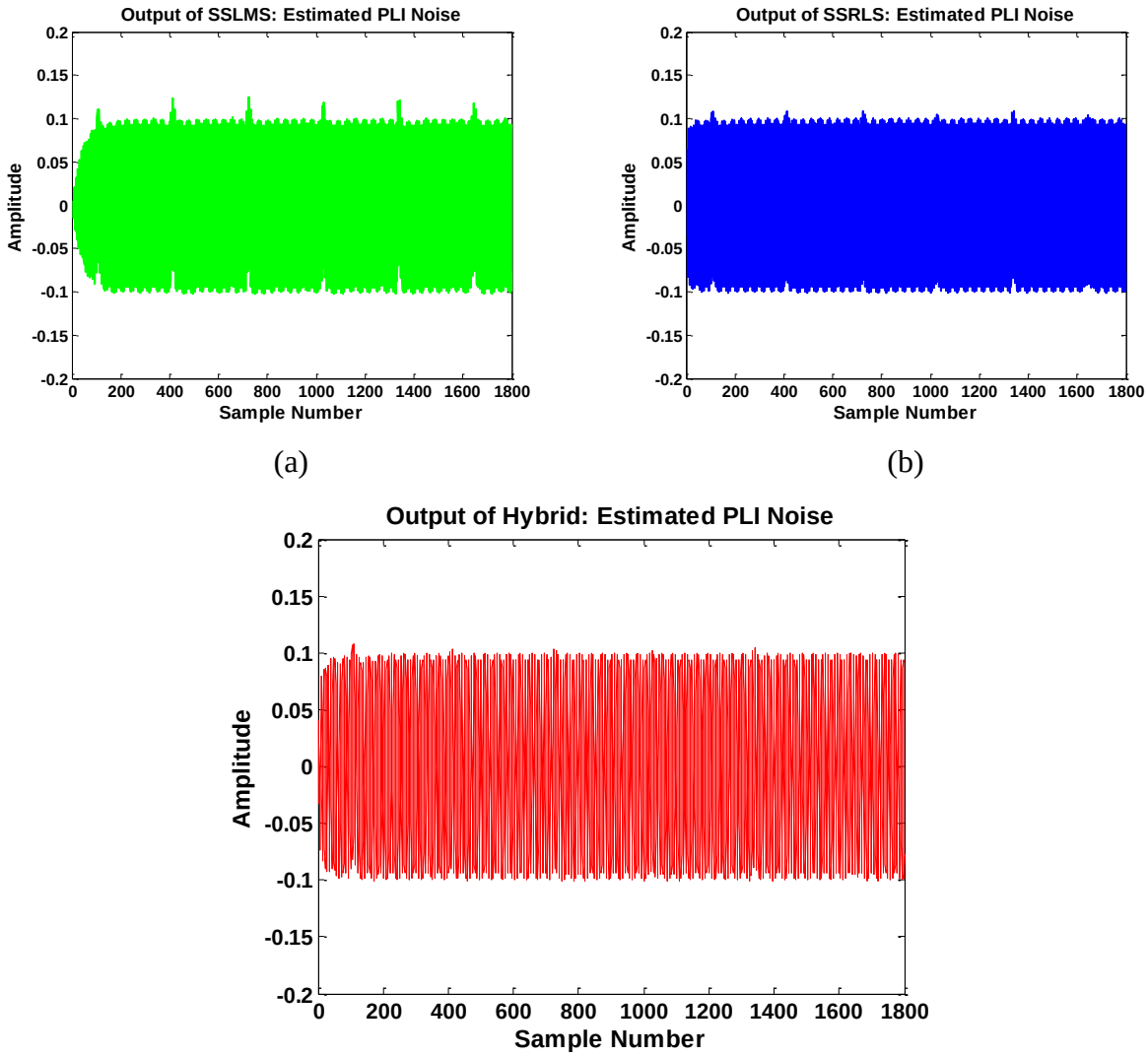

Figure 8.3.2: Estimated PLI of (a) SSLMS (b) SSRLS (c) Hybrid $_{\text{SSRLS-SSLMS}}$ based ANCs

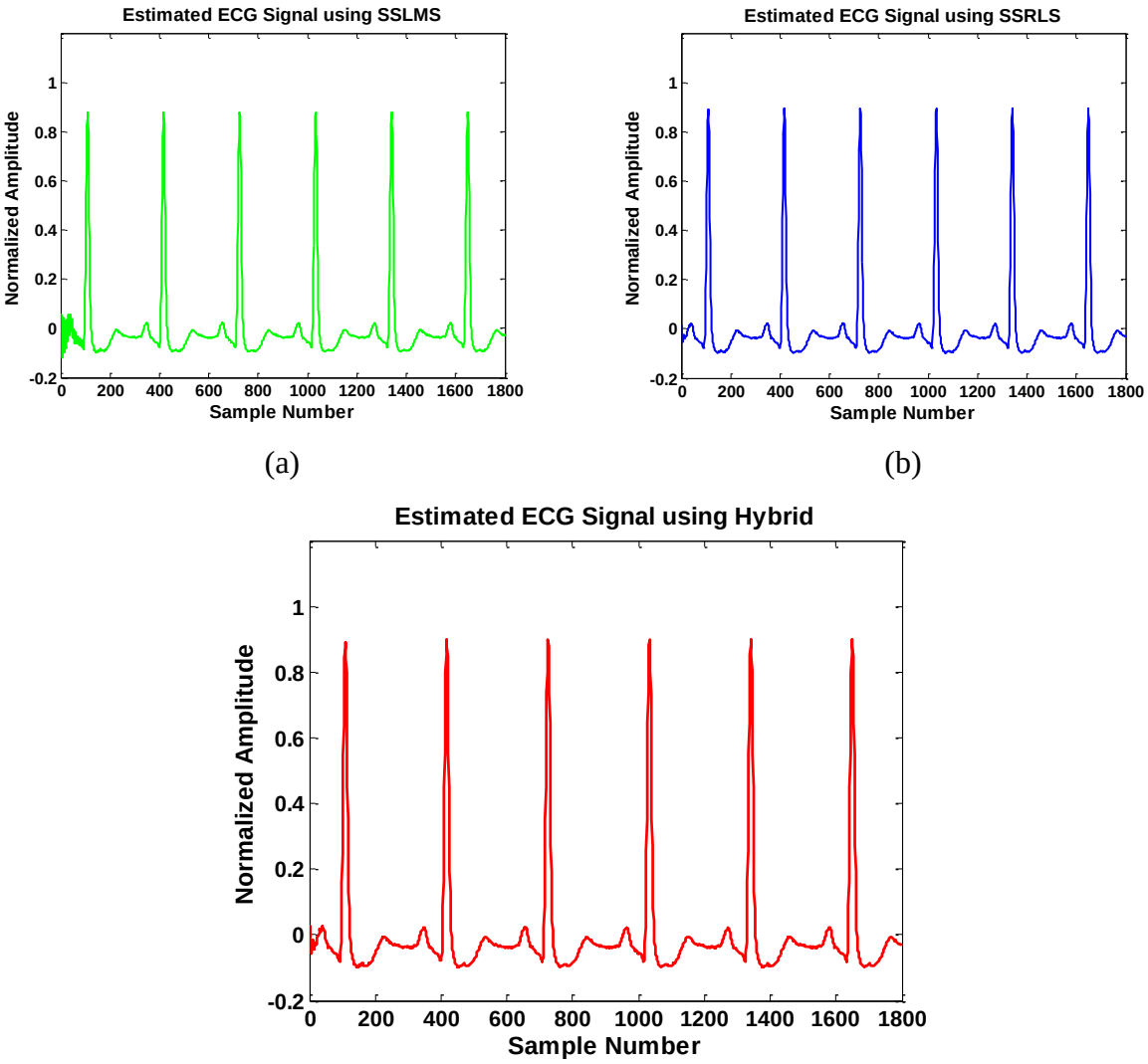

Figure 8.3.3: Estimated ECG of (a) SSLMS (b) SSRLS (c) Hybrid $_{\text{SSRLS-SSLMS}}$ based ANCs

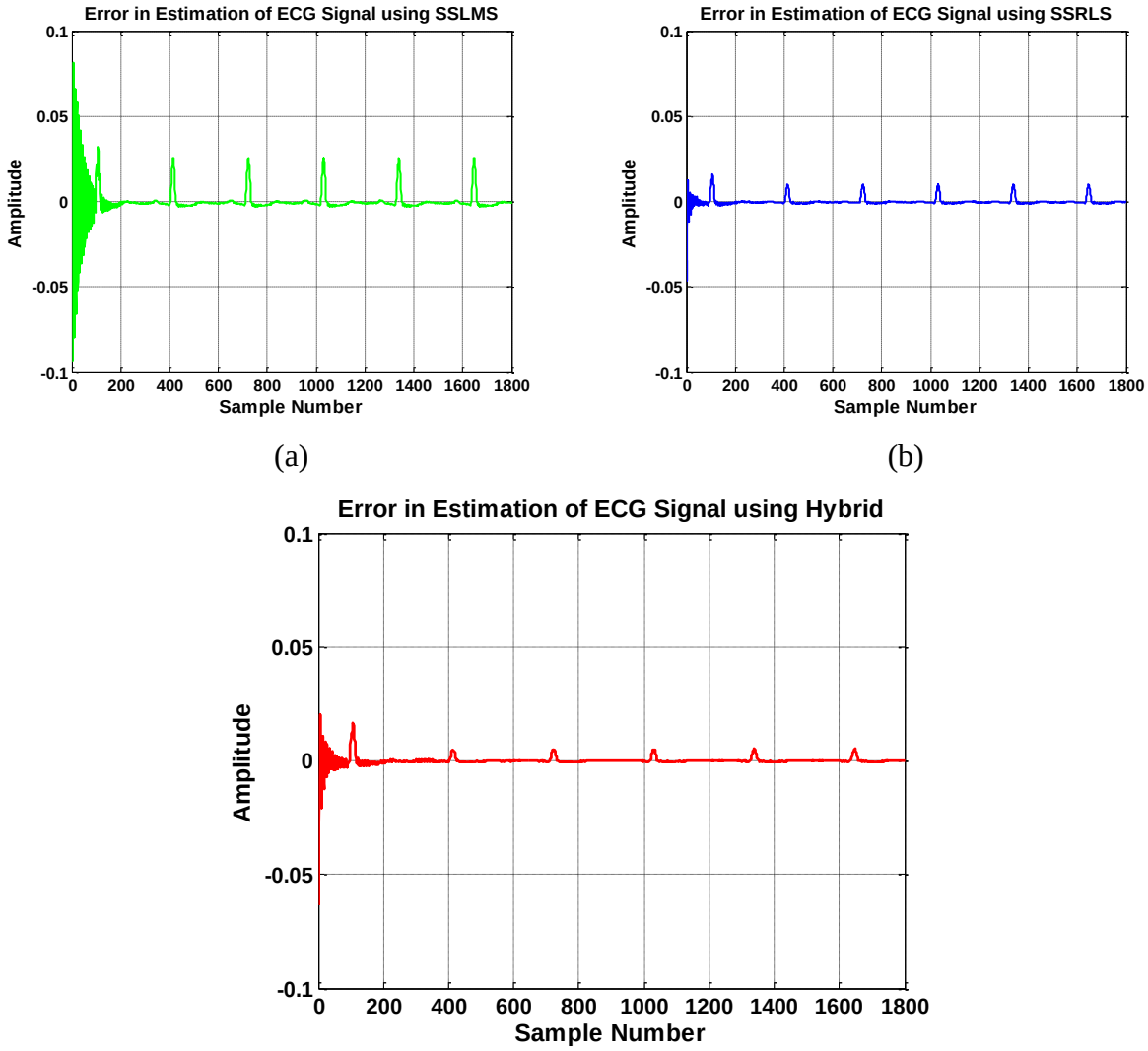

Figure 8.3.4: Estimated error of (a) SSLMS (b) SSRLS (c) Hybrid $_{\text{SSRLS-SSLMS}}$ based ANCs

Table 8.3-1 shows the comparison of elapsed time for MATLAB simulations mentioned above. It shows that Hybrid algorithm has slightly higher elapsed time than that of SSLMS algorithm but is much faster than SSRLS.

Table 8.3-1: Elapsed time of MATLAB simulations for algorithms

Algorithm	Elapsed Time
SSRLS	0.178354 seconds

SSLMS	0.019853 seconds
Hybrid	0.029893 seconds

Hence, it is proved from the simulations that SSRLS-SSLMS Hybrid algorithm has better convergence, MSE and computational speed that both SSRLS and SSLMS algorithms.

8.4 Computational Complexity analysis of SSRLS-SSLMS Hybrid Algorithm

Table 8.4-1 shows the computational complexity of SSRLS algorithm being implemented on first ψ iteration. During these iteration, hybrid algorithm converges reducing the mean square error.

Table 8.4-1: Computational complexity for the first ψ iterations using SSRLS algorithm

Eq's	**Operation**	$\times$	$\pm$	$\div$
1	$\bar{x}[k]_{L\times1} = A[k-1]_{L\times L}\hat{x}[k-1]_{L\times1}$	L^2	$L^2 - L$	$-$
2	$\bar{y}[k]_{1\times1} = C[k]_{1\times L}\bar{x}[k]_{L\times1}$	L	$L-1$	$-$
3	$\varepsilon[k]_{1\times1} = y[k]_{1\times1} - \bar{y}[k]_{1\times1}$	$-$	1	$-$
4	$\phi[k]_{L\times L} = \lambda(A_{L\times L}^{-T}\phi[k-1]_{L\times L}A_{L\times L}^{-1} + C_{L\times1}^{T}C_{1\times L})$	$2L^3 - 2L^2$	$2L^3 - L^2$	1
5	$K[k]_{L\times1} = \phi^{-1}[k]_{L\times L}C^{T}[k]_{L\times1}$	L^2	$L^2 - L$	$-$
6	$\hat{x}[k]_{L\times1} = \bar{x}[k]_{L\times1} + K[k]_{L\times1}\varepsilon[k]_{1\times1}$	L	$-$	$-$
7	$\hat{y}[k]_{1\times1} = C[k]_{1\times L}\hat{x}[k]_{L\times1}$	L	$L-1$	$-$
8	$e[k]_{1\times1} = y[k]_{1\times1} - \hat{y}[k]_{1\times1}$	$-$	1	$-$
	Total	$\boldsymbol{2L^3 + 4L^2 + 3L}$	$\boldsymbol{2L^3 + L^2}$	**1**
		$\boldsymbol{4L^3 + 5L^2 + 3L}$		**1**

Similarly, Table 8.4-2 shows the computational complexity, of SSLMS algorithm, for the samples after the convergence has been attained.

Table 8.4-2: Computational complexity for the remaining iterations using SSLMS algorithm

Eq's	**Equation**	×	±	÷
1	$\bar{\boldsymbol{x}}[\boldsymbol{k}] = A[\boldsymbol{k}-\mathbf{1}]\hat{\boldsymbol{x}}[\boldsymbol{k}-\mathbf{1}]$	L^2	$L^2 - L$	−
2	$\bar{y}[k] = C[k]\bar{x}[k]$	L	$L-1$	−
3	$\varepsilon[k] = y[k] - \bar{y}[k]$	−	1	−
4	$K[k] = \mu C^T[k]$	L	−	−
5	$\hat{x}[k] = \bar{x}[k] + K[k]\varepsilon[k]$	L	−	−
6	$\hat{y}[k] = C[k]\hat{x}[k]$	L	$L-1$	−
7	$e[k] = y[k] - \hat{y}[k]$	−	1	−
	Total	$\boldsymbol{L^2 + 4L}$	$\boldsymbol{L^2 + L}$	−
		$\boldsymbol{2L^2 + 5L}$		−

As mentioned in previous section, $\psi = 300$ which means that for 300 iterations the computational complexity is $4L^3 + 5L^2 + 3L$ and for remaining 1500 iteration, according to the simulations in Section 8.2, it is $2L^2 + 5L$. Computing the average of this complexity over total 1800 iterations, the approximate complexity is $0.667L^3 + 2.5L^2 + 4.667L + 0.1667$ as shown in Table 8.4-3.

Table 8.4-3: Average computational complexity of Hybrid SSRLS-SSLMS algorithm over 1800 iterations with $\psi = 300$

Samples	**Multiplication and Addition**
1-300 (SSRLS)	$300(4L^3 + 5L^2 + 3L + 1)$
201-1800 (SSLMS)	$1500(2L^2 + 5L)$
Average computation per sample	$0.667L^3 + 2.5L^2 + 4.667L + 0.1667$

As sinusoidal model is used to estimate PLI. So $L = 2$ for above mentioned computational complexity analysis. Table 8.4-4 shows the approximate number of computations per iteration it

takes for the three algorithms under study by putting the value of L in Table 8.4-1, Table 8.4-2 and Table 8.4-3. It is clear from the results that Hybrid algorithm has its computational complexity improved that that of SSRLS algorithm.

Table 8.4-4: Number of computations per iteration for Hybrid, SSRLS and SSLMS algorithms

Algorithm	**Number of Computations (L =2)**
SSRLS	59
SSLMS	15
Hybrid	24

8.5 Conclusion

In this chapter, simulation results and MATLAB elapsed time have proved $Hybrid_{SSRLS-SSLMS}$ to be better than SSLMS and SSRLS algorithms. Comparative analysis has been carried out for analyzing convergence, MSE, robustness and computational complexity of algorithms under consideration.

CHAPTER 9; CONCLUSION AND FUTURE WORK

After detailed description and performance comparison of proposed solutions overall conclusion and future recommendations are presented in this chapter.

9.1 Conclusion

In this this, SSLMS based adaptive noise cancellation technique has been proposed in order to estimate and remove impulsive component of PLI from ECG signal. The simulation results and comparison with existing techniques show that SSLMS has better overall performance.

Moreover, sinusoidal PLI with known, unknown and drifting frequency have also been removed from ECG signal using SSLMS Algorithm. Simulations have proved that SSLMS based ANC cancels out PLI efficiently. Step size parameters for SSLMS and adaptive tracking schemes have also been compared to decide the values giving better results. Proposed technique has also been compared with SSRLS based ANC and has proved to give better estimation performance.

In the end, a hybrid algorithm has been proposed that benefits from fast convergence, mean square error (MSE) and computational complexity of both SSRLS and SSLMS algorithm. It has been implemented to remove sinusoidal PLI with known frequency from ECG signal. Better performance of hybrid algorithm has been proved by simulation results along with its computational complexity analysis.

9.2 Future Work

$Hybrid_{SSRLS\text{-}SSLMS}$ Algorithm has implemented where the convergence of SSRLS is better than SSLMS. In case of unknown and drifting sinusoidal PLIs, SSLMS has better estimation performance than SSRLS algorithm. In order to have better performance, $Hybrid_{SSRLS\text{-}SSLMS}$ must be analysed for such frequency cases.

9.3 Research Contribution

- J Habib, A Zeb, A Mirza, SA Sheikh, “SSLMS Algorithm based Impulsive Noise Cancellation from ECG Signal”, IEEE International Conference of Multimedia Systems and Signals Processing, New Taipei, Taiwan, 3-5 September, 2016
- Journal “PLI Removal from ECG signal using Adaptive Algorithms”-submitted

REFERENCES

[1] http://www.who.int/mediacentre/factsheets/fs317/en/.

[2] Global status report on non-communicable diseases 2010. World Health Organization, 2014.

[3] Mathers CD, Loncar D. Projections of global mortality and burden of disease from 2002 to 2030. PLoS Med, 2006, 3(11):e442.

[4] H. V. Pipberger et al., "AHA Committee Report: Recommendations for standardization of leads and of specifications for instruments in electrocardiography and vectorcardiography," Circulation, vol. 52, pp. 11–31, 1975.

[5] J. J. Bailey et al., "AHA Scientific Council Special Report: Recommendations for standardization and specifications in automated electrocardiography," Circulation, vol. 81, pp. 730–739, 1990.

[6] Martin J. Burke and Denis T. Gleeson, "A micropower dry-electrode ECG preamplifier," IEEE Transactions on Biomedical Engineering, vol. 47, No. 2, Feb. 2000.

[7] "Electrocardiography," https://en.wikipedia.org/wiki/Electrocardiography.

[8] Mujagic, Muris. "Characterization of ECG Noise Sources."

[9] Van Rijn, A.M., Peper, A. and Grimbergen, C.A., 1990. High-quality recording of bioelectric events. *Medical and Biological Engineering and Computing*, *28*(5), pp.389-397.

[10] Martens, Suzanna MM, Massimo Mischi, S. Guid Oei, and Jan WM Bergmans. "An improved adaptive power line interference canceller for electrocardiography." IEEE transactions on Biomedical Engineering 53, no. 11 (2006): 2220-2231.

[11] B. Widrow et al., “Adaptive noise cancelling: Principles and applications,” IEEE proceedings, vol. 63, no. 12, pp. 1692-1716, Dec. 1975.

[12] J. R. Glover,“Adaptive noise canceling applied to sinusoidal interferences,” IEEE Trans. on Acoust. Speech, Signal Process., vol. 25, no. 6, pp.484–491, Dec. 1977.

[13] S. Martens, M. Mischi, S. Oei, and J. Bergmans, “An improved adaptivepower line interference canceller for electrocardiography,” IEEE Transactions on Biomedical Engineering, vol. 53, no. 11, pp. 2220 –2231, Nov. 2006.

[14] Panda, R.; Pati, U.C., “Removal of artifacts from electrocardiogram using digital filter,” 2012 IEEE Students’ Conference on Electrical, Electronics and Computer Science (SCEECS), pp.1,4, 1-2, March 2012.

[15] M. Makundi, T. I. Laakso, and L. Yaohui, “Asynchronous implementation of transient suppression in tunable IIR filters,” Int. Conf. on Digital Signal Process., vol. 2, pp. 815–818, 2002,

[16] P. S. Hamilton, “A comparison of adaptive and non-adaptive filters for reduction of power line interference in the ECG,” IEEE Trans. on Biomed. Eng., vol. 43, no. 1, pp. 105–109, Jan. 1996.

[17] N. V. Thakor and Y. S. Zhu, “Application of adaptive filtering to ECG analysis: Noise cancellation and arrhythmia detection,” IEEE Trans. on Biomed. Eng., vol. 38, no. 8, pp. 785–794, Aug. 1991.

[18] W. K. Ma, Y. T. Zhang, and F. S. Yang, “A fast recursive-least-squares adaptive notch filter and its applications to biomedical signals,” Med. Biol. Eng. Comput., vol. 37, no. 1, pp. 99–103, Jan. 1999.

[19] Piskorowski, J., “Digital Q-Varying Notch IIR Filter With Transient Suppression,” IEEE Transactions on Instrumentation and Measurement, vol.59, no.4, pp.866, 872, April 2010.

[20] Li Tan; Jean Jiang; Liangmo Wang, “Pole-Radius-Varying IIR Notch Filter With

[21] Transient Suppression,” IEEE Transactions on Instrumentation and Measurement, vol.61, no.6, pp.1684,1691, June 2012.

[22] Islam, Syed Zahurul, Syed Zahidul Islam, Razali Jidin, and Mohd Alauddin Mohd Ali. "Performance study of adaptive filtering algorithms for noise cancellation of ECG signal." In Information, Communications and Signal Processing, 2009. ICICS 2009. 7th International Conference on, pp. 1-5. IEEE, 2009.

[23] Maniruzzaman, Md, Kazi Md Shimul Billah, Uzzal Biswas, and Bablu Gain. "Least-Mean-Square algorithm based adaptive filters for removing power line interference from ECG signal." In Informatics, Electronics & Vision (ICIEV), 2012 International Conference on, pp. 737-740. IEEE, 2012.

[24] Chandrakar, Chinmay, and M. K. Kowar. "Denoising ECG signals using adaptive filter algorithm." International Journal of Soft Computing and Engineering (IJSCE) 2, no. 1 (2012): 120-123.

[25] S. Haykin, Adaptive Filter Theory, 4th ed., Upper Saddle River, NJ: Prentice-Hall, 2002.

[26] A. K. Ziarani and A. Konrad,“A nonlinear adaptive method of elimination of power line interference in ECG signals,” IEEE Trans. on Biomed. Eng., vol. 49, no. 6, pp. 540–547, Jun. 2002.

[27] Soumyadipta Acharya, Dale H. Mugle, Bruce C. Taylor, “A fast adaptive filter for electrocardiography”, Proceedings of the IEEE 30th Annual Northeast Bioengineering Conference, April 2004.

[28] I. S. Badreldin, D. S. EI-Kholy, and A. A. EI-Wakil, “Modified adaptive noise canceler for electrocardiography with no power-line reference,” Cairo International Biomedical Engineering Conference, Cairo, Egypt, Dec. 2010.

[29] I. S. Badreldin, D. S. EI-Kholy, and A. A. EI-Wakil, “Harmonic adaptive noise canceler for electrocardiography with no power-line reference,” Electrotechnical Conference (MELECON), Mediterranean, March 2012.

[30] Butt, M., Razzaq, N., Sadiq, I., Salman, M. and Zaidi, T., 2013, March. Power line interference removal from ECG signal using SSRLS algorithm. In Signal Processing and its Applications (CSPA), 2013 IEEE 9th International Colloquium on (pp. 95-98). IEEE.

[31] Mohammad Bilal Malik “State-Space Recursive Least Squares: part I ,” Signal Processing, vol. 84/9, pp. 1709-1728, 2004.

[32] M.B. Malik, State-space recursive least squares with adaptive memory, Signal Process. J. 86 (2006) 1365–1374.

[33] Bharath, H. N.; Prabhu, K. M M, "A new LMS based adaptive interference canceller for ECG power line removal," 2012 International Conference on Biomedical Engineering (ICoBE), pp.68,73, 27-28, Feb. 2012.

[34] T. Kanachareon, J. Koseeyaporn, R. Punchalard, and P. Wardkein, “New

Adaptive Filter Algorithm for Noise Cancellation in ECG Signals,” The 31th Electrical Engineering Conference, Thailand, Oct. 2008.

[35] Koseeyaporn, P.; Koseeyaporn, J.; Wardkein, P., “An enhanced adaptive algorithm for PLI cancellation in ECG signals,” 7th International Conference on Information, Communications and Signal Processing ICICS 2009, pp.1,5, 8-10 Dec.

2009.

[36] Manpreet Kaur, Birmohan Singh, “Powerline Interference Reduction in ECG Using Combination of MA Method and IIR Notch”, Electronic Letters, International Journal of Recent Trends in Engineering, vol 2, no. 6, Nov. 2009.

[37] Tong T J, ChenY, Tong J J, eta.l, “A new application of lock-in amplifieradaptive noise canceller”, The 3rd International Conference on Bioinformatics and Biomedical Engineering, New York, 2009.

[38] S. X. Li, L. Y. Liu, “Design of wavelet domain median filter”, Journal of UEST of China, pp: 18-21, 2003.

[39] Zhi-Dong Zhao; Yu-quan Chen, “A New Method for Removal of Baseline Wander and Power Line Interference in ECG Signals,” International Conference on Machine Learning and Cybernetics, pp.4342, 4347, 13-16, Aug. 2006.

[40] Huang.N.E, et al, “The empirical mode composition and the Hilbert spectrum for nonlinear and non-stationary time series analysis”, Proceeding of R.Soc.Lond.A, vol 454, pp. 903-995, 1998.

[41] Flandrin. P, Rilling. G, Goncalves.P, “Empirical mode decomposition as a filter bank”, IEEE Signal Processing Letters, vol. 11, no. 2, pp. 112-114, 2004.

[42] Rilling.G, Flandrin. P, Goncalves. P, “Empirical mode decomposition, fractional Gaussian noise and Hurst exponent estimation”, Proceedings of IEEE International Conference on Acoustics, Speech, and Signal Processing, vol 4544, pp. 489-492, 2005.

[43] Norden E. Huang, “HHT basics and applications for speech, machine health monitoring, and bio-medical data. Analysis,” pp.1-78, March 2003.

[44] Junling Li; Bohu Liang; Xiaodong Su, “Research on ECG signal filtering algorithm based on the fusion of multiple algorithms,” International Conference on Measurement, Information and Control (MIC), vol.1, pp.370,373, 18-20 May 2012.

[45] Kavya, G.; Thulasibai, V., “Parabolic Filter for Removal of Powerline Interference in ECG Signal Using Periodogram Estimation Technique,” International Conference on Advances in Computing and Communications, pp.106,109, 9-11 Aug.

[46] Malik, M.B. and Salman, M., 2008. State-space least mean square. Digital Signal Processing, 18(3), pp.334-345.

[47] Malik, M.B. and Bhatti, R.A., 2004, October. Tracking of linear time-varying systems using state-space least mean square. In Communications and Information Technology, 2004. ISCIT 2004. IEEE International Symposium on (Vol. 1, pp. 582-585). IEEE.

[48] W.J. Rugh, Linear System Theory, second ed., Prentice Hall, Upper Saddle River, NJ, 1996.

[49] A. L. Goldberger et al., “PhysioBank, PhysioToolkit and Physionet: Components of a new research resource for complex physiologic signals Circulation,” Circulation, vol. 101(23), June 2000, doi: http://dx.doi.org/10.1161/01.CIR.101.23.e215

[50] Malik, M.B. and Salman, M., 2006, July. Adaptive tracking of a noisy sinusoid/chirp with unknown parameters. In 2006 IEEE International Symposium on Industrial Electronics (Vol. 1, pp. 593-598). IEEE.

[51] Richard G. Lyons, Understanding Digital Signal Processing, 2nd Ed, Pearsan Education, 2004.

[52] Tario,P., Sanchez, MG., Cuinas, I., "An Algorithm to Simulate Impulsive Noise," 19th International Conference on Telecommunications and Computer Networksm Split, Croatia, p 1-4, 2011.

Completion Certificate

It is to certify that the thesis titled "**PLI Removal from ECG Signal using Adaptive Algorithms**" submitted by **NS Javeria Habib** Registration No. **NUST201464399MCEME35014F** is satisfactory for completion of the partial fulfillment of requirement for Degree of Master of Science in Electrical Engineering.

Thesis Advisor: _____

(Dr Shahzad Amin Sheikh)